



***A Survey of Methods for  
Analysing Groundwater  
Recharge in Arid and  
Semi-arid Regions***



**A Survey of Methods for Groundwater Recharge in Arid and  
Semi-arid regions**



UNEP/DEWA  
UNESCO/IHP

This publication was compiled with contributions from:  
Wolfgang Kinzelbach, IHW, ETHZ, Zurich, Switzerland  
Werner Aeschbach, EAWAG, Zurich, Switzerland  
Carmen Alberich, IHW, ETHZ, Zurich, Switzerland  
Ibrahim Baba Goni, Dept. of Geology, University of Maiduguri, Nigeria  
Urs Beyerle, University of Berne, Berne, Switzerland  
Philip Brunner, IHW, ETHZ, Zurich, Switzerland  
Wen-Hsing Chiang, S.S. Papadopoulos Associates, Bethesda, MD, USA  
Joerg Rueedi, University of Berne, Berne, Switzerland  
Kai Zoellmann, ETHZ, Zurich, Switzerland.

ISBN: 92-807-2131-3

For bibliographic and reference purposes, this publication should be cited as Kinzelbach W., Aeschbach W., Alberich C., Goni I.B., Beyerle U., Brunner P., Chiang W.-H., Rueedi J., and Zoellmann K. (2002) A Survey of Methods for Groundwater Recharge in Arid and Semi-arid regions. Early Warning and Assessment Report Series, UNEP/DEWA/RS.02-2. United Nations Environment Programme, Nairobi, Kenya. ISBN 92-80702131-3

Design layout, editing and production by Salif Diop, Ralph Johnstone, Patrick M'anyi, Dennis Lisbjerg and Audrey Ringler.

Cover photograph: UNEP/Thomas Dressler, 1999. Supporting photos, from top: Lauren Goodsmith/The Image Works CGM0736, 1991; Loic Giorgi, 2001; Abdoul Aziz Tandia, 2001.

Copyright © 2002, United Nations Environment Programme

This publication may be reproduced in whole or in part and in any form for educational or non-profit purposes without special permission from the copyright holder, provided acknowledgement of the source is made. UNEP would appreciate receiving a copy of any material that uses this publication as a source. No use of this publication may be made for resale or for any other commercial purpose whatsoever without prior permission in writing from the United Nations Environment Programme.

To obtain copies of this publication, please contact:



Division of Early Warning and Assessment  
United Nations Environment Programme  
P.O. Box 30552  
Nairobi 00100,  
Kenya  
Tel : (254 2) 62 41 05  
Fax : (254 2) 62 42 69  
E-mail: dewainfo@unep.org

#### **Disclaimer**

This publication contains the views expressed by the authors and experts involved acting in their individual capacity and may not necessarily reflect the views or policies of UNEP. The designations of geographical entities in this report and the presentation of the material do not imply the expressions of any opinion whatsoever on the part of UNEP concerning legal status of any country, territory, city or area or its authority, or concerning the delimitation of its frontiers or boundaries. Mention of a commercial company or product in this report does not imply endorsement by UNEP. The use of information from this publication concerning proprietary products for publicity or advertising purposes is not permitted. Trademark names and symbols are used in an editorial fashion with no intention of infringement on trademark or copyright laws. We regret any errors or omissions that may unwittingly have been made.

## Contents

Acknowledgements .....	1
Acronyms .....	2
Foreword.....	3
Executive Summary.....	4
1. Introduction .....	5
2. Overview of the most common methods of recharge estimation .....	7
3. Use of spreadsheets for soil water balance method.....	20
4. The chloride method.....	22
5. Environmental tracers.....	32
6. Use of spreadsheets for age determination with tritium and CFCs.....	38
7. Carbon14 dating .....	44
8. Use of remote sensing for recharge estimation .....	57
9. Groundwater modelling as a tool for data interpretation.....	65
List of contributors .....	70
Appendix: ‘Your First Groundwater Model with PMWIN’ .....	71

The software included on the CD-ROM is available at: [www.unep.org/water/groundwater/](http://www.unep.org/water/groundwater/)

## Figures

Fig. 2.1: Lysimeter .....	7
Fig. 2.2: Soil moisture profiles .....	8
Fig. 2.3: Recession curve .....	9
Fig. 2.4: Cumulative rainfall departure .....	10
Fig. 2.5: Decay of $^3\text{H}$ to $^3\text{He}$ in the subsurface .....	13
Fig. 3.1: Concept of a soil moisture balance model .....	20
Fig. 3.2: Flow scheme for calculating the soil moisture budget .....	21
Fig. 4.1: Idealised solute concentrations developed during percolation .....	23
Fig. 4.2 A: Schematic representation of solute movement and recharge via the unsaturated zone .....	25
Fig. 4.2 B: Conceptualised solute concentrations during percolation, showing steady state section .....	25
Fig. 4.3: Groundwater sampling procedure .....	26
Fig. 4.4: Unsaturated zone chloride and isotope profiles from Cyprus .....	27
Fig. 4.5: Unsaturated zone chloride and isotopes profiles from Senegal .....	28
Fig. 4.6: Chloride profiles in NORTHEAST Nigeria against Maiduguri rainfall using spreadsheet model .....	29
Fig. 4.7: MF unsaturated zone solutes (Cl, Br & $\text{NO}_3\text{-N}$ ) and deuterium profiles .....	30
Fig. 5.1: Tracers with variable input functions .....	33
Fig. 5.2: Radioactive tracer concentration as a function of time .....	33
Fig. 5.3: The ‘mother-daughter isotopes’ $^3\text{H}$ and $^3\text{He}$ .....	33
Fig. 5.4: Groundwater dating with radiogenic noble gas isotopes .....	34
Fig. 5.5: Calculating mean groundwater residence times using CFC-12, $^{85}\text{Kr}$ , and $^3\text{H}$ .....	35
Fig. 5.6: Schematic principle of box models .....	36
Fig. 5.7 a: Piston flow model and corresponding transfer function .....	36
Fig. 5.7 b: Exponential model and corresponding transfer function .....	37
Fig. 5.7 c: Dispersion model and corresponding transfer function .....	37
Fig. 6.1: Output concentration of tritium as a function of time for different exponential models .....	40
Fig. 6.2: Output concentration as a function of the mean residence time $\tau$ for different models and parameters .....	40
Fig. 7.1: $^{14}\text{C}$ decay and activity at time zero .....	44
Fig. 7.2: Atmospheric concentration of $^{14}\text{C}$ .....	44
Fig. 7.3: Atmospheric $^{14}\text{C}$ extended by tree rings and shallow marine corals .....	45
Fig. 7.4: Dependence of carbonic acid equilibrium on pH .....	46
Fig. 7.5: Species of carbonic acid equilibrium for open and closed system conditions .....	50
Fig 8.1: Daily evapotranspiration in mm/day for the 5 <sup>th</sup> of March 1992 calculated from NOAA-AVHRR .....	63

## Tables

Table 4.1: Unsaturated zone profiles and recharge estimates from NORTHEAST Nigeria .....	30
Table 5.1: Timescales of various tracer-based dating methods .....	32
Table 5.2: Example of a groundwater sample taken in January 2000 .....	34
Table 7.1: Bunsen coefficient of $\text{CO}_2$ in L gas/L $\text{H}_2\text{O}$ .....	45
Table 8.1: Sensor characteristics .....	58

## **Acknowledgments**

We would like to thank UNEP/DEWA and UNESCO/IHP for supporting this publication. We are especially grateful to those United Nations officers without whose determination and hard work this document may never have materialised. We would also like to thank Abdelkader Dodo at the University of Niamey and Abou Amani at Agrhymet, who were instrumental in laying the groundwork for this publication. Finally, we acknowledge support by the Swiss National Foundation through Project No. 2000-061498.00.

## Acronyms

AMS	Acceleration Mass Spectrometer
CFCs	Chlorofluorocarbons
CRD	Cumulative Rainfall Departure
DGPS	Differential Global Positioning System
EAWAG	Swiss Federal Institute for Environmental Science and Technology
ETH(Z)	Swiss Federal Institute of Technology (Zurich)
HAPEX-Sahel	Hydrology-Atmosphere Pilot Experiment in Sahel
IHW	Institute of Hydromechanics and Water Resources Management
NDVI	Normalised Difference Vegetation Index
NGO	Non-Governmental Organisations
NOAA	(US) National Oceanic and Atmospheric Administration
PMWIN	Processing Modflow for Windows
SEBAL	Surface Energy Balance Algorithm for Land
SF <sub>6</sub>	Sulfur Hexafluoride
TDIC	Total Dissolved Inorganic Carbon
TDR	Time Domain Reflectometry
UNEP/DEWA	United Nations Environment Programme – Division of Early Warning and Assessment
UNESCO/IHP	United Nations Educational, Scientific and Cultural Organisation - International Hydrological Programme
USAID	US Agency for International Development
ZFP	Zero Flux Plane

## Foreword

*Tim Foresman, Director, Division of Early Warning and Assessment, UNEP*

In arid and semi-arid environments, the amount of recharge received by aquifers is far more critical to the sustainable use of water than it is in humid regions. Despite this fact, little remains known about the quantities of water that are required to sustainably recharge aquifers in such regions. Even after decades of research, there are many different methods that can be applied due to the complex nature of hydrogeology and the different situations in the world's arid and semi-arid lands.

Today, groundwater depletion is increasingly associated with the demands of development. Rapid recent developments have led to the decline of water levels in several major aquifers. In North Africa and the Arabian Peninsula, where fossil water is mined and not replenished, the use of water for agricultural irrigation is fast depleting the regions' last remaining aquifers.

For the sustainable exploitation of groundwater, the ideal situation would be to know the average rate and volume of extraction, and adapt pumping rates to sustainable withdrawal levels. Managed aquifers also require general maintenance of the ecosystem and its dependant inhabitants.

By definition, potential evapotranspiration normally surpasses average rates of precipitation. Groundwater recharge is irregular and our ability to observe and analyse aquifer dynamics is very limited. These factors are compounded by variations in topography, vegetation cover, soil types and hydrology – elements that make the recharge process very difficult to monitor and measure.

The underlying geology presents additional problems, with calcrete (non-porous) layers often buried beneath surfaces that appear perfect for infiltration and recharge.

This publication is a compilation of methods that have been used for analysing groundwater recharge in arid and semi-arid regions around the world. Some of these are direct methods, such as the soil moisture budget by neutron or TDR probes, water balance methods such as the river channel water balance, or rainfall-recharge relationships, which are the most common techniques. Others include the Darcyan methods, such as the numerical flow model, which can use many types of information, and tracer methods, such as the tritium-helium 3 method. Each method is presented with notes on their application and utilisation.

It is hoped that the methods presented will find wide-ranging and practical use among the many technical institutions, universities, NGOs, government institutions, and researchers working to conserve precious water resources in the world's arid and semi-arid lands.



## **Executive Summary**

The rate of recharge is the single most important factor in the analysis and management of groundwater resources in arid and semi-arid regions. At the same time, it is also the most difficult quantity to determine. This document, which is the result of a course held in Niamey, Niger, in 2000, presents an overview of all the methods identified to date for estimating groundwater recharge, including an assessment of the accuracy and suitability of each. It then looks in more depth at a selection of methods best suited to arid and semi-arid environments. Among these are the chloride method, the CFC and Tritium tracer methods, and the radiocarbon method. Excel spreadsheets and programmes are provided for calculating soil water balances, conducting geochemical analyses, dating environmental tracer concentrations, and building comprehensive groundwater flow and transport models.

The key to the successful estimation of groundwater recharge lies in the utilisation of a variety of independent methods. Every method has its strengths and weaknesses, but combined they become much stronger. By bringing together environmental tracers, modern measurement techniques, automatic monitoring equipment, DGPS and remote sensing in a comprehensive groundwater model, the study of the hydrology of arid and semi-arid environments can enter a new era.

# 1 Introduction

*Wolfgang Kinzelbach, IHW, ETHZ, Zurich, Switzerland*

For the sustainable management of groundwater resources, the amount of recharge received by an aquifer is by far the most important figure required. Yet this figure is usually the least well-known quantity in hydrogeology, especially in arid and semi-arid environments. Unfortunately, it cannot be measured directly on any reasonable spatial scale. That so many years of effort have failed to find a single, reliable method for measuring groundwater recharge is due to the complexity of this phenomenon and the large variety of situations encountered.

The depletion of aquifers is continuing at various rates around the world. Many countries report declining water levels in their major aquifers at rates of between one and three metres a year. In many aquifers, such as those in North Africa and the Arabian Peninsula, the fossil waters being mined will never again be replenished. All major aquifer depletions are due to water use for agricultural irrigation, which consumes far greater quantities than any other sector. Thus, the problem of groundwater recharge is closely tied to that of food security.

It is clear that cost will be the final limiting factor in the exploitation of aquifers and efforts to bring their over-exploitation to a halt. A wise way to proceed would be to calculate the average recharge rates in an area and adapt local pumping rates accordingly – keeping reservoirs relatively high, with an easily accessible reserve for times of prolonged drought. In long-term groundwater management, water tables may also play a vital role, with very low water tables impairing vegetation and leading to the collapse of water bearing fractures, while high water tables may lead to salinisation.

Recharge estimates are made particularly difficult in arid and semi-arid lands by the vast variability of hydrological events in time and space. Potential evapotranspiration surpasses average precipitation, which means that only in certain conditions is it sufficient for recharge. As recharge is a sporadic rather than a continuous process in arid areas, it is extremely difficult to observe and analyse. Point measurements with lysimeters do not do justice to the variability of infiltration and evapotranspiration in space caused by the variability of topography, soil type and vegetation cover.

Several natural processes may also influence recharge on different scales: an infiltration front; preferential flow in soil structures such as wormholes, root channels and termite hills; localised enhanced seepage in topographic depressions, wadis, rivers and irrigated fields. It is debatable whether the contributions of such processes can be realistically measured or compared. Even the driving force for recharge – precipitation – may be only vaguely understood or monitored, particularly in large countries with limited infrastructure. It is certainly risky to try and relate recharge by a constant factor to precipitation in an arid zone.

The determination of specific fluxes is just one side of the problem. For an assessment of the total recharge, the areas associated with the specific fluxes have to be known. A sandy area that may look ideal for infiltration on the surface may not contribute to recharge because of a calcrete layer buried beneath it.

It is very difficult to learn from one case to another, due to the broad range of processes involved. That is why so many

methods and techniques have been brought to bear on the analysis of groundwater recharge. We want to discuss these methods and formulate conclusions as to their relevance for the arid and semi-arid lands of Africa.

## 2 The Most Common Methods of Recharge Estimation

Wolfgang Kinzelbach, IHW, ETHZ, Zurich, Switzerland

The task of this chapter is to describe and classify the most important methods available for estimating groundwater recharge, to weigh their advantages and disadvantages, and then to judge their accuracy and reliability.

The following categories will be considered:

- Direct measurements
- Water balance methods (including hydrograph methods)
- Darcyan methods
- Tracer methods.

Accuracy ratings will be given in three classes, according to regional recharge estimates:

- Class 1: Within a factor of 2
- Class 2: Within a factor of 5 (of the same order of magnitude)
- Class 3: Within a factor of 10 or more (with large errors likely)

### 2.1 Direct Measurements

#### Lysimeters

A lysimeter is a device consisting of an in situ weighable soil column of a  $1\text{m}^2$  or greater cross-sectional area. The flux by rainfall into the column, the outflow by seepage in 1-2m depth and the weight are continuously measurable by modern lysimeters. From them, a 'water budget' can be reconstructed and the missing term – evaporation – calculated. Recharge is directly measured if it can be assumed that

the lower end of the lysimeter is below the zero (upward) flux plane (ZFP).

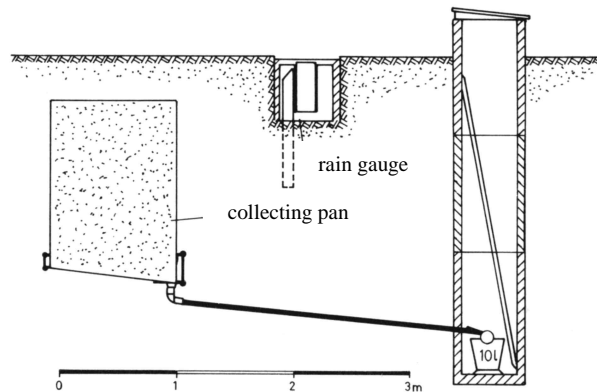


FIG. 2.1: LYSIMETER (FROM FRIEDRICH AND FRANZEN, 1960)

**Advantages:** Seepage below 1-2m is a directly measured quantity. Results from a lysimeter can be used for calibration of some of the following methods.

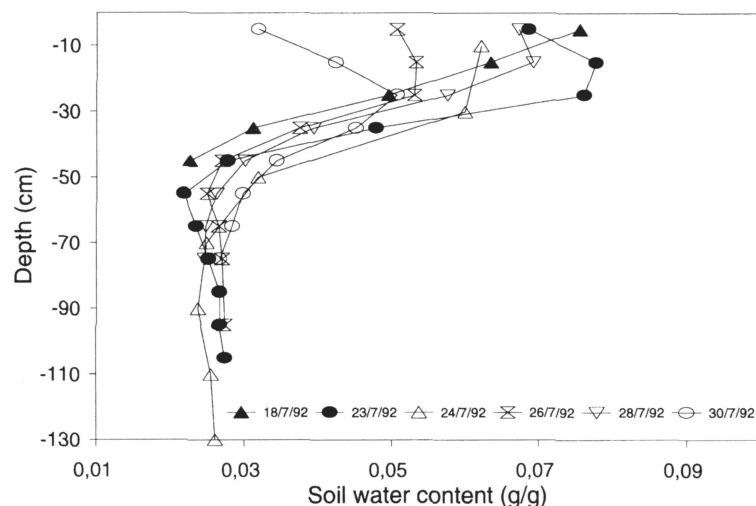
**Disadvantages:** One obtains only a local value for one type of soil, vegetation and soil structure. The method may be irrelevant in arid regions where singular recharge features are dominant over areal recharge. Finally, surface runoff cannot be taken into account.

**Accuracy:** The accuracy of the method for regional estimates is not quantifiable due to spatial variability. However, temporal variation is of more generic nature and therefore of higher reliability.

**Rating:** For point values: Class 1.

## Soil moisture budget by neutron probe or TDR probes

The neutron probe method relies on the fact that water molecules will scatter neutrons. The amount of scattering is proportional to the amount of water present, which essentially determines the vertical distribution of the soil's water content. The TDR method is a more modern method, which is less accurate but has the advantage of not requiring a neutron source. Both methods measure soil water content and not fluxes. They therefore constitute part of the data needed for the determination of a soil water balance from variation in soil moisture



distributions.

FIG. 2.2: SOIL MOISTURE PROFILES (FROM BRUNNEL ET AL., 1997)

**Advantages:** A direct measure of soil water content for budgeting is provided. It can be used for calibration of some of the following methods.

**Disadvantages:** The methods yield again only a local value. More information is needed to get a complete water balance. Interpretation of subsequent profiles may not be accurate, if there is disturbance by lateral flow, which makes the assumption of 1D vertical flux doubtful.

**Accuracy:** Accuracy for estimation of regional values is not quantifiable due to spatial variability.

**Rating:** For point values: Class 1 to 2.

## 2.2 Water Balance Methods (Including Hydrograph Methods)

### Soil moisture budgets

For all fluxes involved in the soil water balance, some empirical formulae exist. For example, evaporation can be computed by Penman's formula and others. The usual inputs for such a model are meteorological data from a nearby weather station, including precipitation, radiation budget, wind speed, relative humidity, air temperature, and soil data such as the field capacity. One variant of this method is explained further in Chapter 3.

**Advantages:** The calculation from standard data is simple and can be done in a spreadsheet.

**Disadvantages:** All methods of this type are basically very inaccurate when applied to recharge estimation. The reason is that recharge is the

difference between two inaccurately known large quantities (precipitation and evapotranspiration), with inaccuracies being particularly large under conditions of weak infrastructure and the peculiarities of the arid environment. The difference between two such quantities is prone to error and is often insignificant.

**Accuracy:** Accuracy is low. At best some sensitivity analyses are possible, which could be used for the estimation of recharge contrasts.

**Rating:** Class 3.

### River channel water balance

If recharge is confined to seepage from a river channel, the observations necessary

could in principle be very simple. If flow is measured between two points along the river, the difference will at least convey some information about seepage and give an upper bound for recharge.

**Advantages:** Measurements of river flow are easily carried out.

**Disadvantages:** Flow measurements are inaccurate and differences may be insignificant if the stretch of river is short. But if the total flow infiltrates, the method is especially interesting.

**Accuracy:** River flows vary in time, and to obtain a significant mean the measurements have to be repeated over time. On a long river stretch recharge may be compensated by tributary flow, which would also have to be accurately known.

**Rating:** Class 1 to 2.

### Water table rise method

A water table rise is the clearest indicator of recharge if all abstractions remain unchanged and atmospheric pressure effects can be ruled out. If the storage coefficient of an aquifer is known, the spatially interpolated water table rise can be converted into a volume of water. If a closed basin is considered, the water volume corresponding to a complete cycle of water table variation will allow the researcher to obtain recharge directly if the discharge is known, as both quantities are then

equal. In this case the storage coefficient of the aquifer is not required.

**Advantages:** This is a straightforward and simple method, especially when a full cycle of water table variation is considered.

**Disadvantages:** Basins or parts of aquifers considered are usually not closed, and in/out-flows not completely known. The storage coefficient is also usually unknown, especially in the situation of confined aquifers.

**Accuracy:** Storage coefficients from pumping tests are local and would have to be estimated for the region. The water table can often not be interpolated to any reasonable accuracy, as the density of observation boreholes in a typical arid zone is small. Also, water table information obtained from pumped boreholes is often unreliable.

**Rating:** Class 2 (if in-outflows are known or are negligible) or Class 3.

### River baseflow method

This method is based on the presumption that low flow conditions in the river represent pure groundwater outflow. On a long-term basis, this outflow must balance the inflow, i.e. be equal to the recharge. The flow measurement integrates all outflows along the river upstream of the gauging station, and therefore only estimates for the whole catchment are possible. Yet this method is one of the few that estimates an integral regional value instead of an insignificant local result. In the humid zone it is probably the best method available.

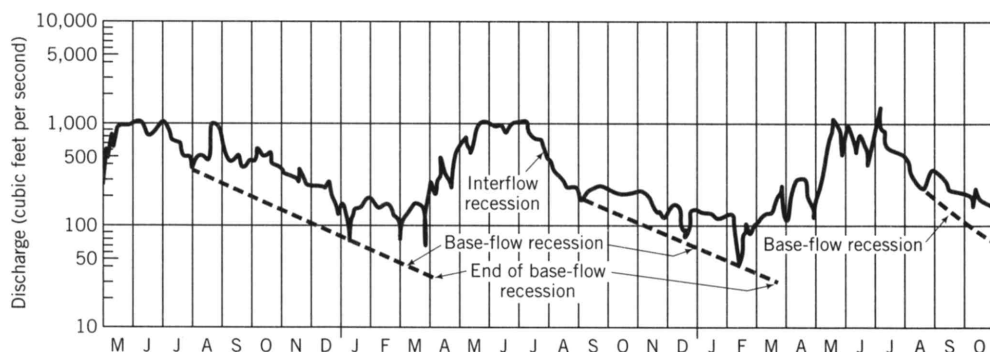


FIG. 2.3: RECESSON CURVE (FROM MEYBOOM, 1961, COPYRIGHT OF THE AMERICAN GEOPHYSICAL UNION)

**Advantages:** This method is one of the few integrative measures of recharge.

**Disadvantages:** The method is not feasible for ephemeral rivers where low flow reaches zero. There is also some ambiguity about the point in time when the discharge curve of a river has reached base flow.

**Accuracy:** Problems may arise when recharge to aquifers deeper than the one draining to the observed river are considered. The base flow then has no relation to the recharge of the deeper aquifer, the discharge of which is not contained in the measured flux.

**Rating:** Class 1 in humid zone, not applicable in arid zone.

### Spring or river flow recession curves

In this method the outflow of a catchment after the passage of the surface water wave is parametrized by an exponential curve. The typical time constant of outflow is determined. With some estimates on the storage volume of the drained aquifer, the recession constants allow an estimate of recharge.

**Advantages:** This is another integrative method. Observations of heads can be used.

**Disadvantages:** The catchment area must be known. The method is only applicable when there are springs or perennial rivers. The storage coefficient (porosity) must also be known.

**Accuracy:** As two estimates are involved, the method is inherently inaccurate. Long-term observations are necessary to obtain reliable results.

**Rating:** Class 2 to 3 in humid zone, often not applicable in arid zone.

### Rainfall-recharge relationships

It is common practice to express recharge as a percentage of better-known rainfall. However, it is usually unclear where the relationship comes from. This method is thus not a stand-alone method, and must be verified by other methods. The method can be upgraded by starting the linear relationship only after some threshold value of minimum rainfall required to observe recharge.

**Advantages:** The method is very simple.

**Disadvantages:** To establish the rainfall-recharge relationship, a reliable method of recharge determination is required. If the recharge is known, why then use the simple linear relationship? A linear relationship between the two quantities is inadequate in arid climates.

**Accuracy:** Poor.

**Rating:** Class 3.

### Cumulative Rainfall Departure Method

Using some simple assumptions, it can be shown that in a closed spring catchment the cumulative rainfall departure curve (CRD) is proportional to the water level response. This can be converted to a volume if the storage coefficient is known.

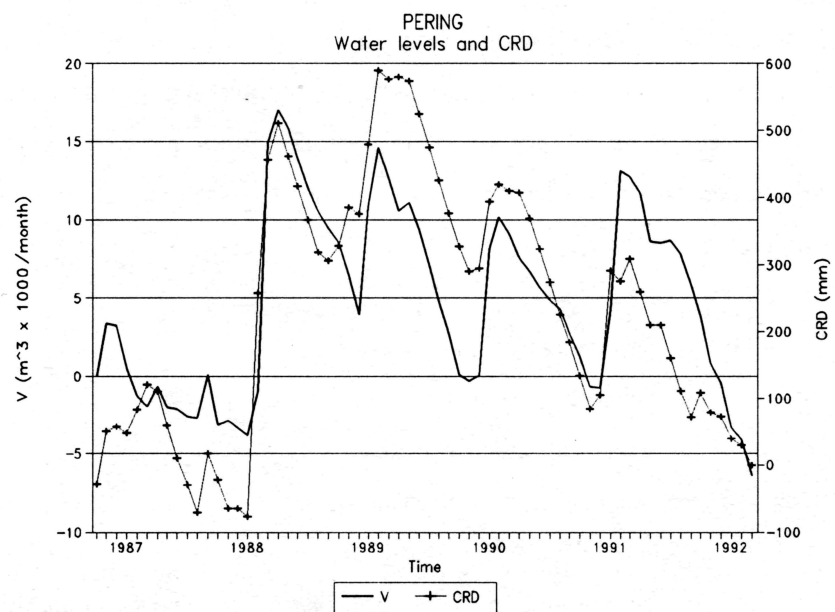


FIG. 2.4: CUMULATIVE RAINFALL DEPARTURE (FROM BREDEKAMP ET AL., 1995)

**Advantages:** The method is simple, and a long time series stabilises the error.

**Disadvantages:** Long time series are required in addition to a good estimate of the storage coefficient. The method is only applicable in a closed spring catchment. All abstractions have to be known.

**Accuracy:** The accuracy depends on the estimates of storage coefficient and abstraction rates.

**Rating:** Class 2 to 3.

### 2.3 Darcyan Methods

All Darcyan methods estimate the flux from a head gradient and a hydraulic conductivity. They therefore require an accurate determination of these two quantities representative of the scale on which the flux is to be determined.

#### Unsaturated zone Darcy law based on measurements of matrix potential

**Advantages:** All quantities involved on the right-hand side of Darcy's equation are measurable.

**Disadvantages:** The hydraulic conductivity of a soil is poorly known due to heterogeneity and varies with saturation. The functional relationship between the two quantities is hard to obtain. The values of water flux determined are very local. Water suction pressure is very hard to measure in arid climates.

**Accuracy:** Accuracy is poor due to the inaccuracy of unsaturated hydraulic conductivity.

**Rating:** Class 3.

#### Saturated Zone Darcy law based on pumping tests and head measurements

**Advantages:** As in the unsaturated case, measurable quantities are involved. The hydraulic conductivity is constant over time in the saturated medium.

**Disadvantages:** Hydraulic conductivity is very poorly known and is usually a log-normally distributed, heterogeneous quantity, which makes the estimation of a representative areal value difficult.

**Accuracy:** As above.

**Rating:** Class 3.

#### Unsaturated Zone: Solving Richards' equation

**Advantage:** This approach mimics the infiltration process. Required quantities can be measured. The method can be adapted to any soil, weather conditions or vegetation type.

**Disadvantage:** The measurements are rather tedious. Homogeneity is required and no lateral flow permitted. The results are only valid for one location. Macropore flow requires a more complex model with even more unknown parameters.

**Accuracy:** This is another method that yields point values instead of an integral areal value.

**Rating:** Class 3.

#### Numerical flow model

**Advantage:** Such a model can use many types of information. It presents an integrative view. A transport model can also be added (see section on tracers).

**Disadvantage:** Calibration of the model is required. Calibration with head data is usually not unique. Many combinations of recharge rate and transmissivities (and in the time varying case storage coefficients) can yield the observed heads. Transmissivities and recharge cannot be estimated at the same time.

**Accuracy:** Large scale transmissivity values are usually known with even less accuracy than recharge, therefore the calibrated quantity is usually transmissivity. Recharge estimates must come from other methods.

**Rating:** Class 3, with time-varying data and tracer information as described below: Class 2.



## 2.4 Tracer Methods

Environmental tracers are dissolved substances introduced into the large scale water cycle either by nature or by mankind over long periods. They are able to trace water movements over long time periods differently from artificially applied tracers, which show water movements over small spatial and temporal scales. Three basic philosophies can be distinguished in environmental tracing: the dating methods, the signature methods as a basis for mixing calculations, and the flux estimation methods.

Environmental tracers can be used in both unsaturated and saturated zones. All tracer methods may show a more averaged behaviour over time than hydraulic variables, owing to the fact that pressure travels faster in the aquifer than solute. The pattern of tracer distribution may therefore not correspond to momentary piezometric head distributions and recharge.

### Chloride method

**Advantages:** Chloride is a conservative tracer, which indicates evaporation. This method is based on the fact that precipitation contains chloride from sea salt aerosol. During evaporation the concentration increases, and the increase is a measure of the evaporation. Together with rainfall data, and under the assumption of negligible runoff, recharge can be computed. The method is cheap and can be carried out in less sophisticated laboratories. It follows the chloride profile in the unsaturated zone, but can also be applied more readily to concentrations in the top layer of the saturated zone. The chloride method is a flux method as it estimates directly the recharge flux. The method is elaborated further in Chapter 4.

**Disadvantages:** There are several instances in which the method can fail. This is especially the case if there are sources of chloride in the soil (eg. halites) other than the chloride contained in the

rainwater. Recycling of dried salt by wind, unaccounted runoff and uptake by harvested plants may also distort the results.

**Accuracy:** In the unsaturated zone, the method again yields a very local recharge value. The input function is difficult to obtain, as a local time series of chloride in precipitation as well as of dry deposition is required. Such data are still rarely available and, where they are, the time series is not yet long. It will take another decade to establish such data for West Africa. Finally, the area associated with the recharge rate has to be determined.

**Rating:** Class 2 to 3.

### Tritium method

**Advantages:** Tritium is a time marker due to its radioactive decay. It moves with the water molecule and can therefore be used to determine water ages. Wherever tritium has entered the soil, it has done so with the same concentration over a large region at a given time. The method is further elaborated in Chapter 5.

**Disadvantages:** Tritium, which came into the atmosphere during the nuclear tests of the 1960s, is declining, as its half-life is only 13.2 years. In the southern hemisphere, its application is very difficult as the peak was less pronounced, the sources being in the northern hemisphere. As tritium moves with the pore velocity, only a pore velocity and not the desired Darcy velocity can be determined. This is the common problem of all tracers that indicate age and travel time.

**Accuracy:** A good estimate of the porosity is required, which is reasonably easy in unconsolidated media but rather difficult in fractured media. When interpreting samples from wells, which mix waters of different age (travel time), a model is needed to interpret the measured values using an assumption on travel time distribution. In unsaturated profiles a very local value is also obtained.

**Rating:** Class 2 to 3.

## Tritium-Helium 3 method

**Advantages:** This method utilizes the fact that tritium (T) decays into Helium3 ( $^3\text{He}$ ). In surface waters and in the unsaturated zone,  $^3\text{He}$  partitions off into the air phase where it can rapidly be diluted. In the saturated zone, however, it moves with the remaining tritium. The ratio between T and  $^3\text{He}$  is then a function of travel time, with zero  $^3\text{He}$  in the beginning and zero tritium in the limit of long travel time. This ratio is independent of the input function.

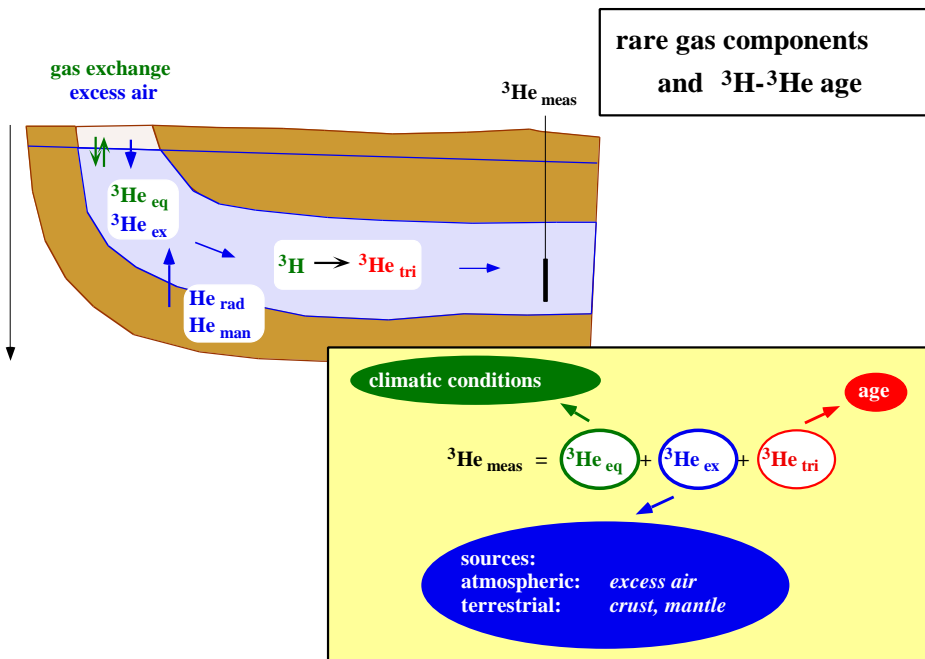


FIG. 2.5: DECAY OF  $^3\text{H}$  TO  $^3\text{He}$  IN THE SUBSURFACE

**Disadvantages:** The method is expensive and requires a strict sampling procedure. Travel times indicated by the method are no longer total travel times of water from ground surface to a well, but basically the time spent in the saturated zone. As in the tritium method, only a pore velocity can be estimated directly. For conversion a porosity figure is required.

**Accuracy:** Accuracy is limited by the estimate of porosity. For mixed water samples the same limitations apply as with tritium alone.

**Rating:** Class 2 to 3.

## Stable isotopes D, $^{18}\text{O}$

**Advantages:** These two stable isotopes can today easily be measured. They can be indicators of evaporation (but not plant transpiration). They are utilisable both in the unsaturated and saturated zones. Temperature and altitude effects cause differences in  $^{18}\text{O}$  or D concentrations over a catchment area, which can be used as indicators for mixing ratios of waters from different origins. The deviations of the two isotope concentrations from a standard are

measured and plotted against each other. The corresponding graph for rainwater yields the so-called meteoric water line.

**Disadvantages:** The method is not always applicable. No evaporation signal is seen if recharge happens in extreme events without much evaporation. On

the other hand, spurious signals may be generated in large diameter wells where evaporation from the water surface can occur. The isotopic composition of rain has to be monitored over a long time to obtain the local meteoric water line. Evapotranspiration by plants does not produce a shift away from the meteoric water line.

**Accuracy:** Often the method is less a quantitative tool for recharge computation than an indicator, which can support other data such as chloride data.

**Rating:** Class 3.

## Carbon 14

**Advantages:** The decay of  $^{14}\text{C}$  can be used as a geochronological tool. With a half-life of 5,200 years,  $^{14}\text{C}$  can be applied to long residence times only. As far as estimation of recharge is concerned, this method therefore yields only very long-term averages. The method is further discussed in Chapter 7.

**Disadvantages:** Due to its long half-life,  $^{14}\text{C}$ -derived recharge rates are not relevant for present day recharge.  $^{14}\text{C}$  is a reactive tracer if carbonates are present. Corrections are necessary. For short residence times, the  $^{14}\text{C}$  from bomb fallout is seen in the groundwater and long-term dating becomes impossible.

**Accuracy:** Corrections for admixing of 'dead' carbon introduce new errors. As for other tracers indicating residence time, a porosity is required for conversion to specific flux. This porosity can be larger than the one relevant for short time tracers such as tritium, as long residence times allow diffusion into the total porosity of the medium.

**Rating:** Class 3.

## Chloride 36 in unsaturated zone (from fallout)

**Advantages:** This tracer can be applied in two respects. It has a long half-life and can be used for dating of very old water. On the other hand, it is contained in the bomb fallout and can be considered stable for short-term applications after the bomb peak, where it presents a clear time-marker. Here only the application of Chloride 36 from fallout is considered. It shows its usefulness mainly in the unsaturated profile.

**Disadvantages:** As this tracer indicates a pore velocity instead of a Darcy flux, porosity has to be known. A profile represents a local value of recharge. Plant uptake is possible and can disturb the profile.

**Accuracy:** The input function has possibly to be interpolated. The porosity must be

known. The local profile may not be representative of the areal situation.

**Rating:** Class 2 to 3.

## Bromide in unsaturated zone

**Advantages:** This tracer has been used as an artificial tracer, bringing bromide out into fields with a certain mass at a certain time. Areas that can realistically be seeded are large in comparison to that for which a single soil profile or a lysimeter are representative.

**Disadvantages:** This tracer indicates pore velocities. The area that can be seeded is limited to single fields. The sampling must be sure to get a high enough number of samples to cover local variability, which is a costly procedure. The profile cannot be followed to a larger depth than about 1 metre. The sampling cannot consecutively be performed in exactly the same place as the sample is removed.

**Accuracy:** The porosity must be estimated. Each time samples are taken from a different location rather than continuously following a single path. This causes stochastic scatter and requires large sample numbers.

**Rating:** Class 2 to 3.

## New gas tracers CFC and SF<sub>6</sub>

**Advantages:** The CFC and SF<sub>6</sub> show until recently exponentially increasing concentrations in the atmosphere. This behaviour can be interpreted much more stably than a peak as in the case of tritium. They are time markers for the past 50 years. They can be used in the southern hemisphere, where tritium levels are low. The method is further discussed in Chapter 5.

**Disadvantages:** Gas tracers do not follow the water movement in the unsaturated zone. They therefore basically only show residence time in groundwater. Solubility in hot climates is low. The input function in industrial countries is not well known as long-term records are only available at

clean air stations, where these substances have been monitored since the 1950s.

**Accuracy and Rating:** This method is still under development, and no statement is currently possible.

## 2.5 Other Relevant Methods

A number of other methods are also related to the determination of recharge. They are applicable if special mechanisms of recharge or recharge related quantities are already known to dominate. Some of these methods are not very quantitative but due to their ability to provide a spatial pattern may allow the step from the point into the area. In this respect, they can also be combined with many of the point measurements discussed above.

### Measuring evaporation fluxes (areally, single trees)

Given a precipitation budget, evaporation is definitely an indicator of where the excess water for recharge may be located and at which time of the year. If vegetation is sparse and evaporation from groundwater only possible through deep-rooting trees, a tree count combined with individual measurements of sap flow in trees may give a much more meaningful estimate of areal losses than any other indirect measurement. Remote sensing data allows for determination of a vegetation index such as the NDVI, which integrates and summarises information on where water is concentrated in the landscape.

### Remote sensing methods for indicators

Spatial distribution of precipitation can be obtained from Meteosat images aggregated over 10 days and on a grid of 5 by 5 km. When looked at over the years, the distribution of rain in space may improve the estimation of recharge more than any other quantity as the inaccuracy of

precipitation in the semi-arid and arid environments is usually much greater than the recharge rate itself. The spatial distribution should, however, be calibrated against measured point values from rain gauges.

The spatial distribution of ponding water is of interest if it is known that depressions contribute preferentially to deep percolation. This is the case, for example, in Niger. A density of lakes forming after the rainy season hints at a potential recharge distribution. These lakes form during cloudy periods, where the usual remote sensing in visible and infrared channels cannot be applied. Yet radar images might be used that show water surfaces under the cloud cover by the lack of any reflected signals.

The spatial distribution of soil temperatures allows one to judge where soil is cooling due to evaporation and where it is heating up due to the rapid percolation of rainwater. In the future, soil moisture distribution recorded by microwave and radar sensors will also be able to help in locating potential recharge areas.

Density of lineaments in outcrops is an indicator often used in the siting of boreholes. At the same time it might also indicate where recharge through fractures is possible. Alteration zones can be identified by spectral peculiarities associated with minerals appearing in these zones.

**Advantages:** Prior knowledge is provided, which allows for better extrapolation of point values obtained on the ground to larger areas. In combination with Bayesian techniques, these data can yield the conditioning of models and the reduction of uncertainties in model estimates. Some contributions of remote sensing are further explained in Chapter 8.

**Disadvantages:** These data are usually only proxy data with approximate correlation to the desired quantities. Many

data can only be obtained on days with little or no cloud cover.

## References

*More details on the above methods and concepts can be found in the following publications:*

- Bredenkamp D. B., Botha L. J., van Tonder G. J. and van Rensburg H. J., *Manual on Quantitative Estimation of Groundwater Recharge and Aquifer Storativity*, Water Research Commission, Pretoria, South Africa, 1995.
- Brunnel J.P., Walker G.R., Dighton J.C. and Monteny B., *Use of stable isotopes of water to determine the origin of water used by the vegetation and to partition evapotranspiration*, Case study from HAPEX-Sahel Journal of Hydrology 188-189, 1997, p. 466-481.
- Friedrich W. and Franzen H., *Ein neuer Versickerungsmesser (Lysimeter)*, Deutsche gewässer, Mitt. 4, 1960, p. 105-111, Koblenz/Rhein.
- Gieske A., *Dynamics of Groundwater Recharge*, Ph. D. Thesis, Free University, Amsterdam, 1992.
- Lerner D.N., Issar A.S. and Simmers I., *Groundwater Recharge*, IAH, International Contributions to Hydrogeology, 8, Verlag Heinz Heise, Hannover, 1990.
- Meyboom, *Journal of Geophysical Research*, 66, 1961, p. 1203-1214.
- Moser H. and W. Rauert, *Isotopenmethoden in der Hydrologie*. Lehrbuch der Hydrologie 8, Borntraeger, Stuttgart, Berlin, 1980, p.400.
- Mazor E., *Applied chemical and isotopic groundwater hydrology*, 274 p., Open University Press, Buckingham, 1991.
- Simmers I., Hendrickx J. M. H., Krusemann G.P., Rushton K.R., *Recharge of Phreatic Aquifers in (Semi-) Arid Areas*, IAH Publications, Volume 19, A. A. Balkema, Rotterdam, 1997.

## Formulae for the Methods Appearing in Chapter 2

### Water balance methods

General:

$$\text{Input} - \text{Output} = \text{Storage}$$

### Aquifer water budget

For time period dt:

$$(IL - OL) \cdot dt + \text{Rech} \cdot A \cdot dt - Q \cdot dt = S \cdot A \cdot dh$$

<i>IL</i>	lateral inflow (m <sup>3</sup> in time dt)
<i>OL</i>	lateral outflow (m <sup>3</sup> in time dt)
<i>Rech</i>	recharge (m in time dt)
<i>Q</i>	pumping rate (m <sup>3</sup> in time dt)
<i>A</i>	area of catchment (aquifer) (m <sup>2</sup> )
<i>S</i>	storage coefficient (-)
<i>dh</i>	water table change (m, spatial average)

### Soil moisture budget

For time period dt:

$$(P - R - ET - Perc) \cdot A \cdot dt = V \cdot dq$$

<i>P</i>	precipitation (m in time dt)
<i>R</i>	runoff (m in time dt)
<i>ET</i>	evapotranspiration (m in time dt)
<i>Perc</i>	deep percolation (seepage out of lower boundary becomes recharge after delay) (m in time dt)
<i>A</i>	area (m <sup>2</sup> )
<i>V</i>	volume (m <sup>3</sup> )
<i>q</i>	soil water content (m <sup>3</sup> per m <sup>3</sup> )

### Spring or river flow recession curves

$$Q = Q_0 e^{-kt}$$

<i>Q</i>	discharge at time t (m <sup>3</sup> per time)
<i>Q<sub>0</sub></i>	discharge at time <i>T</i> * where recession starts (m <sup>3</sup> per time)
<i>T</i>	time from <i>T</i> * onward
<i>k</i>	recession constant (inverse time)

$$V = \frac{Q_0 \cdot t_1}{2.3}$$

<i>V</i>	total potential groundwater discharge (m <sup>3</sup> per time)
<i>t<sub>1</sub></i>	time within which flow decreases by a factor of 10

### Cumulative Rainfall Departure Method

$$CRD_i = \sum_{j=1}^{j=i} Rf_j - i \cdot Rf_{av} + CRD_0$$

time is divided into equal intervals, normally months

*CRD<sub>i</sub>* cumulative rainfall departure at end of i-th time interval (mm)

*CRD<sub>0</sub>* initial rainfall departure, normally set to zero

*Rf<sub>j</sub>* rainfall in the j-th interval (mm)

*Rf<sub>av</sub>* average rainfall in the interval (mm)

$$V = a \cdot CRD + b$$

*V* stored volume (m<sup>3</sup>)

*a, b* regression constants

$${}^m_n CRD_i = \frac{1}{m} \sum_{j=i-(m-1)}^i Rf_j - k \frac{1}{n} \sum_{j=i-(n-1)}^i Rf_j + CRD_{i-1}$$

**CRD** cumulative rainfall departure, taking into account the carry over from previous periods  
**m** number of months denoting the short term carry over  
**n** number of months for which the long-term reference rainfall is calculated  
**k** proportionality factor, k=1 reflecting natural conditions, k<1 pumped conditions

$$V = c + a \cdot {}^m_n CRD$$

**V** stored volume (m<sup>3</sup>)  
**c, a** regression constants

### Darcyan methods

$$v = -k \cdot \nabla h$$

**v** Darcy velocity, specific flow rate (m per time)  
**k** hydraulic conductivity (m per time)  
**h** piezometric head (m)

### Unsaturated zone Darcy law based on measurements of matrix potential

$$v = -k(\mathbf{q}) \frac{dh}{dz} \quad \text{with } \mathbf{q} = \mathbf{q}(\mathbf{y})$$

**v** Darcy velocity, specific flow rate (m per time)  
**h** piezometric head with  $h = \mathbf{y} + z$  (m)  
**y** matrix potential (m)  
**z** vertical coordinate (m)  
**q** water content (m<sup>3</sup> per m<sup>3</sup>)  
**k** hydraulic conductivity (function of saturation) (m per time)

### Saturated zone Darcy law based on pumping tests and head measurements

$$Q = A \cdot k \cdot I = b \cdot T \cdot I$$

**Q** flow rate (m<sup>3</sup> per time)  
**A** cross-sectional area (m<sup>2</sup>)  
**k** hydraulic conductivity (m per time)  
**I** hydraulic gradient (m/m)  
**b** width of aquifer (m)  
**T** transmissivity (m<sup>2</sup> per time)

### Unsaturated Zone: Richards' Equation

$$\frac{\partial \mathbf{q}}{\partial t} = \frac{\partial}{\partial z} \left( k(\mathbf{q}) \frac{\partial h}{\partial z} \right) - s(z, t)$$

**q** water content (m<sup>3</sup> per m<sup>3</sup>)  
**t** time  
**h** piezometric head with  $h = \psi + z$  (m)  
**z** vertical coordinate (m)  
**y** matrix potential (m)  
**s** sinks (extraction by roots per area) (m per time)

Further required:  
 Initial and boundary conditions  
 Functions  $k(\mathbf{q})$  and  $\mathbf{y}(\mathbf{q})$

### Numerical flow model (regional 2D)

$$\nabla(T \cdot \nabla h) + q = S \frac{\partial h}{\partial t}$$

**T** transmissivity (m<sup>2</sup> per time)  
**S** storage coefficient (-)  
**q** specific recharge rate and discharge rate (m<sup>3</sup>/m<sup>2</sup> per time)  
**h** piezometric head (m)  
**t** time

**Tracer methods: Chloride method (runoff neglected)**

$$D + P \cdot c_p = Re ch \cdot c_{Re ch}$$

$$Re ch = \frac{c_p P + D}{c_{Re ch}}$$

*P* precipitation (mm per time)

*Re ch* recharge (mm per time)

*D* dry deposition (in mg per m<sup>2</sup> and time)

*c<sub>p</sub>* concentration in precipitation (mg/l)

*c<sub>Re ch</sub>* concentration in recharging groundwater (e.g. average over profile) (mg/l)

**Tracer methods: Tritium and following**

Darcy velocity *v* (m per time)

$$v = \frac{Q}{A}$$

*Q* flow rate (m<sup>3</sup> per time)  
*A* cross-sectional area (m<sup>2</sup>)

Pore velocity: *u* (m per time)

$$u = \frac{v}{n} = \frac{L}{t}$$

*t* travel time

*L* distance travelled (m)

*n* porosity (-)



### 3 Use of Spreadsheet for Soil Water Balance Method

Philip Brunner, IHW, ETHZ, Zurich, Switzerland

A simple model for calculating the soil moisture budget in daily steps over longer periods of time is based on the concept in the following figure (Kinzelbach, 1986):

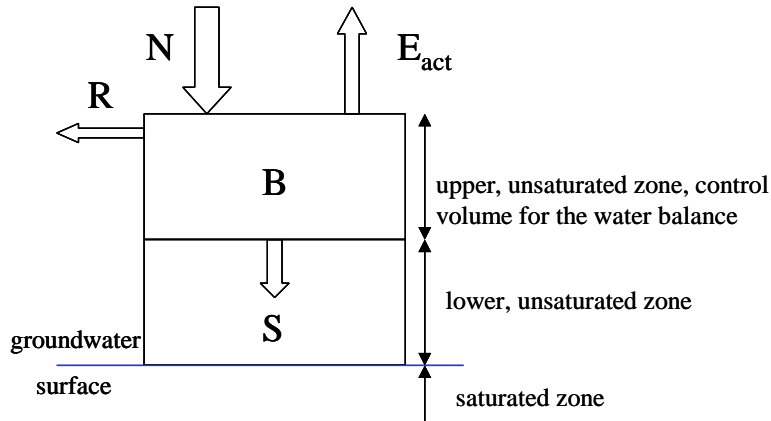


FIG. 3.1: CONCEPT OF A SOIL MOISTURE BALANCE MODEL  
 N = PRECIPITATION  
 E<sub>ACT</sub> = ACTUAL EVAPOTRANSPIRATION  
 R = SURFACE RUNOFF  
 S = DEEP PERCOLATION  
 B = SOIL MOISTURE

A column of 1 metre depth and 1m<sup>2</sup> surface area is considered. Rainfall enters through the surface and increases the soil moisture. Evaporation leaves via the surface and decreases the soil moisture. Neglecting the surface runoff (R), the water balance over the unsaturated zone for a time interval [t, t+Δt] is given by:

$$B(t + \Delta t) = B(t) + (N - E_{act} - S) * \Delta t$$

According to Blau et al. (1983), a partial percolation to the lower unsaturated zone already occurs when 70% of the soil's field capacity (F) is reached. No deep percolation takes place if the soil moisture is less than 70% of the field capacity:

$$S * \Delta t = 0 \text{ if } B(t) + (N - E_{act}) * \Delta t < 0.7 * F$$

$$S * \Delta t = 0.1 * (N - E_{act}) * \Delta t$$

$$\text{if } 0.7 * F \leq B(t) + (N - E_{act}) * \Delta t < F$$

otherwise

$$S * \Delta t = B(t) + (N - E_{act}) * \Delta t - F$$

The actual evapotranspiration (E<sub>act</sub>) depends on various parameters, including vegetation, radiation and soil type. E<sub>act</sub> can be determined using the potential evapotranspiration (E<sub>pot</sub>). When calculating the potential evapotranspiration on the basis of the Penman equation, wind speed,

relative humidity, air temperature and the global radiation are required. If no radiation data are available, it can be estimated by calculating the exo-atmospheric radiation, depending on the date and the latitude of the examined area. Using standard values for the atmospheric transmittance, the global radiation can be obtained. There are numerous approaches describing the relationship between potential and actual evapotranspiration.

Following Renger et al. (1974), the actual evapotranspiration becomes smaller than the potential as soon as the soil moisture content drops more than 30% below field capacity. Reaching this level, the actual evapotranspiration can be described with following equation:

$$E_{act} = E_{pot} * (0.188 + 2 * (B / F) - 1.2 * (B / F)^2)$$

for  $B < 0.7 * F$

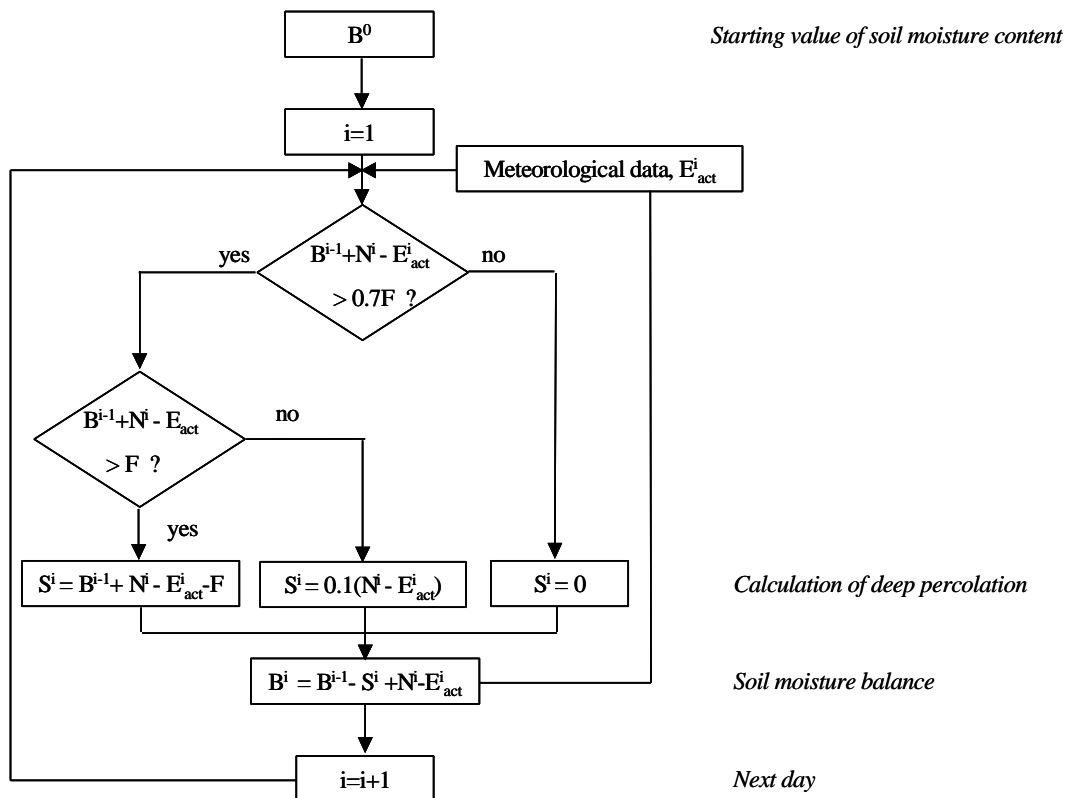
$$E_{act} = E_{pot} \text{ for } B \geq 0.7 * F$$

Note that this equation is a crude approximation, not taking into account the

effects of vegetation. The user is asked to insert a formula according to the relevant climatic and vegetative conditions. The calculation of the soil moisture budget is processed according to the scheme shown in Figure 3.2.

Starting value of soil moisture content (cell Q8).

The units in which these quantities are required are given in the spreadsheet in the accompanying CD-ROM or [www.unep.org/water/groundwater/](http://www.unep.org/water/groundwater/) under the title *soil moisture budget.xls*.



The spreadsheet carrying out these calculations requires the following input data:

- The latitude of the project area in degrees, north positive, south negative (cell A4)
- The field capacity (cell P5)
- The dates of the examined days (column A)
- Global radiation data (column F); if no radiation data are available, the global radiation is approximated in the Excel sheet
- Temperature (column G)
- Wind speed (column J)
- Relative humidity (column K)
- Precipitation (column N)

FIG. 3.2: FLOW SCHEME FOR CALCULATING THE SOIL MOISTURE BUDGET

## References

Blau R.V., Hoehn E., Werner A. and Hufschmied P., *Ermittlung der Grundwasserneubildung aus Niederschlägen*, Gas-Wasser-Abwasser, 63(1), 1983, p. 45-54.

Kinzelbach W., *Groundwater Modelling - An Introduction with Sample Programs in BASIC*, Elsevier Science Publishers, Amsterdam, 333 S, 1986.

Renger M., Strebler O. and Giesel W., *Beurteilung bodenkundlicher, kulturtechnischer und hydrologischer Fragen mit Hilfe von klimatischer Wasserbilanz und bodenphysikalischen Kennwerten*, Z. Kulturtechn, Flurbereinigung, 15, 1974, p. 148-160, 206-221, 353-366.

## 4 Chloride Method in the Unsaturated Zone

*Ibrahim Baba Goni, Dept. of Geology, University of Maiduguri, Nigeria*

### 4.1 Introduction

In homogenous unconsolidated porous media, recharging rainwater often moves through the unsaturated zone by a process similar to piston flow. Groundwater in recent and quaternary formations in many parts of the world conforms to this process, and unsaturated zones are likely to contain an accessible record of water and solute movement. It may be possible to use such records to estimate: 1) recharge rates; 2) recharge history; 3) weathering rates and geochemical processes; and 4) the movement of pollution.

The unsaturated zone may contain an archive of input to the aquifer, ranging from less than a decade to several hundreds or even thousands of years. Unconsolidated sands are developed in all climatic regions and represent a possible medium for comparative global study of environmental change. Consolidated porous media (for example, sandstones and chalk) can provide similar information, but their dual (intergranular and fracture) porosity implies that there is a greater possibility of dispersion, for example due to by-pass flow.

The use of the unsaturated zone to measure recharge started over three decades ago with the use of thermonuclear tritium as a global tracer. Since then it has been widely used in hydrology, mainly in the temperate regions and less commonly in arid regions (Edmunds and Walton, 1980; Allison and Hughes, 1978; Aranyosy and Gaye, 1992; Gaye and Edmunds, 1996) to measure recharge. Tritium may still be used in unsaturated zone recharge studies, but the peak of activity is likely to be at considerable depths in the unsaturated zone (greater than 20 metres in most lithologies). Other notable limitations to

the use of tritium are the cost and specialised sample preparation, the radioactive decay (half-life 12.3 years), the cessation of thermonuclear testing, and the loss of tritium in the vapour phase during evapotranspiration. However, where a tritium profile is obtained, its position and shape in the unsaturated zone provides convincing evidence of the extent to which 'piston displacement' occurs during recharge, as well as providing an estimate of the recharge rate.

As an alternative,  $^{36}\text{Cl}$ , produced both by cosmic bombardment and by thermonuclear testing, has been used to measure recharge in the unsaturated zone (Phillips, 1994; Cook et al., 1994). However,  $^{36}\text{Cl}$  is both difficult and expensive to apply and this has prompted the use of simple techniques, especially the use of chloride, to measure recharge. Chloride inputs from atmospheric deposition are conserved in the soil zone and concentrated due to loss of moisture by evapotranspiration. The accumulation of chloride may therefore be used as a basis for recharge estimation. Although the timing of the tritium spike is well known, the use of chloride relies on knowing the deposition flux and hence details of present and past distributions in rainfall (Edmunds and Gaye, 1994; Allison et al., 1994). Where both techniques have been used (Edmunds *et al.*, 1988), the results have generally matched very well.

To be suitable for the investigation of water and solute movement in the unsaturated zone, tracers should possess several characteristics. The most important is conservative behaviour, meaning that the tracer movement is not slowed or decreased in concentration by interaction with the solid phase and that it is not produced in the soil nor introduced by

man. The tracer's rate of introduction must be known, and it is useful if it has a simple pulse or step input function or a constant rate of input. It is also useful to have tracers that cover a range of timescales.

This paper describes the unsaturated zone chloride profile technique for the estimation of groundwater recharge, citing cases where the technique has been applied.

#### 4.2 Hypothesis for the Technique According to Edmunds et al. (1988)

The total atmospheric fallout of solutes per unit area is made up of rainfall (Fp) and

the net dry deposition (Fd). Solutes will be deposited and transported through the upper soil during the rainy season at rates depending on the rainfall intensity. These solutes will undergo concentration as a result of evapotranspiration (E). Solutes may be removed from solution by plant uptake, by mineral precipitation, or by adsorption. Similarly solutes may be released by the decay of dead plant material, by mineral dissolution, or by desorption. In the absence of knowledge of these ancillary fluxes, only those constituents for which there is no net release or storage by the soil or rock matrix may be used. Chloride is the solute that most frequently and most conveniently meets these requirements. The solute concentrations in the soils or in the upper unsaturated zone will vary seasonally or annually depending upon the intensity of the moisture flux due to the incident rainfall and

evapotranspiration. Complex movements of solutions both upwards and downwards may take place in response to water movement, which in turn depends upon the prevailing water potential gradients. A 'zero flux plane' (ZFP) exists (Wellings and Bell, 1980), which effectively separates moisture and solutes moving upwards (evapotranspiration) from that moving downwards (drainage) (Figure 4.1).

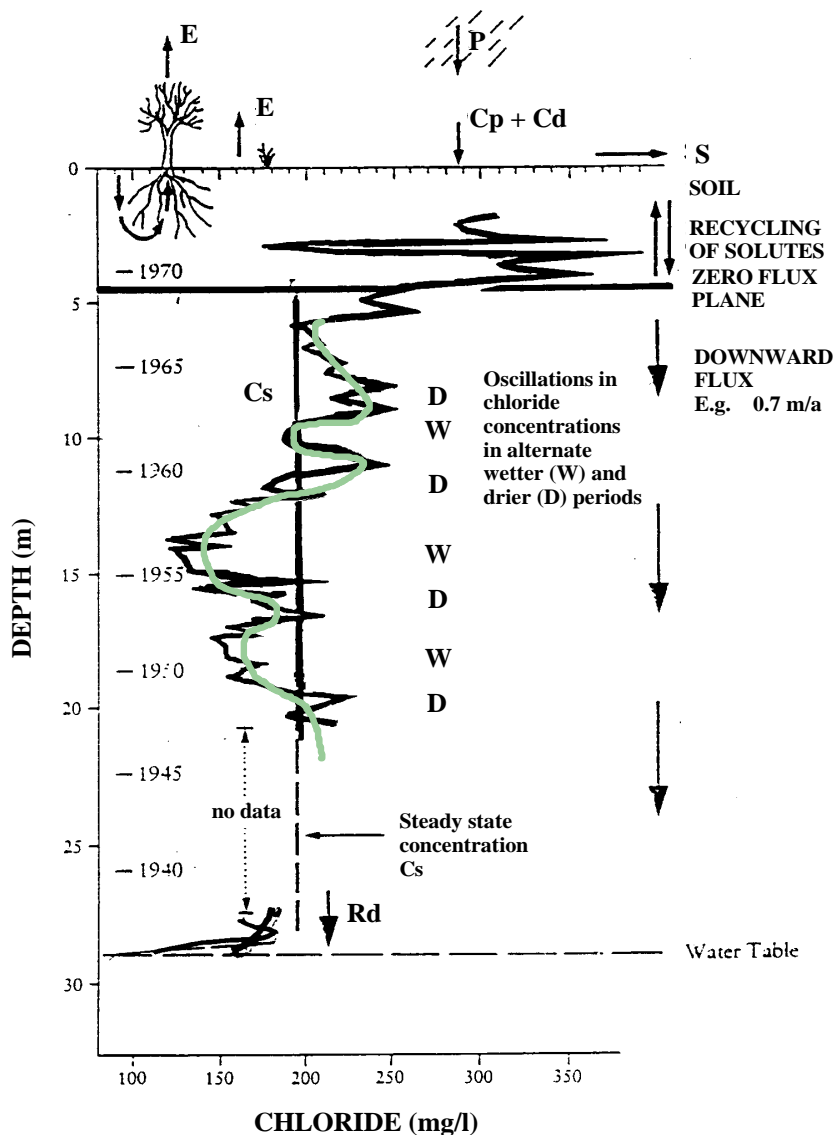


FIG. 4.1: IDEALISED SOLUTE CONCENTRATIONS DEVELOPED DURING PERCOLATION

Under conditions of recharge, a maximum depth can thus be defined at which a net, steady state, moisture and solute transfer should take place towards the water table. The amount of solute crossing the ZFP would be expected to vary in relation to antecedent rainfall over one or more seasons and some oscillation in the solute profile would then occur. A detailed discussion of the transmission of solutes across the ZFP is given in Wellings and Bell (1980). The average composition of interstitial water in this profile ( $C_s$ ) will, under steady state conditions, be proportional to the concentration factor  $P/(P-E)$ , assuming no loss of solute to minerals and that the water and 'inert' solutes are transported at the same rate.

In the steady state, the water balance equation can therefore be given as:

$$R_d = P - E - S \quad (4.1)$$

where  $R_d$  is the direct recharge flux and  $S$  is the surface runoff flux. Note that these quantities are time and space averaged. Providing surface runoff is negligible ( $S \sim 0$ ), this leads to:

$$R_d = P - E \quad (4.2)$$

Similarly the solute balance is given by:

$$F_p + F_d = F_s + F_m \quad (4.3)$$

where  $F_p$  and  $F_d$  are the average precipitation and net dry deposition fluxes (= input) respectively, and  $F_s$  and  $F_m$  are the net steady state output fluxes in the drainage water and the net flux of solute precipitated or adsorbed by minerals respectively (dissolution and desorption give a negative flux).  $F_s$  is given by the output water flux multiplied by the solute concentration (appropriately averaged), in other words:

$$F_s = R_d \times C_s \quad (4.4)$$

Where  $C_s$  is the average concentration of the reference solute in the below-ZFP

water. If we assume  $F_m = 0$ , then Equations (4.3) and (4.4) combine to give:

$$F_p + F_d = R_d \times C_s \quad (4.5)$$

Or on rearranging:

$$R_d = (F_p + F_d)/C_s = (PC_p + F_d)/C_s \quad (4.6)$$

Hence the amount of direct recharge can be estimated from a knowledge of the volume-averaged concentration of the reference solute in the rainfall ( $C_p$ ) and in the deep interstitial water ( $C_s$ ), the long term average annual precipitation ( $P$ ), and the net dry deposition flux of the reference solute ( $F_d$ ). Note that, if  $F_d = 0$ , the fraction of the rainfall contributing to direct recharge is simply given by the ratio  $C_p/C_s$ .

The use of this technique is subject to the following assumptions:

Since there is time lag in solute input to the unsaturated zone and output to the saturated zone, it must be assumed that no major climatic change has occurred over this period;

There have been no external additions, eg. fertiliser, or recent changes in atmospheric pollution;

There is no net change in storage of the 'reference' solute above or below the ZFP, either by plants or animals or by mineral precipitation/dissolution or adsorption/desorption.

Because of its usually conservative nature, chloride is most suitable and reliable as a reference solute. It is possible that only a restricted portion of the unsaturated zone profile may be usable for recharge estimation (Figure 4.2A). For example, the presence of certain lithologies, eg. residual marine bands, may release chloride. The possible development of the solute profile is summarised in Figure 4.2B. Profiles 1 and 2 represent steady state drainage under different vegetation/soil conditions in which evapotranspiration rates differ. Profiles 3 and 4 represent two possible cases in which solute compositions have

been modified by reaction and/or changes in storage. Only the upper part of profiles 3 and 4 would be of value in recharge calculations and, in certain reactive lithologies, no steady state profile may be developed at all.

Differences in solute concentration between unsaturated and saturated zones

exist because, in the latter, concentration is more likely to be modified by incoming lateral flow with higher or lower salinity. Therefore, water table samples are not very reliable for recharge estimation. However, as chloride is not lost during drainage and saturated flow, it can be used to give a minimum recharge rate at a regional scale.

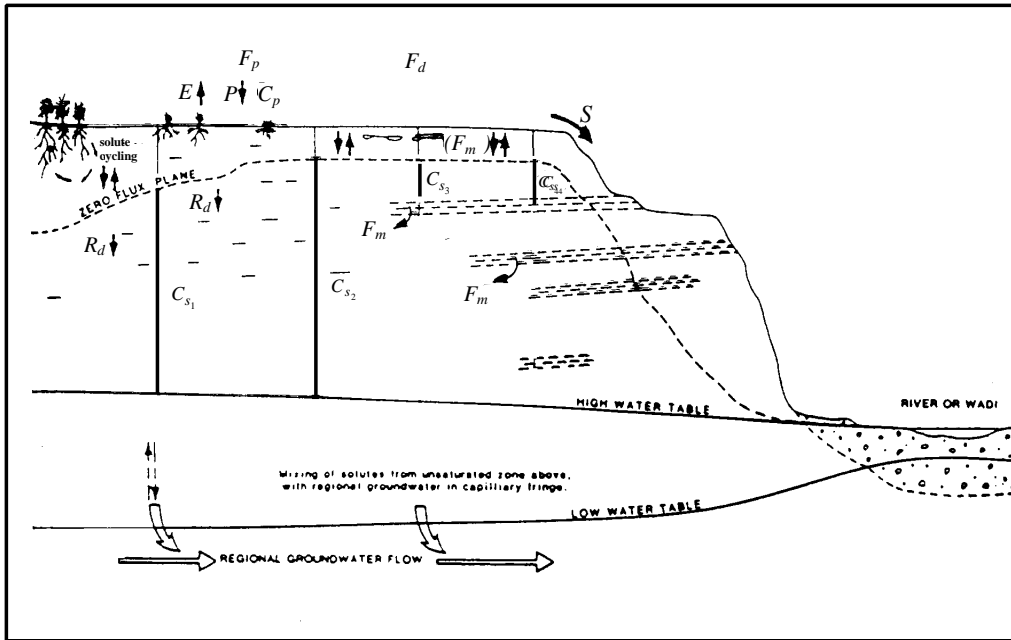


FIG. 4.2 A: SCHEMATIC REPRESENTATION OF SOLUTE MOVEMENT AND RECHARGE VIA THE UNSATURATED ZONE

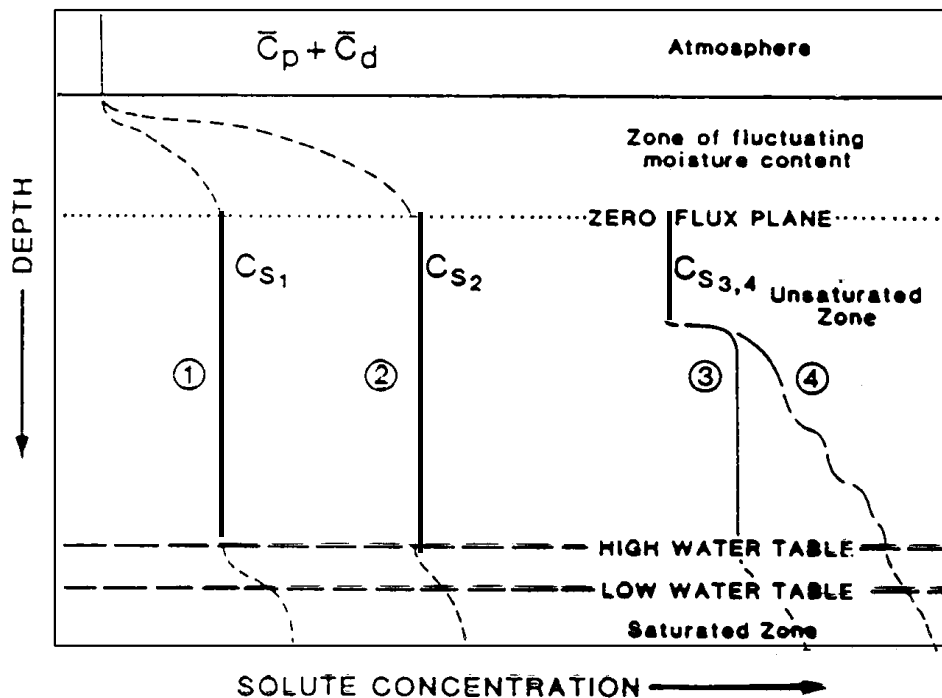


FIG. 4.2 B: CONCEPTUALISED SOLUTE CONCENTRATIONS DURING PERCOLATION, SHOWING STEADY STATE SECTION

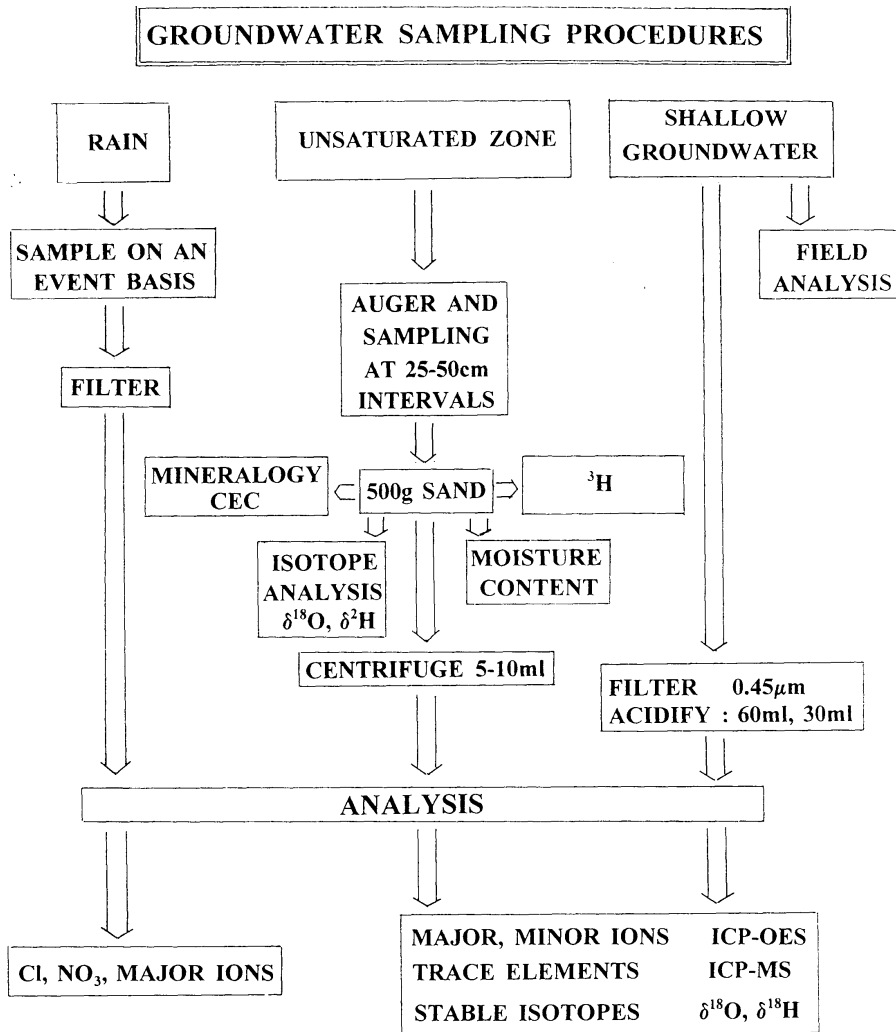


FIG. 4.3: GROUNDWATER SAMPLING PROCEDURE

### 4.3 Data Requirements

Data requirements for this technique are shown in Figure 4.3. Chloride concentration in rainfall as input must be known. An average of mean rainfall and weighted mean chloride concentrations over a minimum of three years for the area are also required.

Augering or other dry drilling techniques are used to obtain unsaturated zone soils at regular intervals. Samples over each interval are mixed and homogenised in a plastic bag and then subsampled into a tight container. Care must be taken to minimise evaporation loss in this process. Moisture content is measured gravimetrically (by weighing before and

after drying), and chloride is determined on samples obtained either by centrifugation or elutriation. Although no single method of extracting interstitial waters from porous media is suitable for all samples, centrifuge methods offer the greatest potential for the routine extraction of water for chemical analysis. The centrifuge may be used for extracting water in two ways:

- Gravity drainage, through which the water is allowed to drain freely through a porous plate supporting the sample and collected in a cup at the bottom of a specially made centrifuge tube;
- Immiscible liquid displacement, through which the excess of a dense, immiscible liquid is added to the sample and displaced water is collected after it has floated to the top. This

method is successful for most soil types, including clay soils.

In the elutriation method, 50 g samples of the moist, disaggregated sediment are dispersed and elutriated in 30 ml aliquots of distilled, demineralised water in a polypropylene beaker for at least an hour, with constant stirring until a constant conductivity is attained. The sample is then filtered through 0.45  $\mu\text{m}$  filter paper, and the filtrate used for chemical analysis. At the end of the analysis, a correction is made for the factor of dilution.

The chloride concentration in the saturated zone is very useful in a regional estimation of recharge and in understanding the mechanism of recharge – whether vertical recharge from rainfall is dominant, or lateral recharge from streams, rivers and ponds also plays an important role.

#### 4.4 Case Studies

Representative single profiles from two semi-arid regions – the Mediterranean (southern Cyprus) and West Africa (Senegal) – are shown in Figures 4.4 and 4.5. These demonstrate a strong agreement between the behaviour of chloride and other isotopes (especially those of the water molecule) in the unsaturated zone, and are significant for the validity of the assumption inherent in this technique of piston flow movement of water in the unsaturated zone. The agreement also helps to calibrate the chloride technique against known tracers (tritium).

The data from Cyprus are from recent dune sediments on the Akrotiri peninsula, where chloride is shown together with tritium profiles from the same percussion drilled borehole (Figure 4.4). These data are described in greater detail in Edmunds et al. (1988). The chloride concentrations below the zero flux plane (around 2 metres in grass vegetation) oscillate about the mean value (Cs) in the profile. These oscillations have been interpreted in terms of seasonal variations related to periods of

wet and dry years. The mean concentration has been used to give an estimate of the recharge rate of 55 mm/year, from a three-year mean rainfall concentration of 16.4 mg/l at this coastal site. The tritium profile serves to confirm the recharge rate given by chloride, the peak marking the position of the 1963 thermonuclear fallout maximum in the rain; the recharge rate obtained using the amount of moisture above the tritium peak is 53 mm/year. The shape of the tritium peak also confirms that at this site downward movement of moisture (and solute) is homogeneous with little or no by-pass flow.

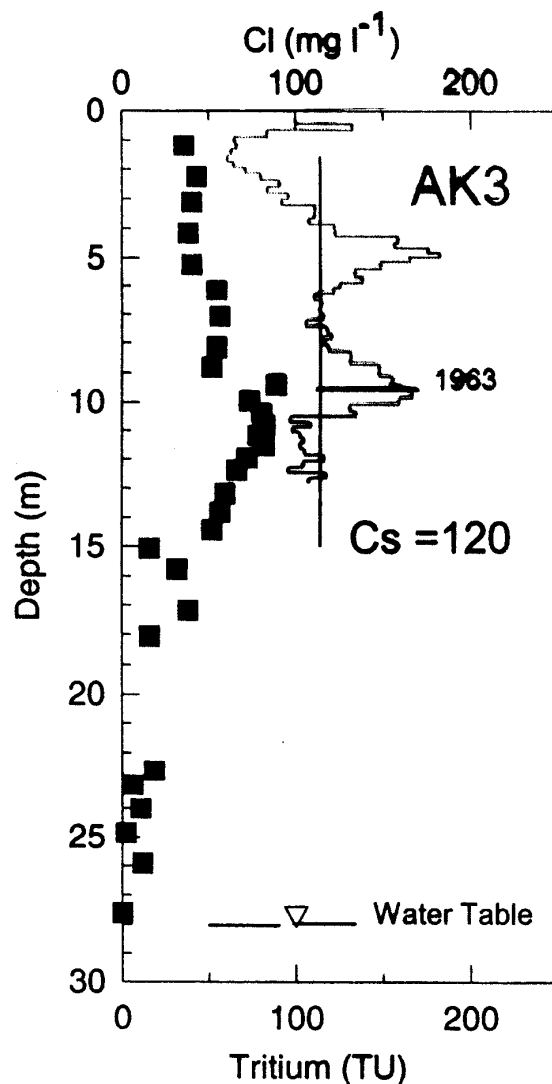


FIG. 4.4: UNSATURATED ZONE CHLORIDE AND ISOTOPE PROFILES FROM CYPRUS



The Senegal case study is another excellent example of an integrated approach to the unsaturated zone profiles study. In this case, chloride, tritium and stable isotopes were used in the same profile (Figure 4.5). (For more details, see Gaye and Edmunds (1996) and Aranyossy and Gaye (1992).) Unsaturated zone samples were obtained from Quaternary dune sands, the moisture of which was used to measure the concentration of chloride and determine the values of tritium and the stable isotopes. The mean concentration of the unsaturated zone chloride is 23.6 mg/l. With chloride in rain of 2.8 mg/l and a rainfall amount of 290 mm/year, a recharge rate of 34.4 mm/year was estimated. The oscillation of the profile indicates variable climatic conditions. The tritium peak clearly defines the 1963 fallout and demonstrates the piston flow movement of moisture in this profile. Estimation of the rate of recharge from the tritium data gives 26 mm/year. The stable isotopes have not been used to quantify recharge, but the fact that their profiles also mirror the chloride profile indicates consistency and agreement of the results obtained.

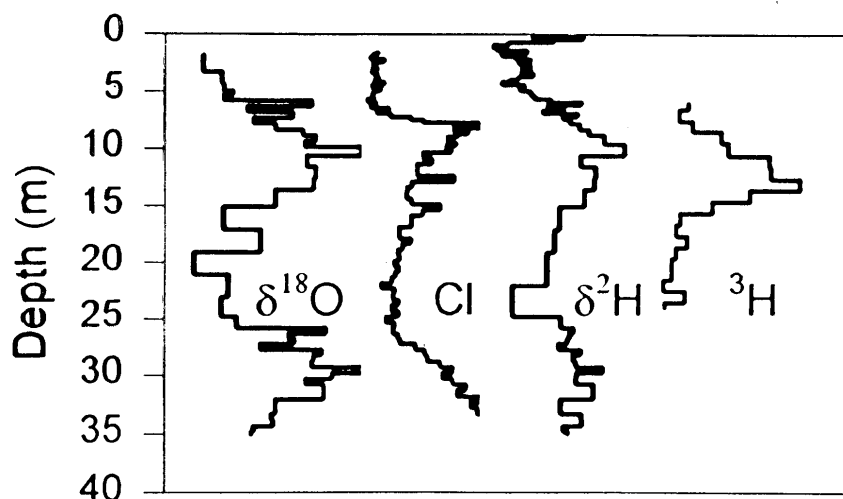


FIG. 4.5: UNSATURATED ZONE CHLORIDE AND ISOTOPES PROFILES FROM SENEGAL

Eight unsaturated zone profiles have so far been obtained in Northeast Nigeria for the

purpose of estimating recharge. The area is generally underlain by wind blown fine sands of variable thickness of 20-50 metres (Goni, 1996), which lie on top of the Chad Formation. These aeolian deposits consist of stabilised longitudinal ancient dunes mostly trending ENE-WSW and actively moving modern barchant dunes with interdunal depressions (oases). Both the ancient and modern dunes are unconsolidated, and deposited in a typical rolling form. They are composed of relatively well sorted fine to coarse grained sand.

A simple spreadsheet model has been produced that can calibrate the profile in terms of timescale represented by the chloride stored in the unsaturated zone (Cook et al., 1992). Cumulative chloride (Cl) in the profiles is proportional to time and a depositional flux measured in modern rainfall is used to provide the timescale using the moisture content and the chloride in the profiles. Modelling of the recharge history is shown for seven of the eight profiles (Figure 4.6) against the annual rainfall records of Maiduguri (1915-1999). The profiles are shown using the ratio 1/Cl; higher values therefore indicate wetter years and may directly be compared with the rainfall records. Some profiles show an excellent match with the rainfall, especially the Magumeri profile, which incidentally is the closest profile to the rainfall station (about 40 km away). There are profiles that do not match with the rainfall records.

Possible explanations for this include the variability in rainfall over the region, although more work needs to be done before reaching a conclusive explanation.

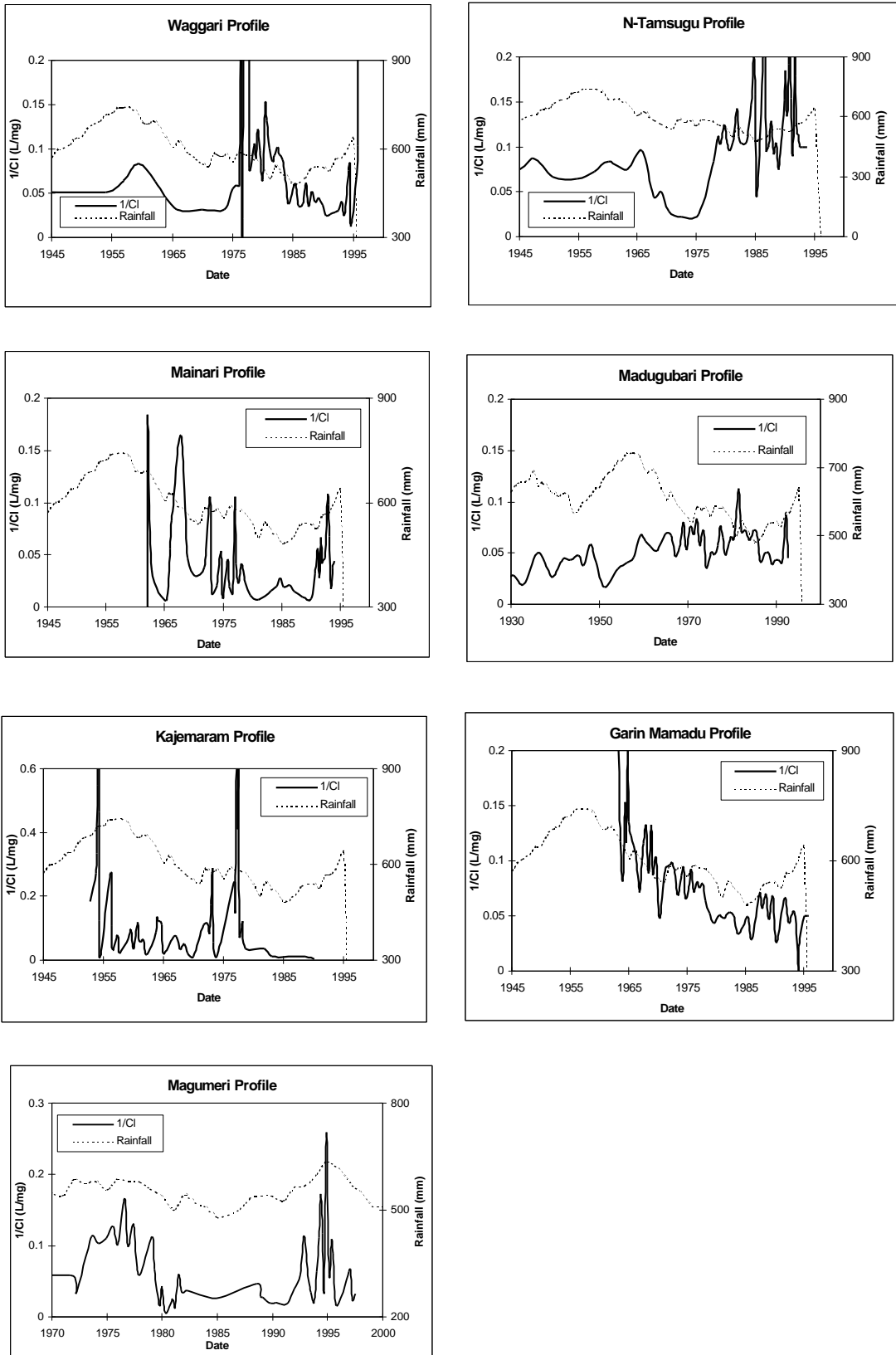


FIG. 4.6: CHLORIDE PROFILES IN NORTHEAST NIGERIA AGAINST MAIDUGURI RAINFALL USING SPREADSHEET MODEL

TABLE 4.1: UNSATURATED ZONE PROFILES AND RECHARGE ESTIMATES FROM NORTHEAST NIGERIA

Profile	Depth (m)	No. Samples (n)	Mean Cl Cs (mg/l)	Mean annual recharge Rd (mm/a)	Residence time (years)
GM 1	15.50	51	14.1	22.03	35
KA 1	14.75	50	18.3	12.32	40
MD 1	22.50	65	11.5	11.34	71
MN 1	16.50	53	41.6	19.90	32
N-TM	18.75	58	11.7	18.88	52
W-Wgg	19.25	60	18.6	20.28	42
MG	16.26	53	20.7	20.71	26

Estimated rates of recharge for the seven profiles range from 11 to 22 mm/year (Table 4.1). Using the concentration of chloride from the saturated zone of 16 mg/l, the same annual rainfall and chloride concentration in rainfall, a rate of 21 mm/year has been estimated. This shows that most of the recharge to the groundwater in the region is from rainfall, with little lateral recharge. Timescales represented by the profiles range from 22 to 71 years, resulting from textural variability.

One of the profiles in Northeast Nigeria (the MF profile) is quite distinct, having a sandy layer to a depth of 3 metres followed by a clayey layer to the total depth drilled. The discussion of this profile is thus carried out on the basis of the lithology. It also underscores the importance of the soil texture in controlling the moisture movement within the unsaturated zone.

The top three metres of the MF profile contain low concentrations of chloride and other conservative solutes – bromide and nitrate (Figure 4.7). This indicates a present day atmospheric origin of these

solutes, which are progressively washed into the profile during the subsequent rainy seasons and account for the lack of accumulation of salts on the surface. The concentrations of chloride in the upper three metres indicate a recharge rate of 14 mm/year – similar to the other profiles in the region.

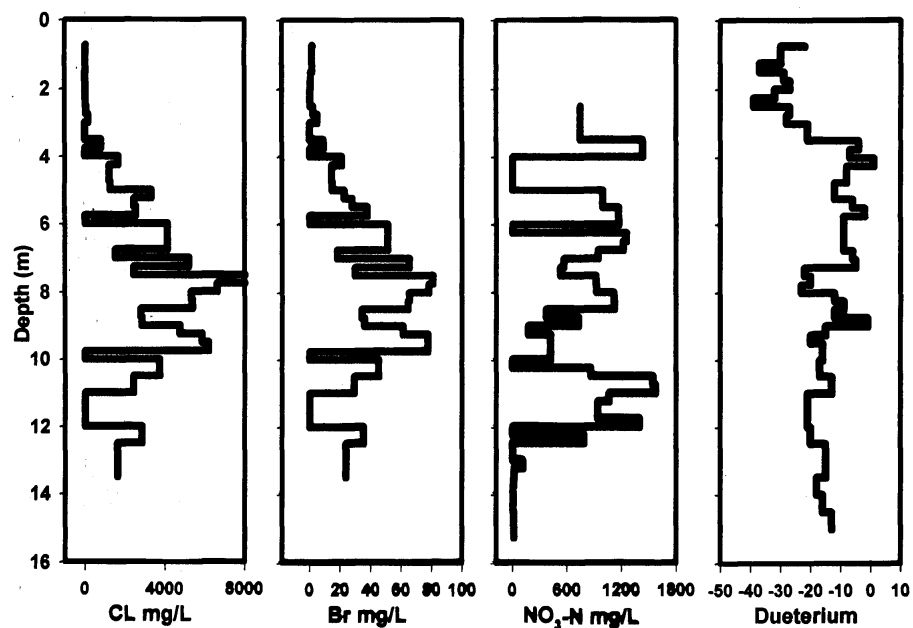


FIG. 4.7: MF UNSATURATED ZONE SOLUTES (CL, BR & NO<sub>3</sub>-N) AND DEUTERIUM PROFILES

The concentration of chloride for the lower part of the MF profile (Figure 4.7) is quite distinct and brackish with one peak at a depth of 9 metres, with chloride concentrations of up to 7000 mg/L. The lower impermeable lacustrine deposits (mainly clays) below 3 metres probably represent the former bed of Lake Chad, where little or no infiltration has been

occurring since the lake extended over this area during the mid Holocene. Schneider (1967) has mentioned the existence of large palaeolake Chad at the 320-metre level at about 6000 yr B.P. During this period it must have invaded large areas, including the area of the MF site and deposited beds that are of low permeability. The lower profile therefore consists of waters of low mobility, a partial relic of the former lake sediment pore waters.

In the MF profile (Figure 4.7), the depth distribution of deuterium clearly separates the upper 3 metres with an average  $\delta^2\text{H}$  of  $-30\text{‰}$  from the lower section with an average  $\delta^2\text{H}$  of  $-12\text{‰}$ . The fact that the lower section of the MF profile has relatively enriched deuterium and a high concentration of solutes shows that the relative evaporative enrichment is the likely control, in line with the Cl results. A small oscillation of deuterium values in the lower MF profile may indicate cycles of flooding of Lake Chad during former climatic conditions.

#### 4.5 Conclusions

In this technique manual augering is used to obtain interstitial waters from the unsaturated zone. The manual hand auger is quite a robust and effective technique in sandy and silty soils. Drilling through clay-rich sediments was also achieved, although with great difficulty (and near impossibility in thick plastic clays). The chloride profile technique is cheap and gives estimates of direct vertical recharge rates, especially in semi-arid and arid regions. It also estimates the residence times of solutes and moisture in the unsaturated zone. Where the chloride profile has been used with other isotopes ( $^3\text{H}$ ,  $^2\text{H}$ ,  $^{18}\text{O}$ , etc.), the results generally matched, indicating the broad effectiveness of this technique. To be effective for areal estimates, further methods are required to regionalise the local values given by the method. The collection of chloride contents in rainwater must be known for a

period of several years before the method can successfully be applied. It is therefore recommended to set up a regional database for West Africa.

#### References

- Allison G.B., Gee G.W. and Tyler S.W., *Vadose-zone techniques for estimating groundwater recharge in arid and semi-arid zones*, Soil Society of America Proceedings, 1994, **58**, p. 6-14.
- Allison G.B. and Hughes M.W., *The use of environmental chloride and tritium to estimate total local recharge to an unconfined aquifer*, Aust. J. Soil Res, 1978, **16**: p. 181-195.
- Aranyosy J.F. and Gaye C.B., *La recherche du pic du tritium thermonucléaire en zone non-saturée profonde sous climat semi-aride pour la mesure de recharge des nappes: première application au Sahel*. C.R.Acad. Sci. Paris, 1992, **315** (ser.II): p. 637-643.
- Cook P.G., Edmunds W.M. and Gaye C.B., *Estimating palaeorecharge and palaeoclimate from unsaturated zone profiles*, Water Resource. Res, 1992, **28**: p. 2721-2731.
- Edmunds W.M., Darling W.G. and Kinniburgh D.G., *Solute profile techniques for recharge estimation in semi-arid and arid terrain*. In: Simmers, I. (ed.) *Estimation of natural groundwater recharge*, D. Reidel Publishing, 1988, p. 139-157.
- Edmunds W.M. and Gaye C.B., *Estimating the spatial variability of groundwater recharge in the Sahel using chloride*, Journal of Hydrology, 1994, **156**: p. 47-59.
- Edmunds W.M. and Walton N.R.G., *A geochemical and isotopic approach to recharge evaluation in semi-arid zones- past and present*, 1980. In *Application of Isotopic techniques in Arid Zone Hydrogeology*, Proc. Advisory Group Meeting, Vienna, IAEA, 1978, p. 47-68.
- Edmunds W.M. and Wright E.P., *Groundwater recharge and palaeoclimate in the Sirte and Kufra basin, Libya*. Journal of Hydrology, 1979, **40**, p. 215-241.
- Gaye C.B. and Edmunds W.M., *Inter comparison between physical, geochemical and isotopic methods for estimating groundwater recharge in north western Senegal*, Environmental geology, 1996, **27**, p. 246-251.
- Goni I.B., *Hydrogeological investigation of the aeolian phreatic aquifer of northern Yobe State, NE Nigeria*, Borno J. Geology, vol.1, No1, 1996, p. 59-70.
- Kiniburgh D.G. and Miles D.L., *Extraction and chemical analysis of interstitial water from soils and rock*, Environ. Sci. Technol, 1983, **17**, p. 362-368.
- Phillips F.M., *Environmental tracers for water movement in desert soils of the American southwest*. Soil Sci. Soc. Am. J., 1994, **58**, p. 15-24.
- Schneider J.L., *Evolution du dernier lacustre et peuplements pré-historiques aux Bas-Pays du Tchad*. Bull. ASEQUA, Dakar, 1967, 14-15: p. 18-23.
- Wellings S.R. and Bell J.P., *Movement of water and nitrate in the unsaturated zone of Upper Chalk near Winchester, Hants, England*. J. Hydrol., 1980, **48**: p. 119-136.

## 5 Groundwater Dating using Environmental Tracers and Black Box Models

*Urs Beyerle, University of Berne, Berne, Switzerland*

### 5.1 Introduction

The age of groundwater – the water’s age or its residence time – is defined as the time elapsed since the water parcel had its last contact with the atmosphere. Water in shallow aquifers can range from days to decades in age, while old groundwater may have residence times from  $10^3$  to  $10^7$  years. Groundwater renewal or recharge is unknown for most aquifers, or associated with great uncertainties as a result of the difficulties in its quantification.

### 5.2 Environmental Tracers

A number of environmental tracers carry information on the age of groundwater. Tritium ( $^3\text{H}$ ) and rare gas tracers such as  $^3\text{He}$ ,  $^{85}\text{Kr}$  and chlorofluorocarbons (CFCs) are used to date groundwater with an age of less than 50 years. For groundwater with ages of a few hundred years, the most useful age indicator is  $^{39}\text{Ar}$ , whereas  $^{14}\text{C}$ ,  $^{36}\text{Cl}$  and radiogenically produced noble gases are normally used to date even older groundwater (Table 5.1).

In industrial areas groundwater is often over saturated with CFCs, indicating either

higher atmospheric concentrations due to the proximity to emission sites or direct input of chlorinated substances into the groundwater flow, eg. from dump sites. In addition, there are indications that CFCs decompose under anoxic conditions (especially CFC-11). Also, a retardation due to adsorption on organic aquifer matter may occur. In general, CFC dating is recommended for water age analysis in sandy aquifers far away from industry.

In principle three different kinds of dating methods have been identified. The first set of methods utilises the fact that certain atmospheric trace components, such as CFCs,  $^{85}\text{Kr}$  and tritium ( $^3\text{H}$ ), have a time dependent input function (Figure 5.1). Thus their atmospheric concentrations are not constant but vary over the past 50 years.

Industrial production introduces most of the CFCs, especially CFC-11 and CFC-12, to the atmosphere, while  $^{85}\text{Kr}$  is released from nuclear reprocessing plants. In the early 1960s, nuclear bomb tests in the atmosphere increased the global tritium inventory by 2 to 3 orders of magnitude. Tritium concentrations have steadily decreased since the nuclear testing of the '60s, but up to today the tritium activity in meteoric water is commonly one order of magnitude greater than the expected

TABLE 5.1: TIMESCALES OF VARIOUS TRACER-BASED DATING METHODS

Tracer	Time scale	Source	Detection
$^{222}\text{Rn}$	days – weeks	$^{238}\text{U}$	$\alpha$ -counting
$^{37}\text{Ar}$	Months	spallation (S)	Low level counting (LLC)
$^3\text{H}$ - $^3\text{He}$	months – decades	S, nuclear bomb testing	Mass spectrometry (MS)
$^{85}\text{Kr}$	months – decades	nuclear power techniques	LLC
CFCs	months – decades	industry	Gas chromatography (GC)
$^{39}\text{Ar}$	$10^2$ years	S	LLC
$^{14}\text{C}$	$10^3$ - $10^4$ years	S	LLC, MS
$^4\text{He}_{\text{rad}}$	$10^2$ - $10^7$ years	U, Th	MS
$^{40}\text{Ar}_{\text{rad}}$	$10^4$ - $10^7$ years	$^{40}\text{K}$	MS

background level due to tritium production by cosmic rays. If a given water parcel is in gas exchange with the atmosphere at time  $t$ , the actual concentration in the water reflects the atmospheric partial gas pressure at this time (Henry's law). As the atmospheric partial pressure of the tracer changes over time, the concentrations of successive water parcels introduced into the aquifer change as well. If mixing processes can be neglected, the concentration of a water parcel basically reflects the time elapsed between the last gas exchange and the sampling date.

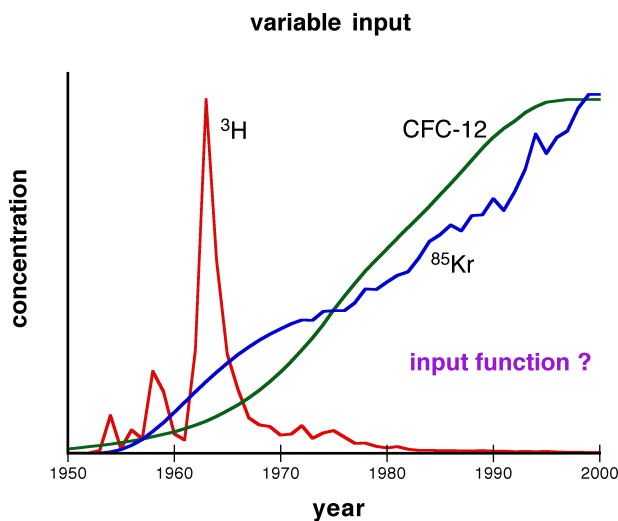


FIG. 5.1: TRACERS WITH VARIABLE INPUT FUNCTIONS

The second set of methods relates mainly to radioactive decay, eg.  $^{14}\text{C}$  decays with a half-life of 5,730 years and  $^{39}\text{Ar}$  decays with a half-life of 269 years. In order to calculate a groundwater residence time using a radioactive tracer, its initial input concentration should be known (Figure 5.2). In contrast to  $^3\text{H}$  and  $^{85}\text{Kr}$ , the fluctuations of atmospheric concentrations of  $^{14}\text{C}$  and  $^{39}\text{Ar}$  are small and their initial concentrations can be estimated.

FIG. 5.2: RADIOACTIVE TRACER CONCENTRATION AS A FUNCTION OF TIME

**mother - daughter isotope**

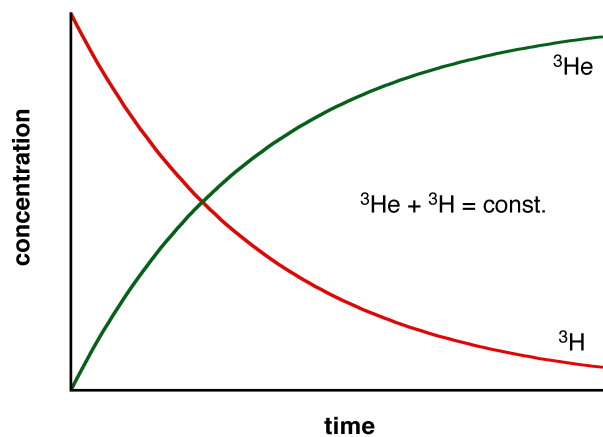
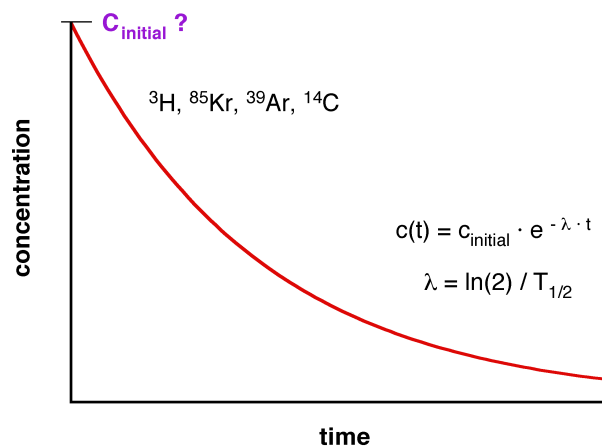


FIG. 5.3: THE 'MOTHER-DAUGHTER ISOTOPES'  $^3\text{H}$  AND  $^3\text{He}$

In a closed system, in which all isotopic changes are purely the result of radioactive decay, the ratio of the stable daughter ( $^3\text{He}$ ) and radioactive mother ( $^3\text{H}$ ) is a direct measure for the time elapsed since the water was last in contact with the atmosphere. As this so-called  $^3\text{H}$ - $^3\text{He}$  Dating relies only on the radioactive decay, it does not depend on the knowledge of the atmospheric tritium input function (Figure 5.3).

The third set of groundwater dating methods relies on a continuous increase of a particular tracer. For example, the stable noble gas isotopes  $^4\text{He}$  and  $^{40}\text{Ar}$  have the

**radioactive decay**



potential to be used for dating very old groundwater. The production of these radiogenic noble gas isotopes is controlled by long-lived nuclides in minerals and rocks, such as U, Th isotopes and  $^{40}\text{K}$ . Groundwater ages derived from  $^4\text{He}$  or  $^{40}\text{Ar}$  concentrations are based on the assumption that the radiogenic noble gases accumulate continuously during groundwater flow (Figure 5.4). The radiogenic noble gases are expected either to diffuse out of minerals within the aquifer or to emanate from deeper strata into the aquifer. In order to obtain groundwater residence times, the respective accumulation rates must be known. They can, however, only be crudely estimated.

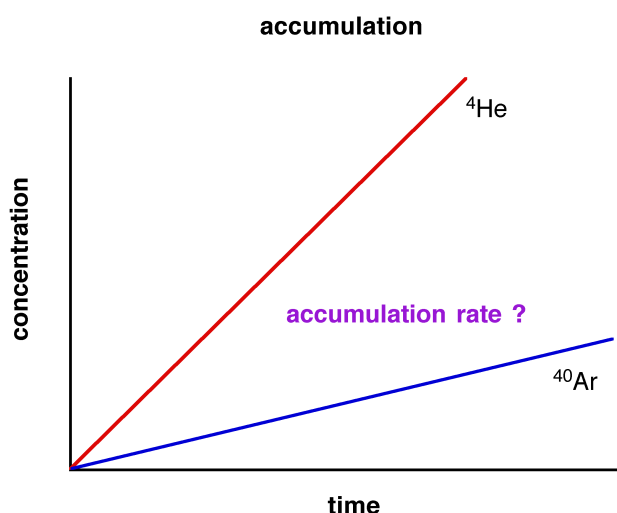


FIG. 5.4: GROUNDWATER DATING WITH RADIOGENIC NOBLE GAS ISOTOPES

The combination of dating methods restricts the mean residence time of an aquifer to a much greater extent than the use of only one technique. Therefore mixing processes in the groundwater can be addressed if several tracers are available. Since the tracers used are both chemically and biologically inert, they take part in the physical groundwater processes only. They can serve as a scale marker for other substances, which undergo additional chemical and biological alterations in the aquifer.

The various dating methods exploit different ways of tracer introduction into the groundwater body. CFCs and rare gas isotopes are dissolved as gases in the water, whereas tritium is bound in water molecules as  $^1\text{H}^3\text{HO}$  and is therefore part of the moving water. CFCs and rare gases are therefore influenced by gas exchange to a much greater degree than tritium. In addition, gas tracers only measure the time since the groundwater reached the saturated zone (ie. the start of its complete isolation from the atmosphere), whereas tritium travels as a component of the water molecule through the unsaturated zone.

TABLE 5.2: EXAMPLE OF A GROUNDWATER SAMPLE TAKEN IN JANUARY 2000

Tracer	Concentration	Mean residence time (see Fig. 5.5)
CFC-12	$390 \pm 10$ pptV <sup>(1)</sup>	15 years
$^{85}\text{Kr}$	$25.7 \pm 1.1$ dpm/cc Kr <sup>(2)</sup>	12 years
$^3\text{H}$	$18.8 \pm 0.9$ TU <sup>(3)</sup>	46, 42, 39, 21, 19 years

(1) pptV = parts CFC per trillion ( $10^{12}$ ) parts air by volume. An atmospheric CFC-12 concentration of 390 pptV corresponds to 243 pg/kg (=  $10^{-12}$ g/kg) measured in groundwater (at T = 20°C, atmospheric pressure = 954 mbar)

(2) dpm/cc Kr = decays per minute per  $\text{cm}^3$  STP Kr

(3) TU = Tritium Unit = 1TU =  $^3\text{H}/^1\text{H}$  ratio of  $10^{-18}$

### 5.3 Testing the Methods

In Table 5.2, an example of a groundwater sample is given. The sample was taken in January 2000 and concentrations of CFC-12,  $^{85}\text{Kr}$  and  $^3\text{H}$  were measured. Using the measured tracer data and assuming piston flow conditions, mean groundwater residence times were calculated (Table 5.2 and Figure 5.5). The piston flow assumption implies that the water parcel basically remained unmixed after its entry into the aquifer, and preserved its original identity.

For CFC-12 the measured concentration is given as the equivalent atmospheric concentration linked to it by Henry's law. Assuming no decomposition of CFC-12 (ie. no anoxic conditions), all we have to do is to compare at what time in the past the atmospheric concentration was equal to the measured concentration. We draw a horizontal line at the equivalent atmospheric value of the sample and look for the intersection with the input curve. As the input curve is monotonically increasing, there is only a single intersection.

In the cases of krypton and tritium, we do the same but take into account the decay. This requires a backward extrapolation from the concentration still remaining in 2000 to the original value. As the plots are semi-logarithmic we go back in a straight line, the slope of which is given by the decay constant. At the intersection with the input curve, we find a possible candidate for the time at which the parcel started its travel. Note that for tritium, several solutions are feasible as the input curve is not monotonic.

### 5.4 The Box Model Approach

The simplest interpretation of environmental tracer data is based on the box model approach (Fig. 5.6).

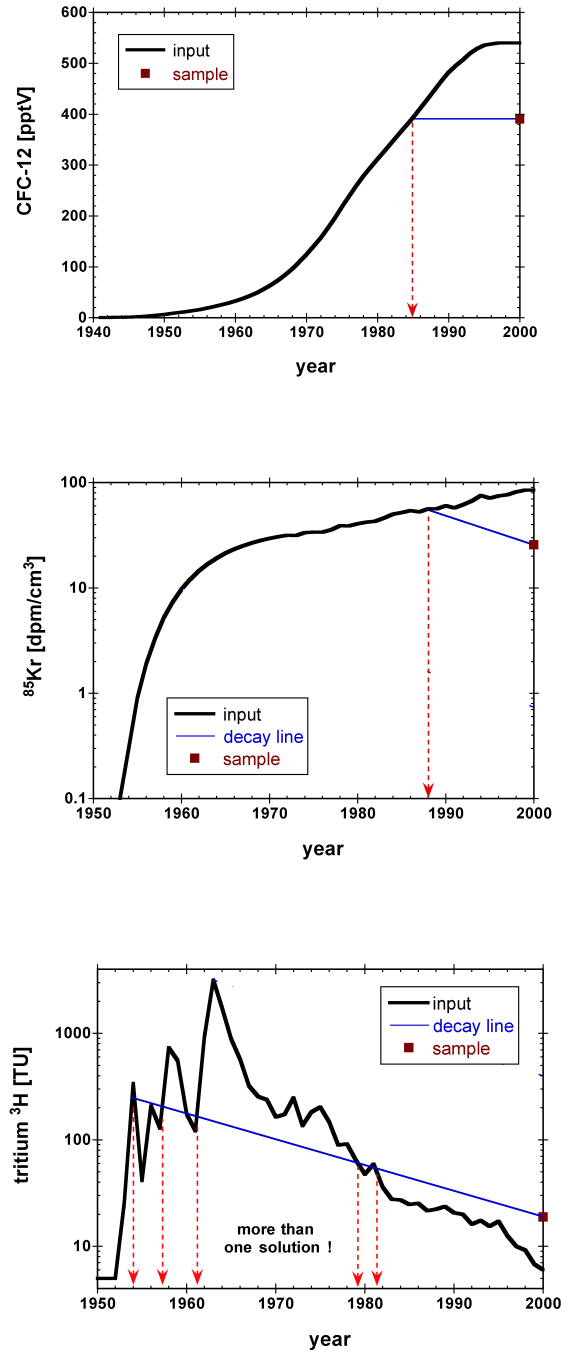


FIG. 5.5: CALCULATING MEAN GROUNDWATER RESIDENCE TIMES USING CFC-12,  $^{85}\text{KR}$ , AND  $^3\text{H}$  (ASSUMING PISTON FLOW CONDITIONS)

For a given tracer input function, a box model calculates the convoluted theoretical output depending on:

- the transfer function (either for a piston flow, an exponential or a dispersion model, see Fig. 5.7a-c); and



- the parameters of this particular transfer function (mean residence time  $\tau$ , dispersion parameter  $\delta$ ).

By comparing observed and calculated concentrations, one can identify these parameters.

**"black box" or "lumped parameter" models**

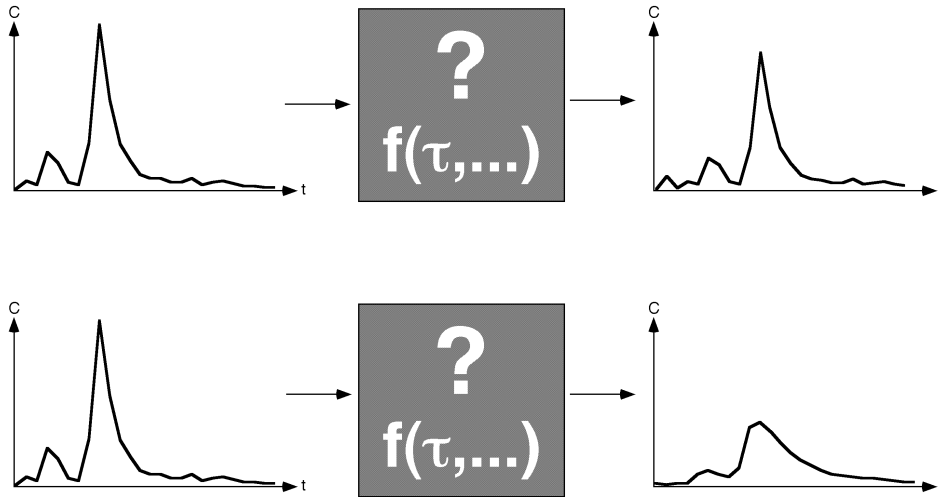


FIG. 5.6: SCHEMATIC PRINCIPLE OF BOX MODELS

**Piston Flow Model (PM)**

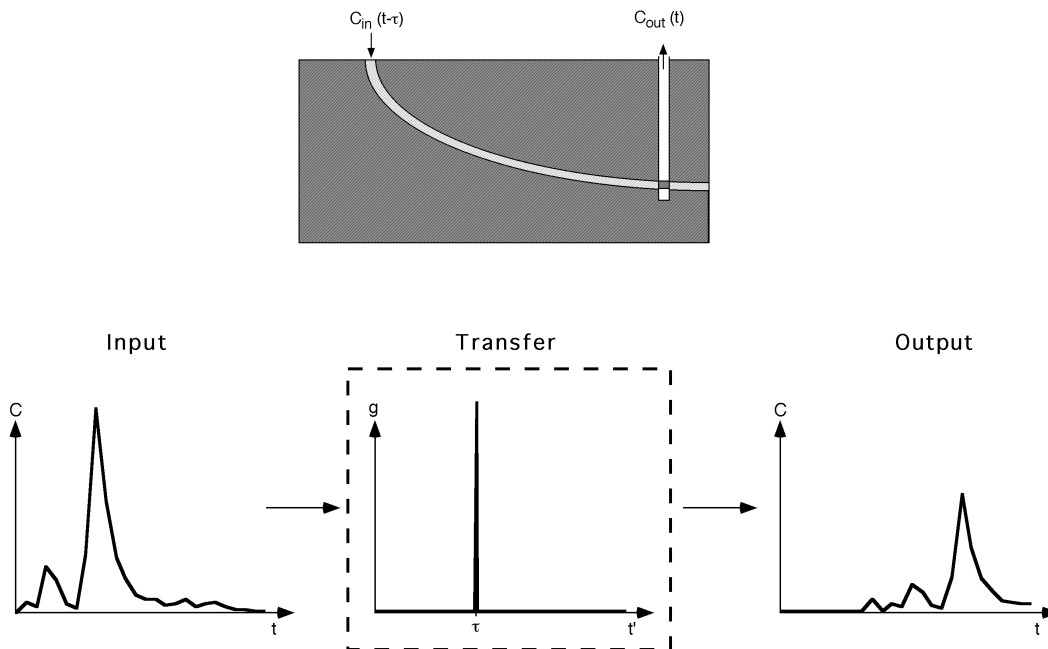


FIG. 5.7 A: PISTON FLOW MODEL AND CORRESPONDING TRANSFER FUNCTION (THE OUTPUT CONCENTRATION IS ADDITIONALLY INFLUENCED BY RADIOACTIVE DECAY)

### Exponential Model (EM)

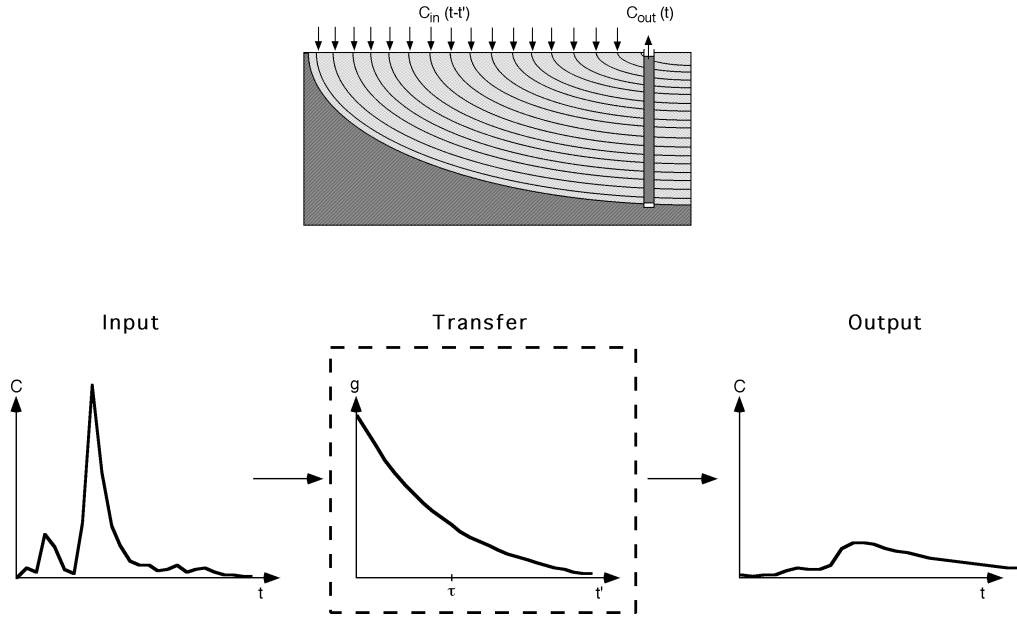


FIG. 5.7 B: EXPONENTIAL MODEL AND CORRESPONDING TRANSFER FUNCTION (THE OUTPUT CONCENTRATION IS ADDITIONALLY INFLUENCED BY RADIOACTIVE DECAY)

### Dispersion Model (DM)

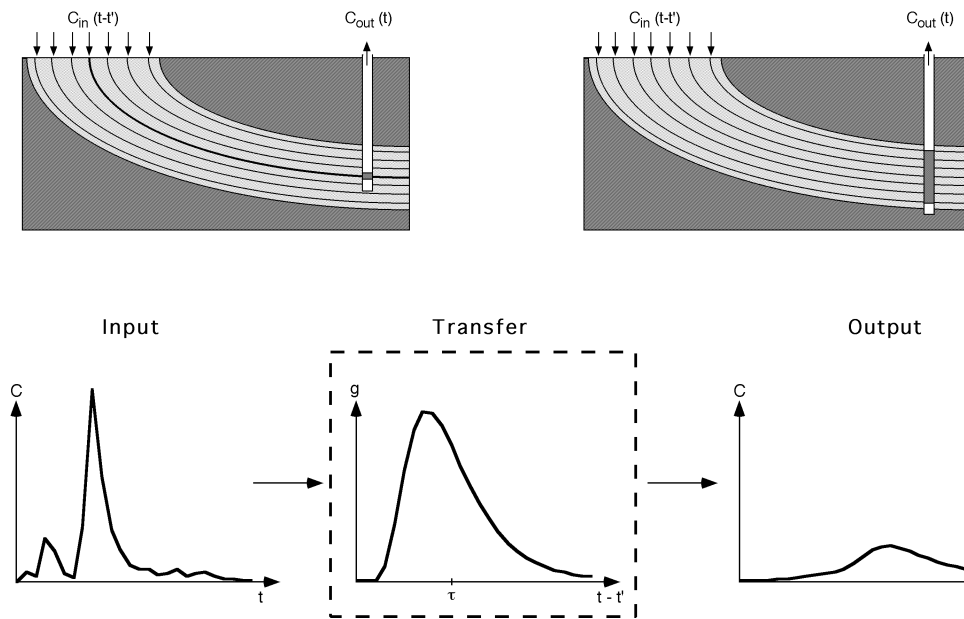


FIG. 5.7 C: DISPERSION MODEL AND CORRESPONDING TRANSFER FUNCTION (THE OUTPUT CONCENTRATION IS ADDITIONALLY INFLUENCED BY RADIOACTIVE DECAY)

The mathematical basis of box models, as well as a spreadsheet for working with them, are provided in the next chapter.

The choice of the box model should respect the general aquifer situation, as characterised by the figures above.

## 6 Use of Spreadsheets for Age Determination with Tritium and CFCs

*Kai Zoellmann, ETHZ, Zurich, Switzerland*

*Werner Aeschbach, EAWAG, Zurich, Switzerland*

The box model approach described in Chapter 5 is implemented with an Excel Workbook, provided as *Boxmodel\_V3.xls* in the CD-ROM accompanying this report (or [www.unep.org/water/groundwater/](http://www.unep.org/water/groundwater/)). This spreadsheet software allows for the interpretation of environmental tracer data taken from groundwater samples ( $^3\text{H}$ ,  $^3\text{He}_{\text{tri}}$ ,  $^{85}\text{Kr}$  and CFCs), based on the box model approach (see Figure 5.6).

The use of the Excel Workbook in the interpretation of measured concentrations of environmental tracers in wells is described below. All you need to run it is a computer equipped with standard Excel software. A simplification used in this Workbook is that the input data are assumed to be constant over the year, which could be unrealistic for systems with very small residence times.

The Workbook consists of 17 separate sheets (INTERFACE, Tr in Graph, CFC in Graph, Kr in Graph, Transfer Exp Graph, Transfer Disp Graph, Output Graph, Tau Graph, Tritium Input, CFC Input,  $^{85}\text{Kr}$  Input, Piston Flow Model, Exponential Model, Dispersion Model, Output (tau), Output (t) and CFC Converter) which are described in detail below.

### Interface

The Interface sheet contains the following input parameters that can be changed by the user (black bordered cells):

*Model Code* - Enter the desired transfer function (pm, exp or dm) that is used for convoluting the input function (pm = Piston Flow Model, exp =

Exponential Model, dm = Dispersion Model).

*Tau [a]* - Enter a value for the mean residence time in years for the pm, exp or dm model. The Transfer Function Graph is calculated for this value only. In the Tau Graph, on the other hand, the output concentrations for the required year are shown as function of Tau for a whole range of Tau values.

*Tau Step [a]* - This value determines the step width for the Tau Graph in years.

*Delta [a]* - Dispersion Parameter for the Dispersion Model. This value has no effect if the Piston Flow or the Exponential Model is used.

*Tritium Factor* - Defines a scaling factor for the tritium input function.

*Tracer Code* - Enter a code (tr, cfc, kr, he) for the desired tracer:

tr = tritium; cfc = chlorofluorocarbons CFC-11 or CFC-12 depending on the input function provided (see sheet CFC Input); kr =  $^{85}\text{Kr}$ ; and he = tritiogenic  $^3\text{He}$  (i.e.  $^3\text{He}$  which originates from the tritium decay during groundwater flow).

*Year of Observation* - This value determines the time for which the concentrations are calculated (Tau Graph). This should be the year of your tracer measurement.

*C\_obs* - Enter here the measured tracer concentrations in the same units as the corresponding input function. These values are not needed for the

computation of the other graphs. But the comparison of those lines with the computed graphs allows the age dating, and they are therefore drawn in the same graph as the computed output. Note that the measured CFC concentration of the groundwater sample [eg. in pg/kg] must be transformed to pptV according to the solubility, which depends on the groundwater temperature and the altitude of the recharge area (see CFC Converter sheet) as the input function is given in these units.

### **Tr in Graph, CFC in Graph, Kr in Graph**

These three sheets show the input functions of tritium ( $^3\text{H}$ ), CFC-12 or CFC-11, and  $^{85}\text{Kr}$  derived from the Tritium Input, CFC Input and  $^{85}\text{Kr}$  Input data sheets.

### **Transfer Exp Graph, Transfer Disp Graph**

These sheets show transfer functions based on the parameters (Tau and Delta) given in the User Interface Sheet.

### **Output Graph**

This sheet shows the resulting output concentration for the desired transfer function as a function of time  $t$  (year of observation) for the given parameters Tau and Delta. The intersection of this curve with the observed concentration (red line) should be in agreement with the chosen residence time (Tau). You can obtain this agreement iteratively. But you can also proceed to the Tau Graph for a more convenient method.

### **Tau Graph (=Residence Time Graph)**

This sheet shows the resulting output concentration for the desired transfer function as a function of the parameter Tau (and implicitly Delta) for a given time  $t$  (the year of observation). The intersection of this curve with the observed concentration (red line) identifies the 'correct' mean residence time (Tau).

### **Tritium Input, CFC Input, $^{85}\text{Kr}$ Input**

These three sheets contain the data of the input functions of tritium ( $^3\text{H}$ ), CFC-12 or CFC-11, and  $^{85}\text{Kr}$ . The tritium concentrations were derived from monthly averaged precipitation and have to be adapted to your local tritium input function. They are given in Tritium Units (TU). The CFC data are given in pptV and are derived from global CFC measurements. If necessary they will have to be adjusted to local conditions. The  $^{85}\text{Kr}$  input function can be strongly dependent upon the investigated area and should be modified if local atmospheric concentrations are known.

### **Piston Flow Model, Exponential Model, Dispersion Model, Output(tau) and Output(t)**

These five sheets contain the calculation algorithms providing the data for the different graphs. The user should not change them.

### **CFC Converter**

This sheet allows one to convert the measured CFC concentration in pg/kg in water to the corresponding atmospheric concentration in pptV.

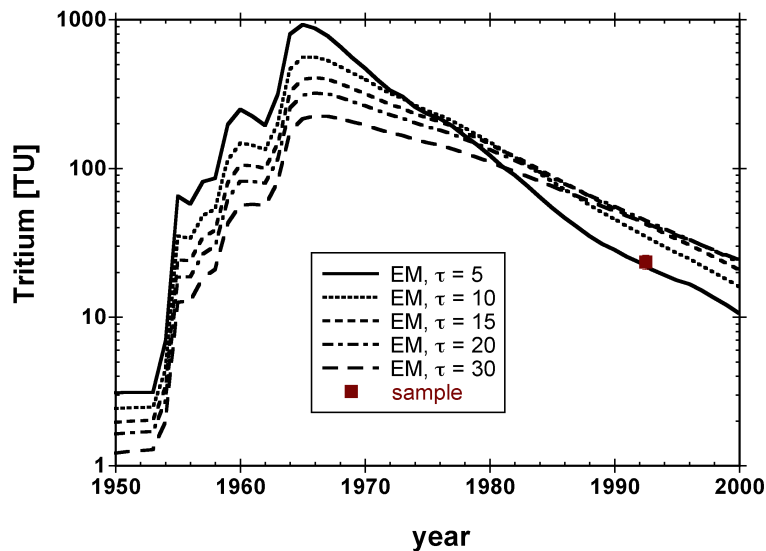
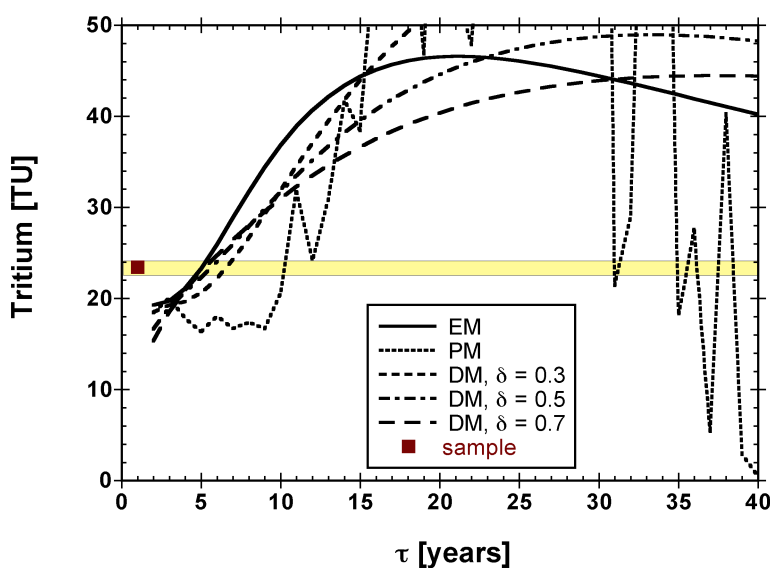


FIG. 6.1: OUTPUT CONCENTRATION OF TRITIUM AS A FUNCTION OF TIME FOR DIFFERENT EXPONENTIAL MODELS ( $\tau$  = MEAN RESIDENCE TIME)

### 6.1 Example

As an example, the Output Graph and the Tau Graph for different models (EM, PM, DM) and parameters ( $\tau$ ,  $\delta$ ) are calculated (Figures 6.1 and 6.2) and compared with a sample taken in June 1992 ( $^3\text{H} = 23.4$  TU).

FIG. 6.2: OUTPUT CONCENTRATION AS A FUNCTION OF THE MEAN RESIDENCE TIME  $\tau$  FOR DIFFERENT MODELS AND PARAMETERS (EM = EXPONENTIAL MODEL, PM = PISTON FLOW MODEL, DM = DISPERSION MODEL,  $\delta$  = DISPERSION PARAMETER)



The Output Graph shows a strong agreement of the exponential model (EM) with the measured sample in the case of a mean residence time  $\tau = 5$  years (Figure 6.1). The same result can be obtained from Figure 6.2 (intersection at  $\tau = 5$  years between measured concentration and calculated Tau Output function of the exponential model).

If the investigated aquifer is best described with a piston flow model, a realistic residence time would be around 10 years or between 31 and 38 years (Figure 6.2). Assuming a dispersion model (DM with  $\delta$  between 0.3 and 0.7), a realistic mean residence time would be close to the one calculated using the exponential model, i.e. about 5-7 years.

In general, with one tracer measurement only one parameter can be determined (normally  $\tau$ ). Therefore the type of the model (PM, EM or DM) and eventually additional parameters (eg.  $\delta$ ) should be known. This will require that a conceptual model for the investigated aquifer already exists.

To determine the type of model and additional parameters using tracer data only, either a time series (1 tracer, 1 site, additional measurements over time) or additional tracers (1 site, 1 time, additional tracers such as CFC or  $^{85}\text{Kr}$ ) will be needed. A third possibility would be tracer data from

additional boreholes (1 tracer, 1 time, more sites). But in such cases, black-box models are less suitable because the residence time ( $\tau$ ) has to be determined for each borehole separately. Therefore a better approach

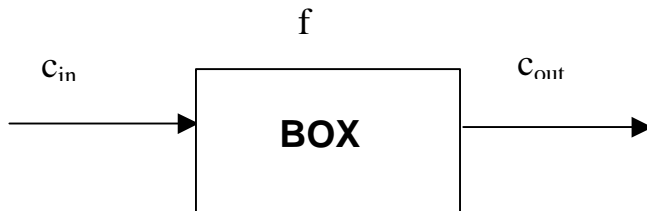
would be to use a numerical flow and transport model. This applies also for strongly time varying recharge rates or cases in which a single average recharge rate is inadequate.

## 6.2 Mathematics of the Black Box Model Approach

Principle: The input signal  $c_{in}(t')$  is convoluted with a transfer function  $f(t,t')$  to yield the output signal  $c_{out}(t)$ .

Assumptions:

- the system is linear;
- with a steady state in its flow properties  $f(t,t') = f(t-t')$ .



$$c_{out}(t) = \int_{-\infty}^t c_{in}(t') \cdot f(t-t') dt'$$

### Plugflow model

$$f(t-t') = \delta(t-t'-\tau)$$

$$c_{out}(t) = \int_{-\infty}^t c_{in}(t') \cdot f(t-t') dt' = c_{in}(t-\tau)$$

### Exponential Model

$$f(t-t') = \frac{1}{\tau} \cdot \text{Exp}\left[-\frac{t-t'}{\tau}\right]$$

By including (radioactive) decay, we obtain:

$$c_{out}(t) = \int_{-\infty}^t c_{in}(t') \cdot \text{Exp}[-\lambda \cdot (t-t')] \cdot \frac{1}{\tau} \cdot \text{Exp}\left[-\frac{t-t'}{\tau}\right] dt'$$

If  $c_{in}(t) = \text{const on } [t', t'+1]$  (Yearly Input Data), the integral can be converted into a sum:

$$\Rightarrow c_{out}(t) = \sum_{t'=-\infty}^{t-1} c_{in}(t') \cdot \frac{1}{\tau} \cdot \int_{t'}^{t'+1} \text{Exp}\left[-\left(\frac{1}{\tau} + \lambda\right) \cdot (t-t'')\right] dt''$$

$$c_{out}(t) = \sum_{t'=-\infty}^{t-1} c_{in}(t') \cdot \frac{1}{t} \cdot \frac{1}{\frac{1}{t} + I} \left\{ \text{Exp} \left[ - \left( \frac{1}{t} + I \right) \cdot (t - t') \right] \right\}_{t'}^{t'+1}$$

The latter equation can be solved for  $\tau$  (iteratively or graphically).

### Dispersion Model

$$f(t-t') = \frac{1/t}{\sqrt{4pd \frac{t-t'}{t}}} \cdot \frac{1}{t-t'} \cdot \text{Exp} \left[ - \frac{\left( 1 - \frac{t-t'}{t} \right)^2}{4d \frac{t-t'}{t}} \right]$$

The convolution yields:

$$c_{out}(t) = \int_{-\infty}^t c_{in}(t') \cdot \text{Exp} \left[ - I t \cdot \frac{t-t'}{t} \right] \cdot \frac{1/t}{\sqrt{4pd}} \cdot \left( \frac{t-t'}{t} \right)^{\frac{3}{2}} \cdot \text{Exp} \left[ - \frac{\left( 1 - \frac{t-t'}{t} \right)^2}{4d \frac{t-t'}{t}} \right] dt'$$

If  $c_{in}(t) = \text{const on } [t', t'+1]$  (Yearly Input Data), the integral can be converted into a sum:

$$c_{out}(t) = \frac{1}{t} \cdot \frac{1}{\sqrt{4pd}} \cdot \sum_{t'=-\infty}^{t-1} c_{in}(t') \cdot \int_{t'}^{t'+1} \left( \frac{t-t''}{t} \right)^{\frac{3}{2}} \cdot \text{Exp} \left[ - \left( I t + \frac{1}{4d} \right) \cdot \left( \frac{t-t''}{t} \right) - \left( \frac{1}{4d} \right) \cdot \left( \frac{t-t''}{t} \right)^{-1} + \frac{1}{2d} \right] dt''$$

with the substitutions:

$$a = I t + \frac{1}{4d}$$

$$b = \frac{1}{4d}$$

$$x = \frac{t-t''}{t}$$

$$x_1 = \frac{t-t'}{t}$$

$$x_2 = \frac{t-t'-1}{t}$$

$$c_{out}(t) = \frac{1}{\sqrt{4pd}} \cdot \text{Exp} \left[ \frac{1}{2d} \right] \cdot \sum_{t'=-\infty}^{t-1} c_{in}(t') \cdot \int_{x_2}^{x_1} x^{-\frac{3}{2}} \cdot \text{Exp} \left[ - a x - \frac{b}{x} \right] dx$$

$$= \frac{1}{4} \cdot \frac{\text{Exp}\left[\frac{1}{2d}\right]}{\sqrt{bd}} \cdot \sum_{t'=-\infty}^{t-1} c_{in}(t') \cdot \left\{ \text{Exp}[2\sqrt{ab}] \cdot \text{Erf}\left[\sqrt{a} \cdot x + \frac{\sqrt{b}}{x}\right] - \text{Exp}[-2\sqrt{ab}] \cdot \text{Erf}\left[\sqrt{a} \cdot x - \frac{\sqrt{b}}{x}\right] \right\}_{\sqrt{x_1}}^{\sqrt{x_2}}$$

with  $\text{Erf}[y] = \frac{2}{\sqrt{p}} \int_0^y \text{Exp}(-t^2) dt$

The Boxmodel\_V3.xls Excel Workbook does not use this closed solution as the calculation accuracy of Excel is not sufficient to deal with the Erf-Functions.

The integral is solved numerically for each year by numerical integration of the previous integral expression instead.



## 7 Groundwater Dating by $^{14}\text{C}$

Joerg Rueedi, University of Berne, Berne, Switzerland

### 7.1 Description of the Method

$^{14}\text{C}$  is a radioactive isotope of carbon with a half life ( $T_{1/2}$ ) of 5,730 years. Its activity follows from the equation:

$$A(t) = A_0 * e^{-\lambda * t}$$

or

$$T = -\ln(A(t)/A_0) * 1/\lambda$$

where  $\lambda = \ln(2)/T_{1/2}$  and  $A_0$  is the activity at time zero (Figure 7.1).

#### $^{14}\text{C}$ in the atmosphere

$^{14}\text{C}$  has been used for groundwater dating since the 1950s. To use  $^{14}\text{C}$  for this purpose, one has to properly correct the measured data because of the manifold processes occurring during groundwater evolution. The  $^{14}\text{C}$  concentrations in the atmosphere have been measured since

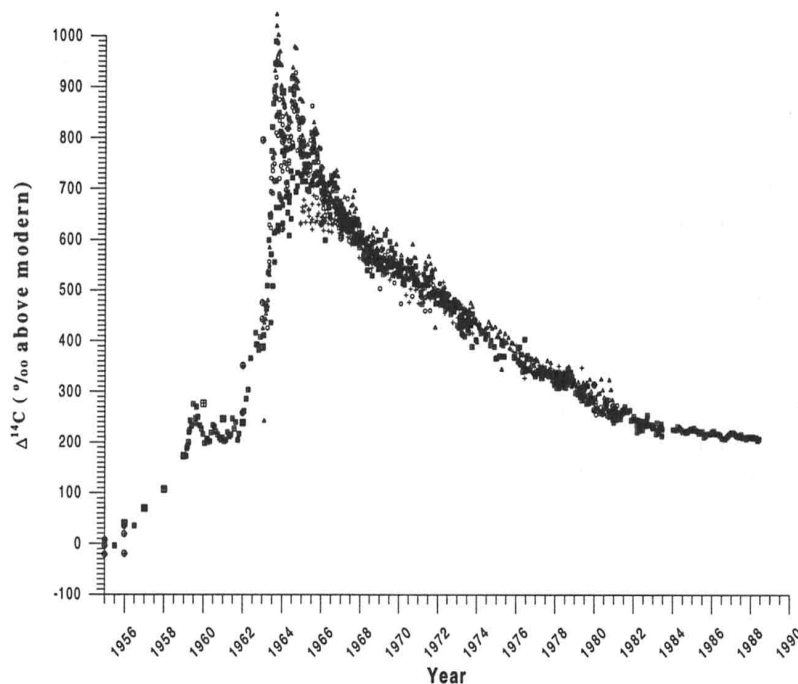


FIG. 7.2: ATMOSPHERIC CONCENTRATION OF  $^{14}\text{C}$  (CLARK & FRITZ, 1997)

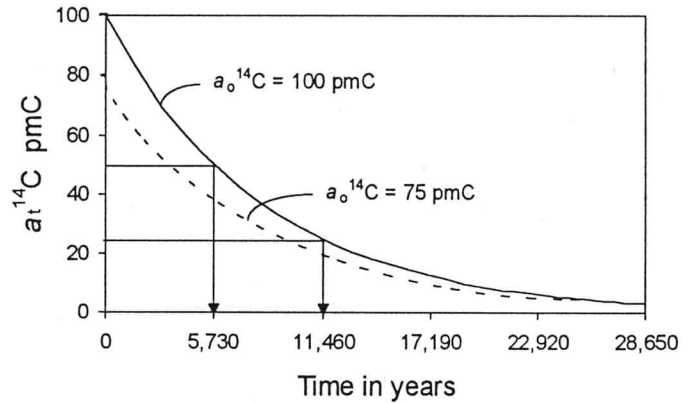


FIG. 7.1:  $^{14}\text{C}$  DECAY AND ACTIVITY AT TIME ZERO (CLARK & FRITZ, 1997)

1959 (Levin, 1980), and can be inferred for years before that time using tree ring (Pearson et al., 1986), coral (Bard et al., 1993) and ice core records (Lal & Peters, 1967; Baumgartner et al., 1998) to up to 50 kyBP (BP = Before Present) (see Figure 7.3). The atmospheric concentration results

from the equilibrium between  $^{14}\text{C}$  production in the atmosphere due to direct spallation and the reaction  $^{14}\text{N}$  (n, p) $^{14}\text{C}$  and the natural decay of  $^{14}\text{C}$  isotopes ( $T_{1/2} = 5,730$  y). As can be seen in Figure 7.2, an abrupt increase occurred during superficial nuclear tests.

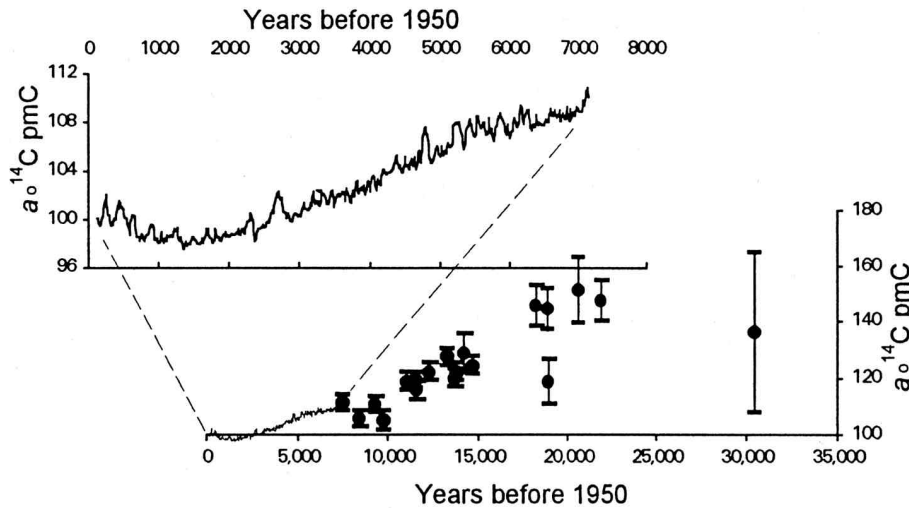


FIG. 7.3: ATMOSPHERIC  $^{14}\text{C}$  EXTENDED BY TREE RINGS AND SHALLOW MARINE CORALS (CLARK & FRITZ, 1997)

Three different notations for  $^{14}\text{C}$  have been identified:

$$\Delta^{14}\text{C} (\%) = 0.9500 * \text{activity OXI (1950)} = 13.56 \text{ dpm/gC} = 100 \text{ pmC}$$

$$\delta^{13}\text{C} (\text{OXI}) = -19.3 \text{ ‰PDB}$$

OXI (oxalic acid I) is the most common standard used in  $^{14}\text{C}$  measurements, although the following alternative standards also exist:

- NOX:  $100 \text{ pmC} = 0.7459 * \text{activity NOX (1950)}^1$ ;
- ANU sucrose;
- Chinese sugar carbon;
- Russian benzene.

TABLE 7.1: BUNSEN COEFFICIENT OF  $\text{CO}_2$  IN L GAS/L  $\text{H}_2\text{O}$

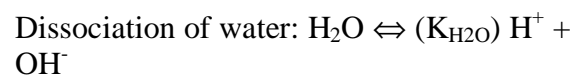
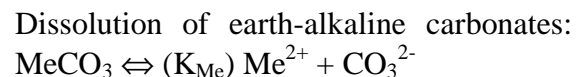
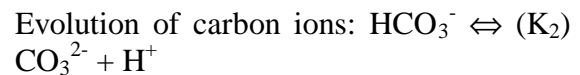
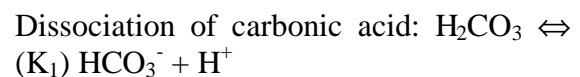
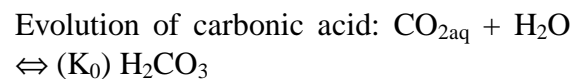
Temperature	b
0	1.7163
10	1.1887
20	0.8704
24	0.7814
28	0.7034
30	0.6678
40	0.5020
50	0.3719
60	0.2747

<sup>1</sup> pmC = percent modern Carbon.

**Introduction of  $^{14}\text{C}$  to groundwater**  
 $\text{CO}_2$  from the atmosphere passes through the unsaturated soil zone and enters the groundwater following Henry's Law:

$$\text{CO}_{2\text{aq}} = \text{pCO}_{2(\text{g})} * \beta (\text{CO}_2) / (\rho_{\text{H}_2\text{O}} * \text{p}_{\text{atm}})$$

where  $\text{pCO}_{2(\text{g})}$  is the partial pressure of  $\text{CO}_2$  of soil air being in contact with the groundwater surface,  $\text{CO}_{2\text{aq}}$  is the dissolved carbon dioxide in L/kg $\text{H}_2\text{O}$ , and  $\beta$  is the Bunsen coefficient in L gas/L  $\text{H}_2\text{O}$ . The partial pressure of  $\text{CO}_2$  is usually higher in soil air than in the atmosphere because of root respiration. During transport of the water package, the following reactions will tend to find an equilibrium between the different species of carbon.



These five reactions define the so-called 'carbonic acid equilibrium'. The reaction constants depend upon temperature and can be calculated with the formulae devised by Langmuir (1971):

$$\text{Log } K = a + b/T + c \cdot T$$

constant	A	B	C
K <sub>0</sub>	-13.417	2229.6	0.01422
K <sub>1</sub>	14.8435	-3404.71	-0.03279
K <sub>2</sub>	6.498	-2902.39	-0.02379
K <sub>Ca2+</sub>	13.870	-3059.0	-0.04035

Depending on the pH of the solution, dissolved carbon can be found in different species. Figure 7.4 shows the different carbon species in dependence of the pH (at 25°C).

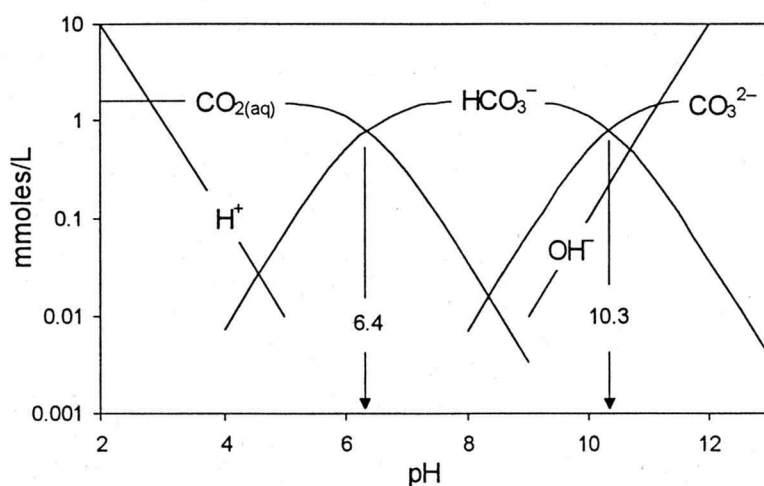


FIG. 7.4: DEPENDENCE OF CARBONIC ACID EQUILIBRIUM ON PH (CLARK & FRITZ, 1997)

Although the above reactions will essentially define the system, the following reactions may alter the carbon balance and lead to errors in <sup>14</sup>C interpretation:

- Weathering of silicates (Vogel & Ehhalt, 1963);
- Dissolution of carbonates due to humic acids (Vogel & Ehhalt, 1963);
- Decomposition of organic material ( $\Rightarrow$  CO<sub>2</sub>, CH<sub>4</sub>) (Brinkmann et al., 1959; Pearson & Hanshaw, 1970);
- Reduction of nitrate and decomposition of organic material (Sander, 1980);
- Reduction of sulfate (Pearson & Hanshaw, 1970).

To find out whether the solution is saturated with respect to a certain mineral, one can calculate the mineral saturation index SI, which is defined as follows:

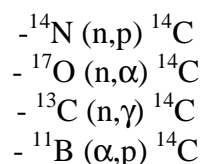
$$SI = \log (IAP / K)$$

where K defines an ion activity (concentration) at equilibrium and IAP the corresponding one found in the solution. As long as IAP is less than K, the solution is undersaturated, leading to SI < 0.

The USGS programmes NETPATH or PHREEQ-C (in the accompanying CD-ROM or [www.unep.org/water/groundwater/](http://www.unep.org/water/groundwater/)) will calculate the saturation indices routinely. The programmes will not run if the pH and the temperature are not defined.

In addition to chemical interaction of water with rock, <sup>14</sup>C can be produced underground due to the following

neutron and  $\alpha$  reactions:



For most aquifers of sandstone or carbonates, this production is negligible compared to the errors of the models. On the other hand, <sup>14</sup>C production in igneous rocks may reach the order of a few pmC.

## 7.2 Interpretation of <sup>13</sup>C Results

### notation

Isotope concentrations in water are usually measured relative to the most abundant

isotope of a certain element compared to the ratio of a defined standard.

$$\delta = [(R_x - R_{St}) / R_{St}] * 1000 \text{ ‰}$$

where:  $R_x = (^{13}\text{C}/^{12}\text{C}, ^2\text{H}/^1\text{H}, \dots)$  sample  
 $R_{St} = (^{13}\text{C}/^{12}\text{C}, ^2\text{H}/^1\text{H}, \dots)$  standard

For  $^{13}\text{C}$  measurements the PDB standard is used normally.

### Isotope fractionation

When incomplete reactions or phase transitions occur in nature, isotope fractionation will alter the isotope ratios of the different species taking part in the reaction. This fractionation depends upon temperature. The usual notations for the separation factors are either  $\alpha$  (-) or  $\epsilon$  (‰), where  $\alpha = 1 + \epsilon/1000$  or

$$\epsilon_{1,2} = (\alpha_{1,2} - 1) * 1000 = (R_1/R_2 - 1) * 1000 \cong \delta_1 - \delta_2$$

The temperature dependence of the fractionation factors was determined by different authors. Recommended values can be taken from the table below.

Reaction	$\epsilon$ [‰]
$\text{CO}_{2g} - \text{CO}_{2aq}$	$-373 / T + 0.19$
$\text{CO}_{2g} - \text{HCO}_3^-$	$-9483 / T + 23.89$
Calcite - $\text{HCO}_3^-$	$-4232 / T + 15.1$

After Craig (1954), the fractionation factor for  $^{14}\text{C}$  is twice the fractionation factor for  $^{13}\text{C}$ . A more recent estimate of this fractionation factor is:  $^{14}\epsilon_{1,2} = 2.3 * ^{13}\epsilon_{1,2}$

### Composition of inorganic carbon sources

Inorganic carbon dissolved in water usually reveals a typical isotope composition for different sources of carbon. The following table contains the most common sources of carbon in groundwater.

Source	$\delta^{13}\text{C}$ range (‰)	Literature
Atmosphere	-9.8 to -7.1	Esser, 1975
C-3 plants (humid climate)	-33 to -22	Bender, 1971
C-4 plants (arid climate)	-20 to -10	Bender, 1971
CAM plants	-31 to -11	Deines, 1980
Volcanic $\text{CO}_2$	-8 to 0	Puchelt & Hubberten, 1980
$\text{CH}_4$	-76 to -21	Deines, 1980
Carbonates:		
Of marine origin	-3 to +3	Craig, 1953
Of terrestrial origin	-19 to -4	Baertschi, 1957
$\text{HCO}_3^-$ in sea water	+1 to +2.5	Mook, 1968

### Calculation of $\delta^{13}\text{C}$ in water samples

The  $\delta^{13}\text{C}$  value of dissolved carbon is defined by two possible boundary conditions:

1.) An **open system**, in which water is in close contact with the  $\text{CO}_2$  source (atmosphere, volcano, etc.). The consequence is that the partial pressure of  $\text{CO}_2$  does not decrease under  $\text{CO}_2$  dissolution. In other words, the  $\text{CO}_2$  reservoir is assumed to be of infinite volume. If the solution is in contact with calcite, for example, it will be dissolved until saturation occurs. The saturation therefore mainly depends on the partial pressure of  $\text{CO}_2$ .

$$\delta = 1/\text{TDIC} * [\text{CO}_{2aq} * (\delta_g - \epsilon_{g,aq}) + \text{HCO}_3^- * (\delta_g - \epsilon_{g,\text{HCO}_3^-})]$$

2.) A **closed system**, in which the partial pressure of  $\text{CO}_2$  is decreasing due to dissolution, as there is no contact with a large  $\text{CO}_2$  reservoir. Thus the following dissolution of calcite will define the concentrations of different species in the equilibrium.

$$\delta = 1/\text{TDIC} * [\text{CO}_{2aq} * \delta_g + 0.5 * \text{HCO}_3^- * (\delta_g + \delta_s)]$$

When sources other than calcite and gaseous CO<sub>2</sub> take part in the carbon balance (cation exchange), or reactions occur that change the pH or the temperature, δ<sup>13</sup>C values are close to zero and A<sub>0</sub> reaches 0 too. In such cases, it is impossible to calculate a <sup>14</sup>C age.

### 7.3 <sup>14</sup>C and <sup>13</sup>C Sampling and Measurement

#### Measurement techniques

There are three different measurement techniques available:

- 1.) **AMS (acceleration mass spectrometer) or S-AMS (small version at ETH Zurich)** with a lower limit of ± 0.1 pmC for AMS and ± 0.3 pmC for S-AMS. The amount of sample needed is of the order of 1 litre of water or a few mg of carbon. This method directly measures the <sup>14</sup>C/<sup>12</sup>C ratio.
- 2.) **Fluid scintillation counters:** the carbon from the sample is transformed into a fluid (benzene), which is filled into the counters. The detection limit of this technique is about 0.1 pmC with a sample volume of 5 g of carbon. Thus large volume samples are needed for this technique.
- 3.) **Proportional counters:** the carbon from the sample has to be filled into copper or quartz tubes (as CH<sub>4</sub> or CO<sub>2</sub>) with a volume of 500-1,000 cm<sup>3</sup>. The β-decay can then be counted in the laboratory at voltages of the order of 4000V. A minimum sample size of 0.7 g carbon leads to a detection limit of 0.1 pmC. This method is used at the University of Bern to measure samples from Niger.

The easiest way to sample large water volumes is to precipitate dissolved carbon in the field. The precipitate can then be taken away easily. When planning a sampling campaign, one has to take into

account the intended measurement technique. In this respect, it is a great advantage if the alkalinity of the water is already known.

#### <sup>14</sup>C Sampling (carbon precipitation)

Depending upon the TDIC of the water and the intended measurement technique, one has to take more or less water in the field and to determine its alkalinity and pH through titration or direct measurement. With these two values, one will be able to calculate the amount of reagents necessary for the two following steps:

**First step:** Fix all dissolved carbon in the form CO<sub>3</sub><sup>2-</sup>, raising the pH above 10 with a strong base (NaOH). The pH can be tested with pH paper or pH meter. Make sure you avoid air contact, which will lead to air CO<sub>2</sub> dissolution and therefore contamination by modern <sup>14</sup>C.

**Second Step:** Add the calculated amount of precipitation reagents (BaCl<sub>2</sub> \* 2H<sub>2</sub>O). The Ba<sup>2+</sup> in the resulting solution will capture the CO<sub>3</sub><sup>2-</sup>, forming an insoluble phase. This process can be supported by flocculation reagents, which will accelerate the precipitation process. The precipitate will be captured in the sampling bottle, while the remaining 'carbon free' water will be spilled.

The pH will stay above 10. The precipitation vessels have to be sealed against the atmosphere. (see open and closed conditions!) We want to have closed conditions without any carbon sources from the atmosphere. When precipitation time is too short the process will be incomplete and fractionation will occur.

#### <sup>13</sup>C Sampling

Due to possible and often observed fractionation during sampling and laboratory preparation of <sup>14</sup>C samples, separate samples for <sup>13</sup>C measurement have to be taken in the field. To avoid sample contamination, it is recommended to use sealed bottles. Contamination can be

caused by CO<sub>2</sub> exchange with the atmosphere or by biogenic reactions. Two sampling techniques can be used:

**First technique:** Using a strong base (NaOH) to fix carbon and suppress biological activity. Advantage: No additional chemicals are needed for fieldwork. Disadvantage: High pH may 'suck in' atmospheric CO<sub>2</sub>.

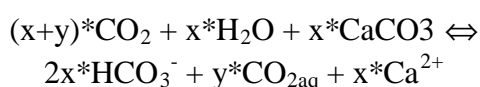
**Second technique:** Sample poisoning (Hg) to suppress biological activity. Advantage: pH is kept stable and there is only a low risk of atmospheric contamination. Disadvantage: Additional chemicals are needed, which are not altogether free of risk.

Both these methods will lead to more accurate measurements than the direct determination of δ<sup>13</sup>C from <sup>14</sup>C preparation. The <sup>13</sup>C/<sup>12</sup>C ratio is measured by mass spectrometry. A total error of 0.5 ‰ (from preparation and measurement) has to be taken into account for water samples (Eichinger, 1982).

## 7.4 <sup>14</sup>C Models

**1.) Model by Vogel:** This model takes a constant A<sub>0</sub> of 85±5 pmC averaged from 100 samples taken from shallow aquifers in Northwest Europe.

**2.) Model by Tamers:** This simple chemistry model is based upon an uptake of soil CO<sub>2</sub> during infiltration, with an ensuing dissolution of carbonate minerals until the carbonate equilibrium is reached. This leads to the following reaction:



It can be seen that this model assumes only two sources of carbon (calcite and soil CO<sub>2</sub>), which mix without the occurrence of fractionation. With these assumptions, A<sub>0</sub> can be calculated as follows:

$$A_0 = [(CO_{2aq} + 0.5*HCO_3^-) * A_g] / (CO_{2aq} + HCO_3^-)$$

This method of A<sub>0</sub> calculation was introduced by Ingerson & Pearson (1964) and discussed in detail by Tamers (1967, 1975) and Tamers & Scharpenseel (1970).

**3.) Model by Pearson (1964):** This simple isotope model is very similar to the chemical model discussed above, but it uses δ<sup>13</sup>C values to determine the mixture of carbon of different origin. It also assumes that there are only two sources of carbon and no fractionation (as in the Tamers model) occurs.

$$A_0 = [(\delta_m - \delta_s) / (\delta_g - \delta_s)] * (A_g - A_s) + A_s$$

Where δ<sub>m</sub> is the measured δ<sup>13</sup>C amount of the solution.

### Isotope Exchange Models

Isotope exchange models take into account that fractionation occurs when carbon changes its phase due to chemical reactions.

**Model by Fontes and Garnier (1979):** In addition to fractionation between gaseous and dissolved carbon, this model also takes into account fractionation between dissolved carbon and the rock matrix. The user also has to take into account that:

- the dissolution of gypsum results in additional Ca<sup>2+</sup> ions;
- cation exchange;
- sodium carbonates may precipitate (at high concentration or pH).

Thus it is recommended to make an ion balance to determine the part of dissolved carbon  $C_s$  originating from the rock matrix:

$$C_s = Ca^{2+} + Mg^{2+} - SO_4^{2-} + (Na^+ + K^+ - Cl^- - NO_3^-)/2$$

In the first step, one has to decide whether the main process is exchange with  $CO_2$  or with the matrix. We therefore have to determine the amount of carbon  $q$  originating from soil  $CO_2$ . In this step we use the balance equation given below, with an  $\epsilon$  for the fractionation between  $CO_2$  and  $HCO_3^-$ :

$$\text{Open system: } \delta_m * TDIC = (C_s - q) * \delta_s + (C_m - C_s) * \delta_g + q * (\delta_g - \epsilon)$$

$$\text{Or transformed: } q = -q' = (TDIC * \delta_m - C_s * \delta_s - \delta_g * (TDIC - C_s)) / (\delta_g - \epsilon - \delta_s)$$

where the subscripts m, s and g mean measured, solid and gaseous carbon respectively.

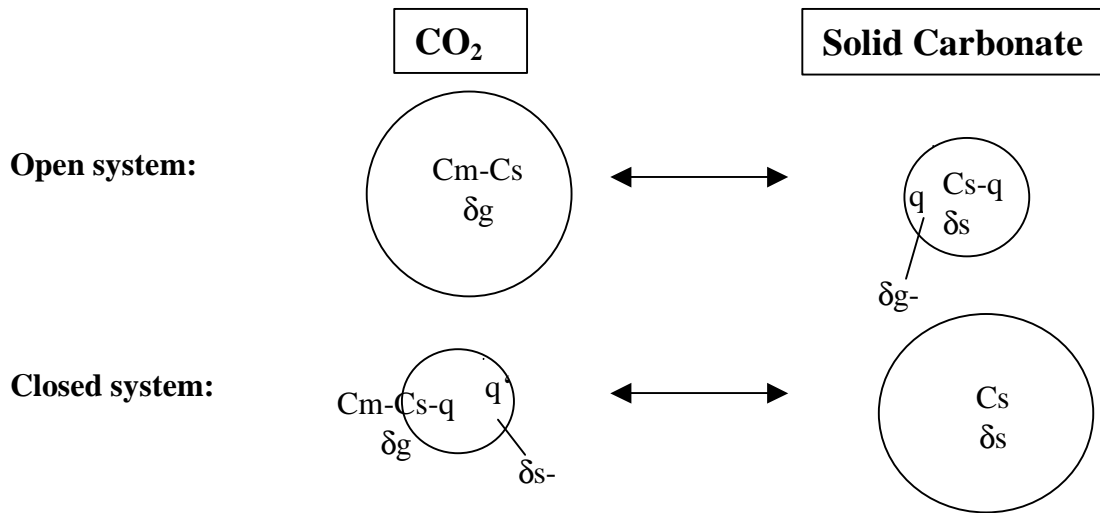


FIG. 7.5: SPECIES OF CARBONIC ACID EQUILIBRIUM FOR OPEN AND CLOSED SYSTEM CONDITIONS

For  $q > 0$  the major process is carbon exchange with soil gas. For  $q < 0$  exchange occurs mainly with solid carbon. This is why we calculate  $q$  again with  $\epsilon$  for fractionation between solid carbonate and  $HCO_3^-$ .

Now  $A_0$  can be calculated with the same balance formula using the fractionation factor  $^{14}\epsilon$  [%] =  $0.23 * ^{13}\epsilon$  [‰]:

$$A_0 = [C_s * A_s + (TDIC - C_s) * A_g + q * (A_g - 0.23 * ^{13}\epsilon - A_s)] / TDIC$$

Both methods discussed above can lead to errors in determination of  $A_0$  when  $\delta_g$  approaches ( $\epsilon_{g,HCO_3^-} + \delta_s$ ). This happens when the denominator of the formula for  $q$  tends to zero, namely in arid regions, in which  $\delta_g$  values of up to  $-12$  ‰ have been detected, or humid regions, in which  $\delta_s$  may reach  $-8$  ‰ (continental sediments) – in other words when  $\delta_s$  and  $\delta_g$  cannot be separated properly.

#### Modelling with NETPATH (Plummer et al., 1994)

The NETPATH code is able to calculate NET balances between two points in the aquifer that should lie on a flow line. One can thus only calculate relative ages. If an absolute  $^{14}C$  age should be determined, the initial value of groundwater flow has to be known. It is therefore of major importance to get samples from the infiltration area.

The following assumptions have to be made:

- today's conditions are the same as the ones a few thousand years ago;
- the infiltration area has to be known;
- the modeller needs to have a clear idea of the processes taking place in the aquifer.

## 7.5 Mixtures

Mixtures of two groundwaters of different ages will produce the following consequences, which have to be kept in mind when groundwater resources are being determined from their residence times. Mixtures may occur either in the aquifer through leakage, or during sampling when different aquifers are captured. The difference can only be detected in the field because the latter case should lead to non-equilibrium conditions. After a short time this non-equilibrium will reach equilibrium again and can no longer be detected.

To determine the amount of both end members, one has to properly treat the data set. Mixtures may be separated by chemistry data when the composition of the end members is known. When a young  $^3\text{H}$ -containing component takes part, it is possible to determine its amount by adding an additional tracer for young ground waters (CFC's,  $\text{SF}_6$  or  $^{85}\text{Kr}$ ).

### Old and young ( $^3\text{H}$ - containing) component

There are two main sources for large errors in modelling the old component:

- 1.) errors of amount calculation are about  $\pm 10\%$ ;
- 2.) activity of the young component depends largely on its age (120-200 pmC).

When resources should be calculated, the young component will dominate the result.

### Two old components (free of $^3\text{H}$ )

When two old waters are mixed, the measured  $^{14}\text{C}$  concentration leads to an underestimation of residence times. If one of both components is  $^{14}\text{C}$  free, the underestimation is even bigger. The reason of this shift is the exponential character of  $^{14}\text{C}$  decay compared to mixture (or dispersion), which is a linear process.

## 7.6 Extending Dating Ranges

There are several different methods for prolonging the dating timescale over 30,000 years – although they all suffer from individual difficulties. Large errors have to be taken into account or kept in mind for interpretations. The following methods can be used:

### $^{81}\text{Kr}$ ( $T_{1/2} = 230'000 \text{ y}$ )

Only a few samples for  $^{81}\text{Kr}$  have yet been taken in the Great Artesian Basin in Australia. The sampling volume of 16,000 litres of water has been degassed in the field and measurements on four samples were performed on a Cyclotron.

**Advantage:**  $^{81}\text{Kr}$  is inert and assumed to have been constant in the past.

**Disadvantages:** A high sampling volume is required. It is very difficult and expensive to measure.

### $^{36}\text{Cl}$ ( $T_{1/2} = 301'000 \text{ y}$ )

$^{36}\text{Cl}$  in groundwater originates from the atmosphere, where its concentration is almost constant and well known over the past 100,000 years. Due to the low sampling volume of  $5\text{mg Cl}^-$ , this method is easy to apply in field studies.

**Advantages:** It is easy to sample. The measurement technique has been developed to routine level.

**Disadvantages:**  $\text{Cl}^-$  concentrations depend on the distance from the sea. The ion can be stored in and dissolved from salt layers. Considerable underground production of  $^{36}\text{Cl}$  leads to problems in interpretation. Dissolution of salt layers (with unknown  $^{36}\text{Cl}/\text{Cl}$  ratio) in the aquifer or during



infiltration may make it impossible to interpret the data.

#### **<sup>4</sup>He (stable)**

This isotope is produced underground and its concentration increases during flow in the aquifer.

**Advantage:** Sampling and measurement have been developed to routine level.

**Disadvantage:** Because the <sup>4</sup>He increase is mostly the sum of *in situ* production and diffusive flux from neighbouring layers, it is difficult to calculate an age from it because it depends very much on the geology and hydrogeology (Andrews et al., 1982).

#### **U-Series**

There have been different methods used for groundwater dating but they are all difficult to interpret because of the complexity of the reactions, which have to be taken into account. For old groundwaters, the most commonly used method is the one based on the ratio <sup>234</sup>U/<sup>238</sup>U where <sup>234</sup>U has got a half life of 246,000 years.

#### **Introductory Literature**

- Clark I. and Fritz P., *Environmental Isotopes in Hydrology*, Lewis Publishers, Boca Raton, 1997.
- Cook P. and Herczeg A.L., *Environmental Tracers in Subsurface Hydrology*, Kluwer Academic Publishers, Dordrecht, 2000.
- Fritz P. and Fontes J.C., *Handbook of Environmental Isotope Geochemistry*, Elsevier, Amsterdam, 1980.
- Taylor R.E., Long A. and Kra R.S., *Radiocarbon After Four Decades*, Springer Verlag, New York, 1992.

#### **References**

- Andrews et al., *Radioelements, radiogenic helium and age relationships for groundwaters from the granites at Stripa*, Sweden, *Geochim. Cosmochim. Acta* 46, 1982, p. 1533-1543.
- Baertschi P., *Messung und Deutung relativer Häufigkeitsvariationen von <sup>18</sup>O und <sup>13</sup>C in Karbonatgesteinen und Mineralien*, Schweiz, *Min. Petr. Mitt.* 37, 1957, p. 73-152.
- Bard E., Hamelin B., Fairbanks R.G. and Hamelin B., *Calibration of the <sup>14</sup>C time scale over the past 30,000*

- years using mass spectrometric U-Th ages from Barbados corals*, *Nature* 345, 1990, p. 405.
- Baumgartner S., Beer J., Masarik J., Wagner G., Meynadier L. and Synal H.-A., *Geomagnetic Modulation of the <sup>36</sup>Cl Flux in the GRIP Ice Core, Greenland*, *Science*, vol. 279, 1998, p. 1330-1332.
- Bender M., *Variations in the <sup>13</sup>C/<sup>12</sup>C ratios of plants in relation to the pathway of photosynthetic carbon dioxide fixation*, *Phytochem* 10, 1971, p. 1239-1244.
- Brinkmann R., Münnich K.O. and Vogel J.C., *<sup>14</sup>C Altersbestimmung von Grundwasser*, *Naturwissenschaften* 46, 1959, p. 10-12.
- Clark I. and Fritz P., *Environmental Isotopes in Hydrogeology*, Lewis Publishers, Boca Raton, New York, 1997. 328 p.
- Craig H., *The geochemistry of stable carbon isotopes*, *Geochim. Cosmochim.* 1953. *Acta* 3, p. 53-92.
- Deines P., *The isotopic composition of reduced organic carbon*, *Handbook of Environmental Isotope Geochemistry*, 1980, Elsevier, Amsterdam, Oxford, New York, p. 329-393.
- Eichinger L., *Bestimmung des Alters von Grundwässern mit Kohlenstoff-14: Messung und Interpretation der Grundwässer des Fränkischen Albvorlandes*, Gesellschaft für Strahlen- und Umweltforschung mbH, München, 1982.
- Esser N., *Messungen der absoluten Konzentration und des <sup>13</sup>C Gehalts von atmosphärischem CO<sub>2</sub>*, Dipl. Arbeit der Universität Heidelberg, Inst. f. Umweltphysik, 1975.
- Fontes J.C. and Garnier J.M., *Determination of the initial <sup>14</sup>C activity of the total dissolved carbon*, *WRR* 15, 1979, p. 399-413.
- Ingerson E. and Pearson F.J.Jr., *Estimation of age and rate of motion of groundwater by the <sup>14</sup>C method, Recent Researches in the Fields of Hydrosphere, Atmosphere and Nuclear Geochemistry*, Maruzen, Tokyo, 1964, p. 263-283.
- Lal D. and Peters B., *Handbuch der Physik*, Springer Verlag, Germany, vol. 46, 1967, p. 551-612.
- Langmuir D., *The geochemistry of some carbonate groundwaters in central Pennsylvania*, *Geochim. Cosmochim. Acta* 35, 1971, p. 1023-1045.
- Matthes G., *Die Beschaffenheit des Grundwassers*, *Hydrologie* vol.2, Bornträger, Berlin, 1973.
- Mook W.G., *Geochemistry of the stable carbon and oxygen isotopes of natural waters in the Netherlands*, Diss., Groningen, 1968.
- Mook W.G., *On the reconstruction of the initial <sup>14</sup>C content of groundwater from the chemical and isotopic composition*, Intern. Conf. Radiocarbon Dating, Wellington, 1972, p. 342-352.
- Mook W.G., *The dissolution-exchange model for dating groundwater with carbon-14, Interpretation of Environmental and Hydrochemical Data in Groundwater Hydrology*, IAEA, Vienna, 1976, p. 213-225.
- Pearson F.J.Jr. and Hanshaw B.B., *Sources of dissolved carbonate species in groundwater and their effect on carbon-14 dating*, *Isotope Hydrology*, IAEA, Vienna, 1970, p. 271-285.
- Pearson G.W., Pilcher J.R., Baillie M.G.L., Corbett D.M. and Qua F., *High Precision <sup>14</sup>C measurement of Irish oaks to show the natural <sup>14</sup>C variations from AD 1840 to 5210 BC*, *Radiocarbon* 28, 1986, p. 911-934.

- Plummer L.N., Prestemon E.C. and Parkhurst D.L., *An interactive code (NETPATH) for modelling net geochemical reactions along a flow path, version 2.0*, U.S. Geological Survey Water-Resources Investigations Report, 1994, p. 94-4169.
- Puchelt H. and Hubberten H-W., *Vulkanogenes Kohlendioxid: Aussagen zur Herkunft aufgrund von Isotopenuntersuchungen*, Tagung: Isotope in der Natur, Leipzig, 1980, p. 198-210.
- Smith D.B., Downing R.A., Monkhouse R.A., Otlet R.L. and Pearson F.J.Jr., *The age of groundwater in the chalk of the London Basin*, WRR 12, 1976, p. 392-404.
- Tamers M.A., *Surface-water infiltration and groundwater movement in arid zones of Venezuela*, Isotopes in Hydrology, IAEA, Vienna, 1967, p. 339-351.
- Tamers M.A., *Validity of radiocarbon dates of groundwater*, Geophys. Survey 2, 1975, p. 217-239.
- Tamers M.A. and Scharpenseel H.W., *Sequential sampling of radiocarbon in groundwater*, Isotope Hydrology, IAEA, Vienna, 1970, p. 241-256.
- Vogel J.C. and Ehhalt D.H., *The use of carbon isotopes in groundwater studies*, Radioisotopes in Hydrology, IAEA, Vienna, 1963, p. 225-240.

## Appendix to Chapter 7: Exercises

### Questions

1. Calculate the initial carbonate content (TDIC) during recharge giving pH, temperature and  $p_{\text{CO}_2}$  values under the assumption of carbonate equilibrium.

pH = 6.3 and pH = 9; T = 30°C;  $p_{\text{CO}_2} = 10^{-2.0}$

Species	pH = 6.3	pH = 9
CO <sub>2(aq)</sub>		
HCO <sub>3</sub> <sup>-</sup>		
H <sub>2</sub> CO <sub>3</sub>		
TDIC		

2. Calculate the  $\delta^{13}\text{C}$  of the HCO<sub>3</sub><sup>-</sup> species for pH = 6.3 values above when the  $\delta^{13}\text{C}$  of soil air is set to be -20 ‰PDB (Note that the sum of all species must be -20‰ again).

3. What is the  $\delta^{13}\text{C}$  of the CO<sub>3</sub><sup>2-</sup> at pH = 10 under the same boundary conditions?

4. Calculate the calcite saturation index SI for the sample from Dan Kassari (see table below).

The following data represent different examples of groundwaters:

Site	<sup>14</sup> C	<sup>13</sup> C	T	pH	Ca <sup>2+</sup>	Mg <sup>2+</sup>	Na <sup>+</sup>	K <sup>+</sup>	Alk.	Cl <sup>-</sup>	SO <sub>4</sub> <sup>2-</sup>	HS <sup>-</sup>
	Pmc	‰	C		meq/l							
Dan Kassari (Niger) CT2	42.0	-19.9	32.8	6.3	0.36	0.74	0.19	0.16 6	1.75	0.02	0.09	
Angoual Banguiro CT3	?	?	31.7	5.25	0.09	0.07	0.17	0.01 7	0.20	0.02	0.05	
Umm er Radhuma	3.3	-2.0	34	7.55	3.59	4.41	6.00	0.27	2.61	6.09	2.63	0.2
Dito (recharge area)	69.8	-6.3	28.0	7.26	2.85	2.25	1.59	0.05	5.94	2.38	0.2	nd

5. Calculate the <sup>14</sup>C ages of Dan Kassari and Umm er Radhuma, applying the correction schemes explained in the theory part.

Sample	uncorrected		Vogel		Tamers		Pearson		Fontes	
	A0 [%]	Age [ky]	A0 [%]	Age [ky]	A0 [%]	Age [ky]	A0 [%]	Age [ky]	A0 [%]	Age [ky]
Dan Kassari										
Umm er Radhuma										

6. Which model do you think is the most adequate one?

## Solutions

1. Calculate the initial carbonate content (TDIC) during recharge giving pH, temperature and  $p_{\text{CO}_2}$  values under the assumption of carbonate equilibrium.

$$\text{pH} = 6.3 \text{ and } \text{pH} = 9; T = 30^\circ\text{C}; p_{\text{CO}_2} = 10^{-2.0}$$

Calculate K values for given temperature (in Kelvin).

$$(\text{CO}_{2\text{g}} - \text{CO}_{2\text{aq}}, 303.15\text{K}): \log K_0 = -1.524$$

$$(\text{CO}_{2\text{aq}} - \text{HCO}_3^-, 303.15\text{K}): \log K_1 = -6.328$$

$$(\text{HCO}_3^- - \text{CO}_3^{2-}, 303.15\text{K}): \log K_2 = -10.288$$

Now for example  $K_1 = [\text{HCO}_3^-][\text{H}^+]/[\text{CO}_{2\text{aq}}]$

so you can calculate the concentrations of the different species.

Species	pH = 6.3	pH = 9
$\text{CO}_{2\text{aq}}$	0.30	$3 \times 10^{-4}$
$\text{HCO}_3^-$	0.28	1.40
$\text{CO}_3^{2-}$	$2.9 \times 10^{-5}$	0.71
TDIC	0.58	2.12

2. Calculate the  $\delta^{13}\text{C}$  of the  $\text{HCO}_3^-$  species for pH = 6.3 when the  $\delta^{13}\text{C}$  of soil air is set to be  $-20\text{‰PDB}$  (Note that the sum of all species must be  $-20\text{‰}$  again).

$$\delta\text{CO}_{2\text{aq}} = \delta\text{HCO}_3^- - \epsilon$$

For this reaction  $\alpha$  can be calculated:  $\alpha(\text{CO}_{2\text{aq}}, \text{HCO}_3^-) = 0.9916\text{‰}$

thus  $\epsilon = 8.4605\text{‰}$

Let's take x as the value we are looking for ( $\delta\text{HCO}_3^-$ ):

$$x * [\text{HCO}_3^-] + (x - 8.4605) * [\text{CO}_{2\text{aq}}] = \text{TDIC} * -20\text{‰}$$

$$\underline{x = -15.6\text{‰} = \delta\text{HCO}_3^-}$$

3. What is the  $\delta^{13}\text{C}$  of the  $\text{CO}_3^{2-}$  at pH = 10 under the same boundary conditions?

$$\epsilon = \delta\text{CO}_3^{2-} - \delta\text{HCO}_3^- = -0.3399\text{‰}$$

$$x = \delta\text{CO}_3^{2-}$$

$$x * [\text{CO}_3^{2-}] + (x + 0.3399) * [\text{HCO}_3^-] = \text{TDIC} * -20\text{‰}$$

$$\underline{x = -20.22 = \delta\text{CO}_3^{2-}}$$

4. Calculate the calcite saturation index SI for the sample from Dan Kassari (see table below).

The following data shall represent different examples of groundwaters:

Site	<sup>14</sup> C	<sup>13</sup> C	T	pH	Ca <sup>2+</sup>	Mg <sup>2+</sup>	Na <sup>+</sup>	K <sup>+</sup>	Alk.	Cl <sup>-</sup>	SO <sub>4</sub> <sup>2-</sup>	HS <sup>-</sup>
	pmc	‰	C		meq/l							
Dan Kassari (Niger) CT2	42.0	-19.9	32.8	6.3	0.36	0.74	0.19	0.166	1.75	0.02	0.09	
Angoual Banguiro CT3	?	?	31.7	5.25	0.09	0.07	0.17	0.017	0.20	0.02	0.05	
Umm er Radhuma	3.3	-2.0	34	7.55	3.59	4.41	6.00	0.27	2.61	6.09	2.63	0.2
Dito (recharge area)	69.8	-6.3	28.0	7.26	2.85	2.25	1.59	0.05	5.94	2.38	0.2	nd

IAP = [Ca]\*[CO<sub>3</sub><sup>2-</sup>] (do not use the total alkalinity!!! Because [HCO<sub>3</sub><sup>-</sup>]≅ [CO<sub>2aq</sub>] as calculated above)

SI (Dan Kassari) = -2.25 (calculated with NETPATH too): so this water is undersaturated with respect to calcite.

5. Calculate the <sup>14</sup>C ages of Dan Kassari and Umm er Radhuma, applying the correction schemes explained in the theory part.

For Dan Kassari we already calculated the amount of the different bicarbonate species! If we do the same for Umm er Radhuma, we'll see that almost all bicarbonate is in the form HCO<sub>3</sub><sup>-</sup>.

Sample	Uncorrected		Vogel		Tamers		Pearson		Fontes	
	A0 [%]	Age [ky]	A0 [%]	Age [ky]	A0 [%]	Age [ky]	A0 [%]	Age [ky]	A0 [%]	Age [ky]
Dan Kassari	100	7.171	85	5.828	76	4.903	90	5.327	117.6	9.591
Umm er Radhuma	100	28.2	85	26.9	50	22.5	13.3	11.5	13.3	11.5

6. Which model do you think is the most adequate one?

Dan Kassari: Obviously the Fontes Model does not work for this sample because there seems to be something wrong with the alkalinity (thus the difference between Cs and TDIC becomes too large). The other models lie very close together and thus reveal similar ages. The Tamers Model seems to overestimate the amount of calcite dissolution and thus reveals an A0 that seems to be too low.

Umm er Radhuma: In this system, ion exchange seems to take place between the solid calcite and our solution, thus all models must fail that cannot include ion exchange (Vogel, Tamers).

## 8 Estimation of the Spatial Distribution of Evapotranspiration using Optical Remote Sensing

*Carmen Alberich, IHW, ETHZ, Zurich, Switzerland*

### 8.1 Introduction

Estimation of evapotranspiration using remote sensing inputs is based on the one dimensional surface energy balance, which in terms of specific fluxes is expressed as:

$$R_n = G + H + IE$$

The net radiation  $R_n$  resulting from the budget of incoming radiation from the sun and the atmosphere towards the surface, and the upward radiation reflected and emitted by the surface, partitions into the soil heat flux  $G$ , the sensible heat flux into the atmosphere  $H$ , and the latent heat flux  $IE$ , which is the energy used for evaporation.

Transport of heat into the soil occurs by diffusion, so that the flux  $G$  depends upon the temperature gradient in the soil, on the soil heat capacity, and on the soil resistance to heat transport. The partitioning of the available energy  $R_n - G$  between  $IE$  and  $H$  depends upon the availability of water for evaporation and on the heat and mass transport conditions between the surface and the atmosphere.

As reviewed by Jackson (1985), Moran and Jackson (1991) and Kustas and Norman (1996), many of the algorithms used to estimate evapotranspiration using remote sensing are based on the calculation of the latent heat flux  $IE$  as a residual term of the surface energy balance equation.

The self-preservation in the diurnal evolution of the surface energy budget is then used to infer meaningful daily evapotranspiration values from the instantaneous latent heat flux estimates

obtained for the time of satellite overpass. Self-preservation makes reference to the fact that the relative partitioning of the energy flux among its main components remains the same during the daytime.

Estimation of the instantaneous flux densities in the surface energy balance equation relies on ground meteorological data and on the estimation of surface properties, such as albedo, surface temperature and vegetation cover, using satellite data. These surface physical properties are extracted from the surface radiances, which are obtained after calibration and atmospheric correction of the spectral signals registered by the satellite sensor. The computation of albedo and vegetation indices from remote sensing requires spectral information of the visible and near infrared ranges. For the estimation of surface temperature a sensor in the far infrared range is necessary. Table 8.1 shows the distribution of the spectral bands of some current meteorological and earth resource satellites.

Since most of the algorithms developed for the estimation of the fluxes are only valid for clear days, a cloud masking procedure has to be applied to the satellite images as a pre-processing step. Accurate georeferencing of the images is also important to guarantee comparison with ground measurements and other geospatial information. While georeferencing and cloud masking are pure pre-processing operations, calibration and atmospheric correction are tightly related to the procedures for the estimation of albedo and surface temperature and deserve further discussion.

TABLE 8.1: SENSOR CHARACTERISTICS

	Platform	Sensor	1 <sup>st</sup> launch	Bands	Spatial resolution	Revisit period	
<b>Meteorological Satellites</b>	Meteosat		Nov_1977	Visible 0.45 - 1.0 $\mu\text{m}$ Water vapour 5.7 - 7.1 $\mu\text{m}$ Infrared 10.5 - 12.5 $\mu\text{m}$	2.5 km 5 km 5 km	30 min	
	GMS	VISSR	Oct_1977	Visible 0.55 - 1.0 $\mu\text{m}$ Infrared 10.5 - 12.5 $\mu\text{m}$	1.25 km 5 km		
	GOES	GOES Imager			0.55 - 0.75 $\mu\text{m}$ 3.80 - 4.00 $\mu\text{m}$ 6.50 - 7.00 $\mu\text{m}$ 10.20 - 11.20 $\mu\text{m}$ 11.50 - 12.50 $\mu\text{m}$	1 km 4 km 8 km 4 km 4 km	26 min
			FENG YUN		Sep_1988	Visible 0.55 - 1.05 $\mu\text{m}$ Water vap. 6.2 - 7.6 $\mu\text{m}$ Infrared 10.5 - 12.5 $\mu\text{m}$	1.25 km 5 km 5 km
	NOAA	AVHRR	Jun_1979	band 1 0.58 - 0.68 $\mu\text{m}$ band 2 0.725 - 1.0 $\mu\text{m}$ band 3 3.55 - 3.93 $\mu\text{m}$ band 4 10.3 - 11.3 $\mu\text{m}$ band 5 11.4 - 12.4 $\mu\text{m}$	1.1 km	12 hours	
<b>Earth Resources Satellites</b>	Landsat	MSS	July_1972	band 4 0.5 - 0.6 $\mu\text{m}$ band 5 0.6 - 0.7 $\mu\text{m}$ band 6 0.7 - 0.8 $\mu\text{m}$ band 7 0.8 - 1.1 $\mu\text{m}$ band 8* 10.4 - 12.6 $\mu\text{m}$ * only on Landsat 3	79 m 79 m 79 m 79 m 237 m	18 days (Landsat 1,2,3) 16 days (Landsat 4,5)	
		TM ETM +	Jul_1982 1999	band 1 0.45 - 0.52 $\mu\text{m}$ band 2 0.52 - 0.60 $\mu\text{m}$ band 3 0.63 - 0.69 $\mu\text{m}$ band 4 0.76 - 0.90 $\mu\text{m}$ band 5 1.55 - 1.75 $\mu\text{m}$ band 7 2.08 - 2.35 $\mu\text{m}$ band 6 10.4 - 12.5 $\mu\text{m}$	30 m 30 m 30 m 30 m 30 m 30 m 120 m (TM) 60 m (ETM+)	16 days	

TABLE 8.1: SENSOR CHARACTERISTICS (CONTINUED)

	Platform	Sensor	1 <sup>st</sup> launch	Bands	Spatial resolution	Revisit period
Earth Resources Satellites	SPOT	HRV HRV <sub>panchro</sub>	Jan_1990	0.50 - 0.59 μm (green) 0.61 - 0.68 μm (red) 0.79 - 0.89 μm (near IR) 0.51 - 0.73 μm (panchrom.)	20 m 20 m 20 m 10 m	26 days
		HRVIR HRVIR <sub>panchro</sub>	Mar_1988	0.50 - 0.59 μm (green) 0.61 - 0.68 μm (red) 0.78 - 0.89 μm (near IR) 0.51 - 0.73 μm (panchrom.)	20 m 20 m 20 m 10 m	26 days
		Vegetation	Mar_1988	0.43 - 0.47 μm (blue) 0.61 - 0.68 μm (red) 0.78 - 0.89 μm (near IR) 1.58 - 1.75 μm (mid IR)	1000 m 1000 m 1000 m 1000 m	26 days
		HRG HRG <sub>panchro</sub>	2002	0.50 - 0.59 μm (green) 0.61 - 0.68 μm (red) 0.78 - 0.89 μm (near IR) 1.58 - 1.75 μm (mid IR) 0.51 - 0.73 μm (panchrom.)	10 m 10 m 10 m 10 m 5 m	26 days
	IRS 1A,1B,1C,P2	LISSI I LISSI II	Mar_1988 Aug_1991	0.45 - 0.52 μm 0.52 - 0.59 μm 0.62 - 0.68 μm 0.77 - 0.86 μm	73 m (LISSI I) 26 m (LISSI II)	22 days (1A,1B) 24days (1C,P2)
		LISSI III	Sep_1997	0.52 - 0.59 μm 0.62 - 0.68 μm 0.77 - 0.86 μm 1.55 - 1.70 μm	23 m	
		Pan	Sep_1997	0.5 - 0.57 μm	10 m	
		Wifs	Sep_1997	0.62 - 0.68 μm 0.77 - 0.86 μm	188 m	
	RESURS-01		1985	0.5 - 0.6 μm 0.6 - 0.7 μm 0.7 - 0.8 μm 0.8 - 1.1 μm 10.4 - 12.6 μm	160 m 160 m 160 m 160 m 600 m	21 days

## 8.2 Estimation of the Fluxes in the Surface Energy Balance Equation

### Net radiation

The net radiation results from the budget of shortwave and longwave radiation reaching and leaving the surface:

$$R_n = S \downarrow - S \uparrow + L \downarrow - L \uparrow = (1 - r_0) S \downarrow + L \downarrow - L \uparrow$$

The incoming shortwave radiation  $S \downarrow$ , solar radiation in the wavelength range 0.3 - 3μm, is partly reflected at the surface. The amount reflected  $S \uparrow$  may be expressed in terms of the incoming shortwave radiation and the surface albedo  $r_0$ . The incoming long-wave radiation  $L \downarrow$  is

thermal radiation emitted by the atmosphere. The outgoing long-wave radiation  $L \uparrow$  is the portion of the atmospheric thermal radiation that is reflected at the surface plus the thermal radiation emitted by the surface itself.

Since thermal radiation obeys Stefan-Boltzmann's law, the estimation of the longwave fluxes requires the knowledge of the temperature and emissivity of the surface and of the atmosphere. The shortwave component is determined by estimating the surface albedo and the incoming shortwave radiation.

While surface albedo and surface temperature can be obtained from satellite-measured radiances, atmospheric temperature and emissivity are usually related to parameters measured at ground



based meteorological stations. The incoming shortwave radiation may be estimated from the exoatmospheric incoming shortwave radiation, obtained from astronomical parameters.

Methods for estimating surface albedo and surface temperature from satellite radiances and methods for estimating incoming shortwave radiation from the exoatmospheric solar radiation necessarily contain some atmospheric correction procedure, but the approaches used are different depending on the parameter to be estimated and on the data availability.

### **Incoming shortwave radiation**

Surface incoming shortwave radiation can be measured directly with a pyranometer. The measurements may be simply extrapolated radially for some distance around the pyranometer site (Moran et al., 1989), or they may be used to calculate atmospheric transmittance.

The atmospheric transmittance – defined as the ratio of surface incoming shortwave radiation to exoatmospheric incoming shortwave radiation – is a lumped attenuation factor that accounts for absorption and scattering effects in the atmosphere. Since atmospheric conditions are usually homogeneous over large spatial scales, the transmittance is considered to be constant over the study area.

The surface incoming shortwave radiation is calculated as the product of the exoatmospheric incoming shortwave radiation calculated for each pixel of the study area times the transmittance estimated for the pyranometer site. Iqbal (1983) provides formulae for the calculation of the exoatmospheric incoming shortwave radiation from astronomical parameters. The input parameters needed are the solar constant, the solar zenith angle, and the julian day (see Chapter 3).

### **Surface albedo**

Albedo is defined as the integral of the hemispherical surface reflectance over the wavelength range of solar radiation, from 0.3  $\mu\text{m}$  to 3  $\mu\text{m}$ . As satellites measure the radiance within discrete spectral intervals, a method is required to derive the total or broadband albedo from the reflectance computed in the range of the single spectral bands. Generally the broadband albedo is obtained as a linear combination of the reflectance of the single bands. The weighting factors are either chosen to be proportional to the percentage of incoming solar radiation in the wavelength range of the band (ie. Brest and Goward, 1987) or are estimated statistically, comparing the continuous spectral reflectance signatures of targets at the ground with the discrete signals registered at the satellite sensor and corrected with a radiative transfer code under different atmospheric conditions (see Valiente et al., 1995).

As summarised by Csiszar and Gutman (1999), the retrieval of surface albedo from satellite-measured reflectances requires besides the narrow to broadband conversion an atmospheric correction procedure and the conversion from directional reflectances to hemispheric albedos, based on a bi-directional reflectance distribution function. The conversion from directional reflectance to hemispheric albedos is often simplified by assuming the surface to be a Lambertian reflector.

The order in which atmospheric correction and the narrow to broadband conversion are applied is not prescribed, but the procedures used must be chosen accordingly. Atmospheric correction of single band reflectances, before the narrow to broadband conversion, is more widely accepted, and can be carried out with an atmospheric correction code like SMAC (Rahman and Dedieu, 1994). If the narrow to broadband conversion is applied first, the broadband surface albedo can be obtained from the planetary albedo using

the linear relationship derived by Chen and Ohring (1983).

## **Surface temperature and surface**

### **emissivity**

Methods applied to estimate surface temperature and emissivity differ, depending upon the spectral information available. For sensors having two bands in the far infrared, the estimation of surface temperature can be accomplished using Split Window Techniques. These techniques base the atmospheric correction on the differential atmospheric absorption of two adjacent bands. Split Window Techniques were first applied for the estimation of sea surface temperature. Later methods that simultaneously provide an estimate of land surface temperature and of emissivity were developed. These techniques have been reviewed by Prata et al (1995).

If only one band in the far infrared is available, as in the case of Landsat Thematic Mapper, an explicit atmospheric correction is required, which can be carried out using a radiative transfer code. Alternatively a linear relationship can be established between single longwave radiance ground truth measurements and the corresponding longwave radiance measured by the satellite sensor. However, as mentioned by Moran and Jackson (1991), this correction procedure only works well on very clear days. The estimation of surface temperature from the blackbody temperature delivered by the atmospheric corrected longwave radiance can be carried out using the empirical relation between surface emissivity and the normalised difference vegetation index (NDVI) proposed by Van de Griend and Owe (1993).

### **Longwave incoming radiation**

The accurate computation of the thermal radiation emitted by the atmosphere requires temperature and humidity profiles,

which are not always available. For this reason, several empirical equations have been developed to calculate longwave incoming radiation from air temperature and humidity measured near the surface at meteorological stations. Most of these empirical approaches deliver satisfactory estimates of daily and long-term averages of the thermal incoming radiation, but show greater errors for estimates at shorter time scales, as they are needed for modelling the surface energy balance.

Brutsaert (1975) proposed a physically based approach for calculating the incoming shortwave radiation, which relies on the assumption of exponential functional relationships for pressure temperature and vapour density profiles and the analytical solution of Schwarzschild's transfer equation. Brutsaert's equation has proven to model closely the measured diurnal trend of the longwave incoming flux (Culf and Gash, 1993), and has the advantage of allowing easy adjustment to local climatological conditions by fitting the constant parameter in the functional relationship for the vapour density profile to the average of measured profiles.

### **Soil heat flux**

The transfer of heat between the surface and the soil occurs by diffusion, so that the soil heat flux is a function of the temperature gradient between the surface and the soil and of the thermal conductivity of the soil. However, since the temperature in the soil and the soil thermal conductivity are not known, except perhaps for a few point measurements, it is necessary to relate the soil heat flux to surface parameters that can be observed from the satellite.

Empirical studies by de Bruin and Holtslag (1982) showed that the ratio  $G/R_n$  is related to the amount of vegetation present. Jackson et al (1987) and Kustas and Daughtry (1990) developed empirical relations between the ratio  $G/R_n$  and the

normalised difference vegetation index (NDVI).

For environments with sparse canopy, Choudhury et al (1984) parameterised the ratio as the product of two quantities  $\Gamma'$  and  $\Gamma''$ , where  $\Gamma'$  describes the conductive heat transfer in the soil, while  $\Gamma''$  is an extinction factor that expresses the attenuation of radiation through vegetation. For completely bare soils, the extinction factor has the value  $\Gamma''=1$ . Studies carried out in the desert of the Qattara Depression (Bastiaanssen, 1995) show that in such an environment the ratio  $G/R_n$  can be described satisfactorily through an empirical relation of surface temperature and albedo. In the presence of vegetation, the extinction factor  $\Gamma''$  is related to the NDVI. Bastiaanssen collected data from different authors to fit a relationship between  $\Gamma''$  and NDVI, and assumed the ratio  $G/R_n$  for a sparse canopy environment to be the product of the empirical relations derived for  $\Gamma'$  and  $\Gamma''$ . This method for the estimation of the soil heat flux was validated during the HAPEX Sahel Experiment (Bastiaanssen, 1998).

### Sensible heat flux

Sensible heat flux can be described through an Ohm-type law as a function of the temperature difference between the surface and the atmosphere, of the heat capacity of the air at constant pressure, and of the aerodynamic resistance to heat transport.

Transport of heat from the surface to the atmosphere occurs both by turbulence and convection. The turbulent transport is affected by the thermal stratification present in the atmosphere. In an unstable atmosphere, as is typical for a clear day in an arid environment, where the surface temperature is much higher than the air temperature, the turbulent transport is enhanced vertically by buoyancy. The aerodynamic resistance to heat transport is calculated as the integral of the inverse eddy diffusion coefficient for heat

transport, which according to the Monin-Obukhov similarity hypothesis is given by the combination of the buoyancy-corrected von Karman equation and the shear stress of the turbulent process (Monteith and Unsworth, 1990).

Bastiaanssen et al (1998) used the relation between surface temperature and albedo in landscapes with heterogeneous hydrological conditions to identify sets of so-called dry pixels, for which the latent heat flux is approximately zero, and of wet pixels, for which the sensible heat flux is assumed to be approximately zero. This allows one to anchor the extreme values of the sensible heat flux and to calculate the extremes of the difference between surface and air temperature. The difference between surface and air temperature for the remaining pixels in the area is calculated by the linear interpolation of the extreme values. The determination of the aerodynamic resistance to heat transport is optimised by using an iterative procedure to update the Monin-Obukhov length and the buoyancy correction parameter that depends on it.

### 8.3 Daily Evapotranspiration from Instantaneous Estimates

The use of remote sensing data for the estimation of the fluxes in the surface energy balance equation implies that these are instantaneous estimates, valid for the instant of satellite overpass. The latent heat flux calculated as a residual term of these flux estimates is also an instantaneous value. In order to obtain more meaningful daily evapotranspiration values from the instantaneous values, the self-preservation in the diurnal evolution of the surface energy budget is used.

Assuming that the ratio of the latent heat flux  $IE$  and some other flux term in the energy budget, here denoted by  $F$ , is self-preserved, the daily latent heat flux can be obtained as the product of the instantaneous ratio times the integral of  $F$

over daytime, provided that the diurnal evolution of  $F$  is known.

Jackson et al (1983) used the self-preservation of the ratio  $IE/S\downarrow$  to infer daily evapotranspiration from one time of the day estimates, taking a sinus function as an approximation for the behaviour of  $S\downarrow$  over the day.

Brutsaert and Sugita (1992) proved the suitability of the self-preservation of the ratios  $IE/(R_n - G)$  and  $IE/R_n$  and  $IE/S\downarrow$  for inferring daily evapotranspiration from instantaneous values calculated from atmospheric profiles and surface temperatures using the bulk similarity approach.

#### 8.4 Operational Methods for the Estimation of Evapotranspiration

Over the past 10 years, research has focused on the development of operational methods that make use of the procedures for estimating the fluxes in the surface energy balance as described above. One of these algorithms is the Surface Energy Balance Algorithm for Land (SEBAL) (Bastiaanssen et al, 1998). The SEBAL algorithm has been validated at experiments in Spain, China and Niger. These validation experiments and others carried out by Kite and Droogers (2000) show that the accuracy attainable is within the 20% level of uncertainty of ground based evapotranspiration measurements.

An example of an evapotranspiration map calculated with SEBAL for the Iullemeden Basin in Niger is given in Figure 8.1.

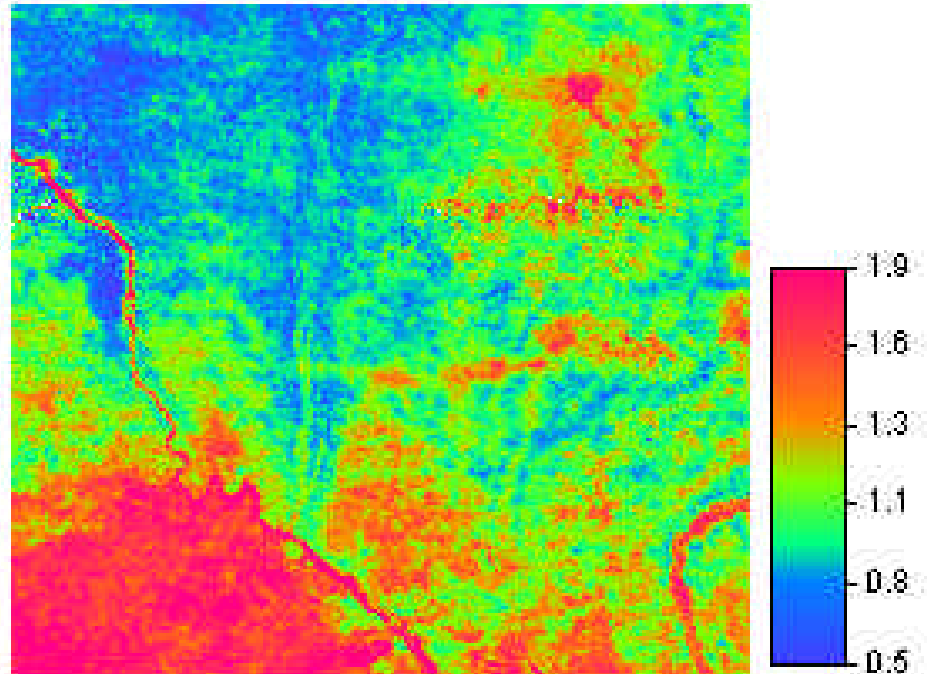


FIG 8.1: DAILY EVAPOTRANSPIRATION IN MM/DAY FOR THE 5<sup>TH</sup> OF MARCH 1992 CALCULATED FROM NOAA-AVHRR

#### 8.5 Further Utilisation of Evapotranspiration Maps

In the context of recharge estimation, the evapotranspiration maps can be applied as one element of the water balance. In a flat area without significant surface runoff, the recharge is the difference between precipitation and evapotranspiration.

The precipitation distribution can be obtained from METEOSAT5 data eventually combined with station data. Ten-day-sums are supplied for Africa by the USAID programme on a 5 km by 5 km grid on the Internet.

From maps of yearly precipitation and evapotranspiration, the difference can be calculated and integrated over available years. The result is an estimate of recharge,

provided that the redistribution by surface runoff and the outflow from the region remain small.

Even if the absolute values of estimated recharge are inaccurate, they can still be used for a meaningful 'zonation' of recharge. In combination with tracer information at points for calibration, a valuable recharge map can be constructed. This method has already been tried out by Brunner et al (2001) for an aquifer in Botswana.

## References

- Bastiaanssen W.G.M., *Regionalization of surface flux densities and moisture indicators in composite terrain*, Ph.D. Thesis, Agricultural University, Wageningen, The Netherlands, 1995.
- Bastiaanssen W.G.M., Menenti M., Feddes R.A. and Holtschlag A.A., *A remote sensing surface energy balance algorithm for Land (SEBAL)*, Journal of Hydrology, 212-213, 1998, p. 198-229.
- Brest C.L. and Goward S.N., *Deriving surface albedo measurements from narrow band satellite data*, International Journal of Remote Sensing 8, No.3, 1987, p. 351-367.
- Brunner, P., Eugster, M. Bauer, P., Kinzelbach, W., *Recharge estimation using remote sensing data and the chloride method*, in preparation, 2001.
- Brutsaert W., *On a derivable formula for long-wave radiation from clear skies*, Water Resources Research, vol. 11, no. 5, 1975, p. 742-744.
- Brutsaert W., *Evaporation into the atmosphere*, Reidel Publishing Company, Dordrecht, The Netherlands, 1982.
- Brutsaert W. and Sugita M., *Application of self-preservation in the diurnal surface energy budget to determine daily evaporation*, Journal of Geophysical Research 97, No. D17, 1992, p. 18337-18382.
- Culf A.D. and Gash J.H.C., *Longwave Radiation from Clear Skies in Niger: Comparison of Observations with Simple Formulas*, Journal of Applied Meteorology 32, 1993, p. 539-547.
- Chen T.S. and G. Ohring, *On the Relationship between Clear-Sky Planetary and Surface Albedos*, Journal of Atmospheric Science 41, 1983, p. 146-148.
- Choudhury B.J., Idso S.B. and R.J. Reginato, *Analysis of an empirical model for soil heat flux under a growing wheat crop for estimating evaporation by an infrared-temperature based energy balance equation*, Agricultural and Forest Meteorology, 39, 1984, p. 283-297.
- Csiszar I. and Gutman G., *Mapping global land surface albedo from NOAA AVHRR*, Journal of Geophysical Research, vol. 104, No. D6, 1999, p. 6215-6228.
- De Bruin H.A.R. and Holtschlag A.A.M., *A simple parameterization of the surface fluxes of sensible and latent heat during daytime compared with the Penman-Monteith concept*, Journal of Applied Meteorology, 21, 1982, p. 1610-1621.
- Iqbal M., *An Introduction to solar radiation*, Academic Press, Toronto, 1983.
- Jackson R.D., *Evaluating evapotranspiration at local and regional scales*, Proceedings IEEE 73, 1985, p.1086-1096.
- Jackson R.D., Hatfield J.L., Reginato R.J., Idso S.B. and Pinter P.J., *Estimation of daily evapotranspiration from one time-of-day measurements*, Agricultural Water Management 7, 1983, p. 351-362.
- Jackson R.D., Moran M.S., Gay L.W. and Raymond L.H., *Evaluating evaporation from field crops using airborne radiometry and ground-based meteorological data*, Irrigation Science 8, 1987, p 81-90.
- Kite G.W. and Droogers P., *Comparing evapotranspiration estimates from satellites, hydrological models and field data*, Journal of Hydrology 229, 2000, p.3-18.
- Kustas W.P. and Norman J.M., *Use of remote sensing for evapotranspiration monitoring over land surfaces*, Hydrological Sciences Journal 41, 1996, p.495-516.
- Kustas W.P. and Daughtry, *Estimation of the soil heat flux/net radiation ratio from spectral data*, Agricultural and Forest Meteorology 49, 1990, p. 205-223.
- Monteith J.L. and M.H. Unsworth, *Principles of Environmental Physics*, Edward Arnold Publishing Division, Hodder and Stoughton Ltd., London, 1990.
- Moran M.S., Jackson R.D., Raymond L.H., Gay L.W. and Slater P.N., *Mapping Surface Energy Balance Components by Combining Landsat Thematic Mapper and Ground-Based Meteorological Data*, 1989.
- Moran M.S. and Jackson R.D., *Assesing the Spatial Distribution of Evapotranspiration Using Remotely Sensed Inputs*, Journal of Environmental Quality 20, 1991, p.725-737.
- Prata A.J., Caselles V., Coll C., Sobrino J.A. and Ottlé C., *Thermal Remote Sensing of Land Surface Temperature from Satellites*, Current Status and Future Prospects, Remote Sensing Reviews, vol. 12, 1995, p. 175-224.
- Rahman H. and Dedieu G., *SMAC: A simplified method for the atmospheric correction of satellite measurements in the solar spectrum*, International Journal of Remote Sensing, Vol. 15, No. 1, 1994, p. 123-143.
- Valiente J.A, Nunez M., Lopez-Baeza E. and Moreno J.F., *Narrow-band to broad-band conversion from Meteosat-visible channel and broad-band albedo using both AVHRR-1 and -2 channels*, International Journal of Remote Sensing 16, No.6, 1995, p. 1147-1166.
- Van de Griend A.A. and Owe M., *On the relationship between thermal emissivity and the normalized difference vegetation index for natural surfaces*, International Journal of Remote Sensing, vol. 14, No.6, 1993, p. 1119-1131.

## 9 Groundwater Modelling as a Tool for Data Interpretation

*Wolfgang Kinzelbach, IHW, ETHZ, Zurich, Switzerland*

*Wen-Hsing Chiang, S.S. Papadopoulos Associates, Bethesda, MD, USA*

Aquifers share a number of features that necessitate the use of models in studies of them. The most obvious is their relative inaccessibility. The hydrogeologist usually knows the underground structure only at a few drilling points or at the occasional outcrop. From these scarce data he must reconstruct the complete aquifer, which is impossible without the use of models and hypotheses.

By simplifying the natural situation a conceptual picture of the aquifer structure is obtained, which has to be filled with quantitative information on, for example, transmissivity or recharge rate distribution, in order to arrive at a numerical groundwater model. The identification of recharge and discharge zones is also important. In arid and semi-arid environments, it should not be overlooked that vegetation may be discharging groundwater by evapotranspiration.

Without models there is no data interpretation in the geosciences. Often models are used unconsciously without accounting for their applicability. A hydrogeologist who uses the Theis formula to evaluate a pumping test is using a very crude model, which implies that the aquifer is two-dimensional, homogeneous, isotropic and of infinite extensions. A numerical aquifer model can take into account much more complex topology and boundary conditions, heterogeneity and vertical structure.

Another reason why models are useful and necessary in hydrogeology is the relatively slow pace of subsurface processes. The fact that timescales are usually long compared to the human lifespan severely restricts the possibility of experimenting and for practical decisions prognostic power – even if only approximate – is

necessary, which can only be come by through modelling. The most important quantities for resource management and ecological evaluations are the amount of water stored, the flow velocity, the recharge rates, total flux through a cross section, and arrival times.

These quantities are not directly measurable, and must be determined indirectly from measurable quantities such as piezometric heads, spring flows, and environmental tracer concentrations. The model is the link between measurable and desired quantities.

In addition, one should bear in mind that drilling an observation well is usually an expensive process, and therefore a significant effort is justified in getting all possible information out of the observation data.

Groundwater models are divided into flow and transport models. While the flow models describe the distributions of piezometric head and Darcy flux in the domain, transport models compute the distribution and migration of substances carried by the water flux.

Further classification is possible, according to the processes involved, dimensionality, the solution methods used, and temporal behaviour. Models can also be used in both forward and inverse directions.

**Processes:** A flow model can be for phreatic, confined or leaky conditions. A transport model can be for an ideal tracer, which does not modify the flow field and is transported passively by it. It can, however, also consider density and chemical reactions. Multiphase flow processes can be taken into account as well as single phase unsaturated flows in the

aerated zone. For the problem of recharge estimation, flow models and transport models for passive tracers in very small concentrations are relevant. In the vadose zone, Richards' equation in all its variants is used to reproduce observed vertical tracer profiles. In the saturated zone, the larger scale transport of tracers in the horizontal directions is modelled.

**Dimensionality:** Before starting a spatially resolving modelling effort, a 0-dimensional model is advisable. This treats the aquifer as a box with inputs and outputs, as well as internal storage. (Box models for environmental tracers are described in Chapter 7.) 1-D models are used in the vadose zone and for laboratory columns. Horizontally 2D models are the most common for regional aquifers, where the thickness is usually much smaller than the horizontal extension. However, if several layers (aquifers) with distinctly different piezometric heads exist, a layered model (2.5 D) or a 3D model becomes necessary. Transport in general requires 3D modelling. When modelling environmental tracers in deep aquifers, it has to be remembered that the penetration depth of the tracer may be small and depth-averaged concentrations of a model are not directly comparable to concentrations measured in shallow wells.

**Solution methods:** The solution methods start out from a discretization in space and time, as the computer cannot treat infinitely many numbers contained in the continuum, but rather only a finite set of numbers. The spatial discretization can be performed by Finite Difference Methods, which cut the continuum into prismatic boxes, or by the more flexible Finite Element or Finite Volume Methods with triangular or more complex shaped elements, including an interpolation function for the distribution of the computed quantity inside these elements. The transport equation is of a different nature to the flow equation. While the flow equation is a diffusion equation for pressure, the transport equation (besides

diffusion-like terms) also contains an advective frontal movement term. This necessitates special caution and eventually dedicated solution methods preserving fronts, such as the Method of Characteristics or random walk methods.

**Time behaviour:** While flow modelling usually starts from a long-term averaged steady state situation, transport can usually not be reduced to steady state but has to be modelled in time varying mode. In arid and semi-arid environments, it has to be remembered that steady state situations are rare due to the highly erratic variations of inputs – even when dealing with larger timescales.

**Forward vs. inverse modelling:** In the forward modelling mode of the flow model all parameters are given, including geometry, boundary and initial conditions, transmissivities or hydraulic conductivities, storage coefficients, specific yields, recharge rates, pumping rates, depth-dependent evapotranspiration rates, water levels in surface water bodies, and leakage factors. From these parameters the piezometric head distribution in space and in time can be computed, which in turn allows one to determine the distribution of Darcy fluxes in space and time. In transport modelling additional input data are required, including porosity, dispersivities, initial and boundary conditions for solute concentrations, and solute input rates.

Usually not all these parameters are available in sufficient accuracy. However, piezometric head and concentration observations do exist. In such cases, the model can be used in inverse mode on the measured data of the past. In this way, the heads and concentrations plus some parameters become known, while the remaining parameters remain unknown. They are then determined by systematic parameter variation, with the goal of matching the observation data as closely as possible. This procedure is also known as 'model calibration'.

In principle all transmissivities on the grid can be considered as unknowns. The presently preferred approach reduces the spatial distribution to a much smaller number of parameter values, either through zones with constant value or by a pivot point method, in which the spatial distribution is obtained by interpolation (e.g. Kriging method) between the values at a smaller number of pivot points. The number of parameter values to be estimated should clearly be smaller than the number of head measurements available. The fitting procedure minimises the sum of squared differences between measured and calculated quantities in a regressive sense.

The basic problem of inverse modelling is a uniqueness problem. If both transmissivities and recharge rates are unknown, a flow model usually cannot find a unique solution to the parameter estimation problem purely from head observations. For the inverse problem, the better known of the two types of data is inserted into the model as known, while the second one is estimated. Usually the better known is the recharge rate, as the transmissivity is log-normally distributed and a good regional representative value cannot easily be estimated from few pumping test data. The suggested procedure therefore is to choose a recharge rate from independent methods (as described above), and then to estimate transmissivities from observation data. To remain conservative for management purposes, the recharge can then be varied to its probable low value and the procedure can be repeated. The transmissivities obtained can be compared to the available pumping test results, and should usually fall within the interval that they span. Only when the transmissivity field is well known can the recharge be taken as the parameter to be identified.

Taking into account other quantities apart from heads helps to better determine the estimation problem. These other quantities

can be observed discharges into rivers or concentrations of environmental isotopes, especially chloride, when the chloride method is applicable. Environmental tracers naturally require new parameters beyond the known input function, such as porosities and dispersivities. But dispersivities are usually not very sensitive parameters for the regional input of environmental tracers, while porosities are in a porous aquifer of loose sediments determined within a factor of 2 at most.

It is often thought that a 'perfect fit' of observation is desirable and should be achieved in any way possible. The way usually chosen is to over-parametrize the model and then reach quasi-perfect agreement between observations and calculated values. In an over-parametrized model, however, such 'perfect' solutions usually exist with rather different parameter combinations. It is more likely that a cruder model, which does not go for the perfect fit, is preferable to an over-parametrized model.

The CD-ROM accompanying this report (or [www.unep.org/water/groundwater/](http://www.unep.org/water/groundwater/)) contains the software for a complete groundwater flow and transport model. The programme PMWIN5, a pre- and post-processor, includes the USG models MOFLOW, UCODE and MOC, as well as MT3D, MT3DMS, PMPATH and PEST. An MSWord tutorial for 'Your first groundwater model with PMWIN' is also provided.

A standard modelling task should proceed with the following steps:

- 1) Identification of the problem to be solved;
- 2) Construction of a conceptual model of the aquifer;
- 3) Data collection;
- 4) Definition of boundaries of the modelled domain;
- 5) Discretization;
- 6) Entry of data into the model;



- 7) Running of the model in forward mode;
- 8) Model calibration;
- 9) Model application.

So how do these steps contribute to the greater purpose of recharge estimation?

- 1) Here our task is to determine the recharge and to find out whether a pumping regime is sustainable or not.
- 2) The conceptual model has to use all the available geological data and possible ideas on the genesis of the aquifer in order to create as realistic a geometric model as possible.
- 3) Data often have to be collected from a variety of institutions and government offices. Sometimes raw data must be obtained from the operational records of local wells. New data can of course also be measured. This step is usually the most costly and time consuming of them all.
- 4) The definition of boundaries implies that a general picture is available of the flow system between recharge and discharge. The boundary conditions will constrain the flow problem and the right choice is therefore of great importance. It is not advisable to use fixed head boundaries excessively. A model that is bounded by fixed head boundary conditions on all sides can only interpolate given data and is not utilisable for predictions of situations in which wells will influence the heads at the chosen boundaries. Natural boundaries, which are preferable, include rivers, water divides, or boundaries where aquifers end. Fixed head boundaries should preferably be used downstream, where the aquifer discharges, while upstream flux boundary conditions are more advisable to guarantee that pumps in the future cannot pump more water (out of a fixed head node) than is available. Streamlines, which are relatively constant in time and which can be obtained from head contour maps, as well as water divides are zero

flux boundaries that are convenient to use. If a river is in steady contact with the aquifer, it is modelled as a fixed (or prescribed) head boundary condition. If colmatation reduces the connection, a third type of boundary condition is more appropriate, which puts a resistance between the groundwater head and the river head.

- 5) Discretization of a flow model should be adequate to resolve the expected gradients. Mesh refinement around wells is advisable if observations close to wells are to be interpreted. Heads in a well are not reproduced in a regional model as the cells are much too large, even after refinement. The head in a model cell represents rather an average over this cell than the real head in the well bore. A finer discretization is usually required in a transport model than in a flow model. For standard FD and FE methods, the mesh size should be not larger than twice the longitudinal dispersivity. But for the method of characteristics this requirement can be relaxed.
- 6) The data entry into the model can be done by a pre-processor, which is provided in PMWIN. The programme accepts the data in an interactive way. Distributed data can first be interpolated and brought into grid form with PMDIS, a tool contained in PMWIN, or with any other contouring software such as SURFER (by Golden Software).
- 7) The model is run with a complete data set in forward mode to check that all inputs are correct. The results can be displayed with various tools in the form of contour maps or a time series. The complete data set may only be obtained by inserting reasonable generic values for all unknown data. One way of handling the situation is to estimate all input data through independent methods, such as the averaging of pumping test results, recharge estimates using environmental tracer data, etc. When the model is run, it can be checked

whether the results for heads and/or concentrations are in agreement with these observations. Such a consistency check is the first and most important task of a groundwater model.

- 8) The model calibration then tries to complete input data in a more organised fashion, such that observed and computed values are in close agreement. We might choose a recharge scenario and adapt transmissivities using head observations. The result can be compared to the available transmissivity data. A variation of the initial assumption to a low or a high scenario with subsequent repetition of the calibration task will show how sensitively the transmissivities react. If the estimated transmissivities fall out of reasonable intervals or a fit becomes impossible, this is a sure sign that our assumed recharge is already outside the realistic range. Of course, we can also proceed by assuming zonal transmissivities from pumping tests and vary recharge such that heads and environmental tracer concentrations are reproduced satisfactorily. Extensive sensitivity analysis is always advisable. In this task, the input parameters are varied and the reaction of computed variables is recorded. Sensitive parameters are easy to estimate. Insensitive parameters are less relevant and the values used need not be accurate.
- 9) The calibrated model can now be used for forecasts. Locations and abstraction rates of wells can be varied. The consequences of draw-downs, the reversal of flow directions and other scenarios can be assessed and plans of action optimised.

It should always be remembered that a model is only a crude manmade picture of nature. All models contain uncertainties. The user of model results should always take this into account when choosing their path of action. There are several techniques that allow one to take robust,

well-informed decisions even if the model results are uncertain. The most traditional of these is to take conservative decisions. If, for example, a recharge rate is determined on the basis of best estimates of transmissivities, one could deliberately take transmissivities on the low side and then through calibration obtain a low value for recharge. Decisions based on such a lower estimate will be safe.

More elaborate ways of taking into account uncertainties exist. Using the techniques of 'stochastic modelling', all parameters are considered as probability distributions instead of single values. The results of one's calculations are therefore also a probability distribution of heads or recharge rates. Practical calculations may follow the so-called 'Monte Carlo method', which requires making many model runs with various combinations of feasible parameters and ordering the results according to statistics. From such statistics, a course of action can be chosen that stays within given limits with a predefined probability. While in fields such as meteorology and air pollution protection, the probabilistic point of view is already common, in the field of groundwater studies the concept is still relatively new – and decision makers still have to get used to it.

## References

- Chiang W.-H., Kinzelbach W. and Rausch R., *Aquifer Simulation Model for WINDOWS*, Gebrüder Borntraeger, Berlin Stuttgart, 1998, 136 p.
- Chiang W.-H. and Kinzelbach W., *3D-Groundwater Modeling with PMWIN – A Simulation System for Modeling Groundwater Flow and Pollution*, Springer Berlin Heidelberg New York, 2000, 346 p.
- Kinzelbach W., *Numerische Methoden zur Modellierung des Transports von Schadstoffen im Grundwasser*, Oldenbourg Verlag, München, 1987, 313 S. 2. ed. 1992.
- Kinzelbach, W., *Groundwater Modelling - An Introduction with Sample Programs in BASIC*, Elsevier Science Publishers, Amsterdam, 1986, 333 S.
- Kinzelbach, W. and Rausch R., *Grundwassermodellierung - Eine Einführung mit Beispielen*, Borntraeger Verlag Stuttgart, 1995, S. 283.

## List of Contributors

### **Carmen Alberich**

Institute of Hydromechanics and Water  
Resources Management,  
ETH-Hoenggerberg,  
8093 Zürich, Switzerland.  
[alberich@ihw.baug.ethz.ch](mailto:alberich@ihw.baug.ethz.ch)

### **Werner Aeschbach-Hertig**

EAWAG/ETH, Postfach 611,  
8600 Duebendorf, Switzerland  
[aeschbach@eawag.ch](mailto:aeschbach@eawag.ch)

### **Ibrahim Baba Goni**

Dept. of Geology,  
University of Maiduguri,  
Maiduguri, Nigeria.  
[ibgoni@infoweb.abs.net](mailto:ibgoni@infoweb.abs.net)  
[ibgoni@yahoo.com](mailto:ibgoni@yahoo.com)

### **Urs Beyerle**

Department of Climate and Environmental  
Physics,  
University of Bern,  
Sidlerstrasse 5,  
3012 Bern, Switzerland.  
[beyerle@climate.unibe.ch](mailto:beyerle@climate.unibe.ch)

### **Philip Brunner**

Institute of Hydromechanics and Water  
Resources Management,  
ETH-Hoenggerberg,  
8093 Zürich, Switzerland.  
[brunner@ihw.baug.ethz.ch](mailto:brunner@ihw.baug.ethz.ch)

### **Wen-Hsing Chiang**

Excel Info Tech, Inc.  
20 Fairbanks, Suite 187  
Irvine, CA 92618  
USA  
[wchiang@neteit.com](mailto:wchiang@neteit.com)

### **Wolfgang Kinzelbach**

Institute of Hydromechanics and Water  
Resources Management,  
ETH-Hoenggerberg,  
8093 Zürich, Switzerland.  
[kinzelbach@ihw.baug.ethz.ch](mailto:kinzelbach@ihw.baug.ethz.ch)

### **Joerg Rueedi**

Department of Climate and Environmental  
Physics,  
University of Bern,  
Sidlerstrasse 5,  
3012 Bern, Switzerland.  
[rueedi@climate.unibe.ch](mailto:rueedi@climate.unibe.ch)

### **Kai Zoellmann**

Formerly: Institute of Hydromechanics and  
Water Resources Management,  
ETH-Hoenggerberg,  
8093 Zürich, Switzerland.  
[kzoe@gmx.de](mailto:kzoe@gmx.de)

## Appendix: Your First Groundwater Model with PMWIN

W.- H. Chiang and W. Kinzelbach

It takes just a few minutes to build your first groundwater flow model with PMWIN. First create a groundwater model by choosing *New Model* from the *File* menu. Then determine the size of the model grid by choosing *Mesh Size* from the *Grid* menu. Specify the geometry of the model and set the model parameters, such as hydraulic conductivity, effective porosity etc. Finally, perform the flow simulation by choosing *MODFLOW > Run...* from the *Models* menu.

After completing the flow simulation, you can use the modelling tools provided by PMWIN to view the results, to calculate water budgets of particular zones, or to graphically display the results, such as head contours. You can also use PMPATH to calculate and save path lines or use the finite difference transport models MT3D or MOC3D to simulate transport processes.

For more detailed information on PMWIN get hold of the book by Chiang and Kinzelbach, PMWIN, Springer Verlag, 2000.

### 1 Overview of the Sample Problem

As shown in Fig.1, an aquifer system with two stratigraphic units is bounded by no-flow boundaries on the North and South sides. The West and East sides are bounded by rivers, which are in full hydraulic contact with the aquifer and can be considered as fixed-head boundaries. The hydraulic heads on the west and east boundaries are 9 m and 8 m above reference level, respectively.

The aquifer system is unconfined and isotropic. The horizontal hydraulic conductivities of the first and second stratigraphic units are 0.0001 m/s and 0.0005 m/s, respectively. Vertical hydraulic conductivity of both units is

assumed to be 10% of the horizontal hydraulic conductivity. The effective porosity is 25%. The elevation of the ground surface (top of the first stratigraphic unit) is 10 m. The thickness of the first and the second units is 4 m and 6 m, respectively. A constant recharge rate of  $8 \times 10^{-9}$  m/s is applied to the aquifer. A contaminated area lies in the first unit next to the western boundary. The task is to isolate the contaminated area using a fully penetrating pumping well located next to the eastern boundary.

A numerical model has to be developed for this site to calculate the required pumping rate of the well. The pumping rate must be high enough, so that the contaminated area lies within the capture zone of the well. We will use PMWIN to construct the numerical model and use PMPATH to compute the capture zone of the pumping well. Based upon the calculated groundwater flow field, we will use MT3D and MOC3D to simulate the contaminant transport. We will show how to use PEST and UCODE to calibrate the flow model and finally we will create an animation sequence displaying the development of the contaminant plume.

To demonstrate the use of the transport models, we assume that the pollutant is dissolved into groundwater at a rate of  $1 \times 10^{-4}$  m<sup>3</sup>/s/m<sup>2</sup>. The longitudinal and transverse dispersivity values of the aquifer are 10 m and 1 m, respectively. The retardation factor is 2. The initial concentration, molecular diffusion coefficient, and decay rate are assumed to be zero. We will calculate the concentration distribution after a simulation time of 3 years and display the breakthrough curves (concentration versus time) at two points [X, Y] = [290, 310], [390, 310] in both units.

## 2 Run a Steady-State Flow simulation

Six main steps must be performed in a steady-state flow simulation:

1. Create a new model
2. Assign model data
3. Perform the flow simulation
4. Check simulation results
5. Calculate subregional water budget
6. Produce output

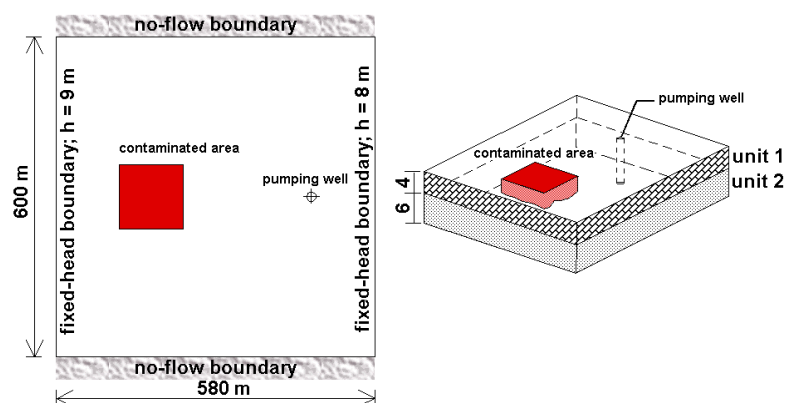


FIG. 1: CONFIGURATION OF THE SAMPLE PROBLEM

### 2.1 Step 1: Create a New Model

The first step in running a flow simulation is to create a new model.

#### ► To create a new model

1. Choose *New Model* from the *File* menu. A *New Model* dialog box will appear. Select a folder for saving the model data, such as C:\PM5DATA\SAMPLE, and type the file name SAMPLE for the sample model. A model must always have the file extension .PM5. All file names valid under Windows 95/98/NT with up to 120 characters can be used. It is a good idea to save every model in a separate folder, where the model and its output data will be kept. This will also allow you to run several models simultaneously (multitasking).
2. Click *OK*.  
PMWIN takes a few seconds to create the new model. The name of the new model name is shown in the title bar.

### 2.2 Step 2: Assign Model Data

The second step in running a flow simulation is to generate the model grid (mesh), specify boundary conditions, and assign model parameters to the model grid.

PMWIN requires the use of **consistent units** throughout the modeling process. For example, if you are using length [L] units of metres and time [T] units of seconds, hydraulic conductivity will be expressed in units of [m/s], pumping rates will be in units of [m<sup>3</sup>/s] and dispersivities will be in units of [m].

In MODFLOW, an aquifer system is replaced by a discretized domain consisting of an array of nodes and associated finite difference blocks (cells). Fig. 2 shows a spatial discretization of an aquifer system with a mesh of cells and nodes at which hydraulic heads are calculated. The nodal grid forms the framework of the numerical model. Hydrostratigraphic units can be represented by one or more model layers. The thickness of each model cell and the

width of each column and row may be variable. The locations of cells are described in terms of columns, rows and layers. PMWIN uses an index notation [J, I, K] for locating the cells. For example, the cell located in the 2nd column, 6th row, and the first layer is denoted by [2, 6, 1].

The model domain is discretized in boxes of horizontal dimensions of 20 m by 20 m. The boxes in the first layer are chosen to have the thickness of the stratigraphic layer (4 m). The second stratigraphic layer is discretized into two layers of boxes of 3 m thickness each for demonstration purposes.

► **To generate the model grid**

1. Choose *Mesh Size* from the *Grid* menu. The *Model Dimension* dialog box appears (Fig. 3).

2. Enter 3 for the number of layers, 30 for the numbers of columns and rows, and 20 for the size of columns and rows.

The first and second stratigraphic units will be represented by one and two model layers, respectively.

3. Click *OK*. PMWIN changes the pull-down menus and displays the generated model grid (Fig. 4). PMWIN allows you to shift or rotate the model grid, change the width of each model column or row, or to add/delete model columns or rows. For our sample problem, you do not need to modify the model grid.
4. Choose *Leave Editor* from the *File* menu or click the *leave editor* button

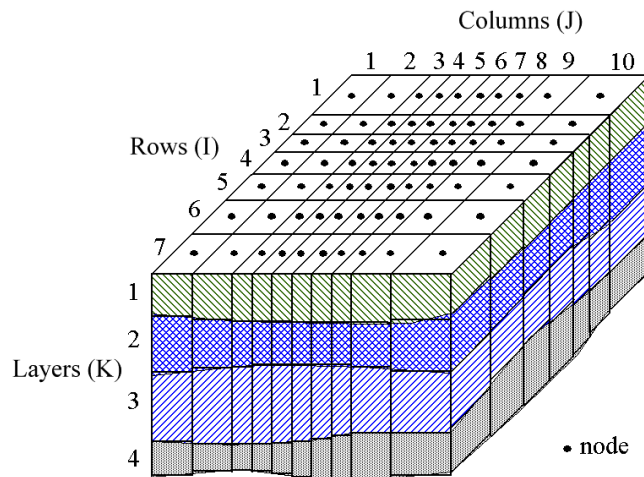


FIG. 2: SPATIAL DISCRETIZATION OF AN AQUIFER SYSTEM AND THE CELL INDICES

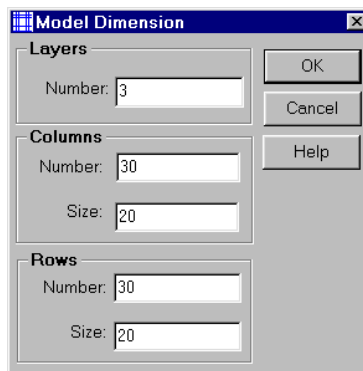


FIG. 3: THE *MODEL DIMENSION* DIALOG BOX

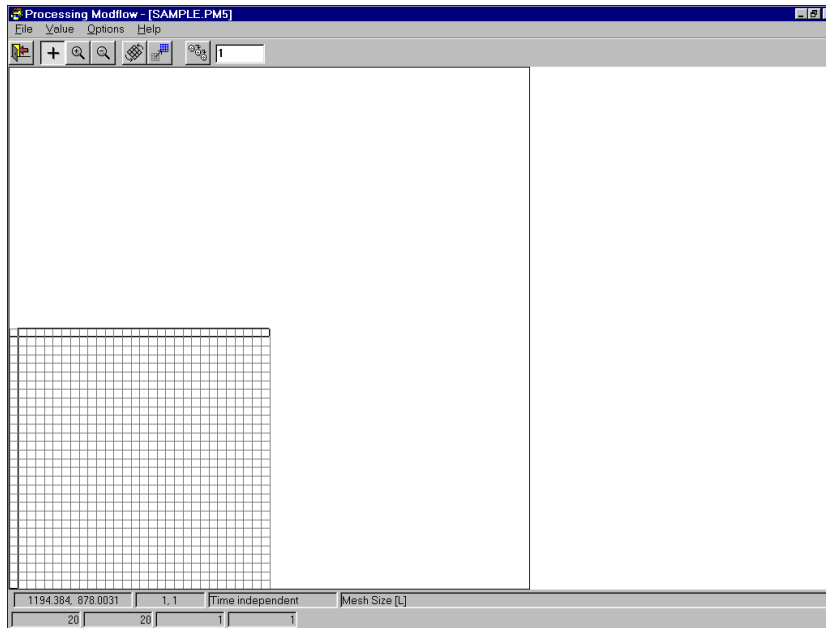


FIG. 4: THE GENERATED MODEL GRID

The next step is to specify the type of layers

► **To assign the type of layers**

1. Choose *Layer Type* from the *Grid* menu.  
A *Layer Options* dialog box appears.
2. Click a cell of the *Type* column, a drop-down button will appear within the cell. By clicking the drop-down button, a list containing the available layer types (Fig. 5) will be displayed.
3. Select *1: Unconfined* for the first layer and *0: Confined* for the other layers then click *OK* to close the dialog box.

MODFLOW is a multi-layer model. The layers are coupled via the leakage principle. The terms *leakance* or *vertical leakance* are used to account for the leakage. As transmissivity and leakance are - by default - assumed to be calculated (see Fig. 5) from conductivities and geometrical properties, the primary input variables to be specified are horizontal and vertical hydraulic conductivities.

You must now specify basic boundary conditions of the flow model. The basic boundary condition array (IBOUND array) contains a code for each model cell that indicates whether (1) the hydraulic head is computed (active variable-head cell or active cell), (2) the hydraulic head is kept fixed at a given value (fixed-head cell or

time-varying specified-head cell), or (3) no flow takes place within the cell (inactive cell). Use 1 for an active cell, -1 for a constant-head cell, and 0 for an inactive cell. For the sample problem, we need to assign -1 to the cells on the west and east boundaries and 1 to all other cells. Any outer boundary cell, which is not a fixed head cell, is automatically a zero flux boundary cell. Flux boundaries with non-zero fluxes are simulated by assigning appropriate infiltration or pumping wells in the corresponding cell via the well package. Third type boundary conditions are modeled by means of the general head boundary package or the river package.

► **To assign the boundary condition to the flow model**

1. Choose *Boundary Condition > IBOUND (Modflow)* from the *Grid* Menu.


The *Data Editor* of PMWIN appears with a plan view of the model grid (Fig. 6). The grid cursor is located at the cell [1, 1, 1], which is the upper-left cell of the first layer. The value of the current cell is shown at the bottom of the status bar. The default value of the IBOUND array is 1. The grid cursor can be moved horizontally by using the arrow keys or by clicking the mouse on the desired position. To move to

another layer, use *PgUp* or *PgDn* keys or click the edit field in the tool bar, type the new layer number, and then press enter.

**Note.** A DXF-map is loaded by using the *Maps Options* dialog box.

2. Press the *right* mouse button. PMWIN shows a Cell Value dialog box.
3. Type -1 in the dialog box, then click *OK*.

The upper-left cell of the model has been specified to be a fixed-head cell.

4. Now turn on duplication by clicking the *duplication* button .

Duplication is on if the duplication button is sunk. The current cell value will be duplicated to all cells passed by the grid cursor, if it is moved while duplication is on. You can turn off duplication by clicking the duplication button again.

5. Move the grid cursor from the upper-left cell [1, 1, 1] to the lower-left cell [1, 30, 1] of the model grid.

The value of -1 is duplicated to all cells on the west side of the model.

6. Move the grid cursor to the upper-right cell [30, 1, 1].
7. Move the grid cursor from the upper-right cell [30, 1, 1] to the lower-right cell [30, 30, 1].


The value of -1 is duplicated to all cells on the east side of the model.

8. Turn on layer copy by clicking the *layer copy* button .

Layer copy is on if the layer copy button is sunk. The cell values of the current layer will be copied to other layers, if you move to the other model layer while layer copy is on. You can turn off layer copy by clicking the layer copy button again.

9. Move to the second layer and then to the third layer by pressing the *PgDn* key twice.

The cell values of the first layer are copied to the second and third layers.

10. Choose *Leave Editor* from the *File* menu or click the *leave editor* button .

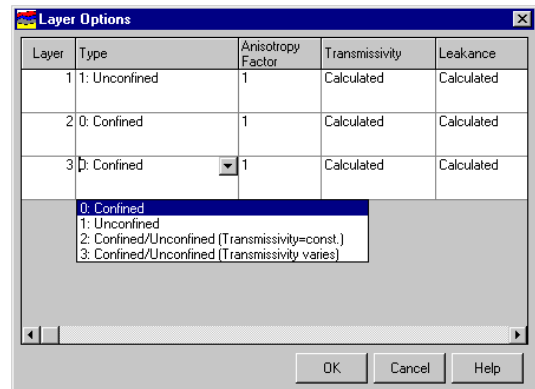


FIG. 5: THE *LAYER OPTIONS* DIALOG BOX AND THE *LAYER TYPE* DROP-DOWN LIST

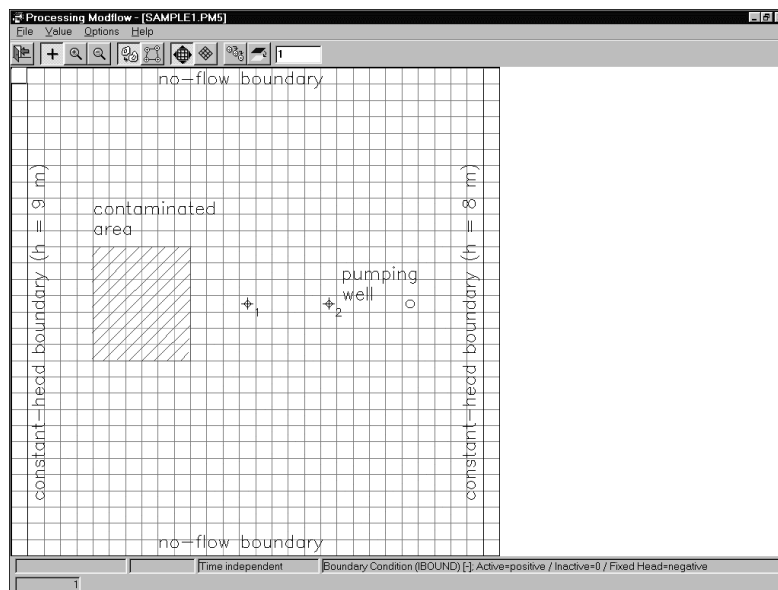



FIG. 6: THE *DATA EDITOR* DISPLAYING THE PLAN VIEW OF THE MODEL GRID.




The next step is to specify the geometry of the model.

► **To specify the elevation of the top of model layers**

1. Choose *Top of Layers (TOP)* from the *Grid* menu.  
PMWIN displays the model grid.
2. Choose *Reset Matrix...* from the *Value* menu (or press Ctrl+R).  
A *Reset Matrix* dialog box appears.
3. Enter 10 in the dialog box, then click *OK*.  
The elevation of the top of the first layer is set to 10.
4. Move to the second layer by pressing *PgDn*.
5. Repeat steps 2 and 3 to set the top elevation of the second layer to 6 and the top elevation of the third layer to 3.
6. Choose *Leave Editor* from the *File* menu or click the *leave editor* button .

► **To specify the elevation of the bottom of model layers**

1. Choose *Bottom of Layers (BOT)* from the *Grid* menu.
2. Repeat the same procedure as described above to set the bottom elevation of the first, second and third layers to 6, 3 and 0, respectively.
3. Choose *Leave Editor* from the *File* menu or click the *leave editor* button .

We are going to specify the temporal and spatial parameters of the model. The spatial parameters for the sample problem include the initial hydraulic head, horizontal and vertical hydraulic conductivities, and effective porosity.

► **To specify the temporal parameters**


1. Choose *Time...* from the *Parameters* menu.  
A *Time Parameters* dialog box appears. The temporal parameters include the time unit and the numbers of stress periods, time steps and transport steps.

In MODFLOW, the simulation time is divided into stress periods - i.e. time intervals during which all external excitations or stresses are constant - which are, in turn, divided into time steps. In most transport models, each flow time step is further divided into smaller transport steps. The length of stress periods is not relevant to a steady state flow simulation. However, as we want to perform contaminant transport simulation with MT3D and MOC3D, the actual time length must be specified in the table.

2. Enter 9.46728E+07 (seconds) for the *Length* of the first period.
3. Click *OK* to accept the other default values.  
This implies that a steady state flow simulation will be carried out.

You now need to specify the initial hydraulic head for each model cell. The initial hydraulic head at a fixed-head boundary will be kept constant during the flow simulation. The other heads are starting values in a transient simulation or first guesses for the iterative solver in a steady-state simulation. Here we first set all values to 8 and then correct the values on the West side by overwriting them with a value of 9.

► **To specify the initial hydraulic head**

1. Choose *Initial Hydraulic Heads* from the *Parameters* menu.  
PMWIN displays the model grid.
2. Choose *Reset Matrix...* from the *Value* menu (or press Ctrl+R) and enter 8 in the dialog box, then click *OK*.
3. Move the grid cursor to the upper-left model cell.
4. Press the *right* mouse button and enter 9 into the *Cell Value* dialog box, then click *OK*.
5. Now turn on *duplication* by clicking the *duplication* button .  
Duplication is on if the relief of the *duplication* button is sunk. The current cell value will be duplicated to all cells passed over by the grid cursor, if *duplication* is on.

6. Move the grid cursor from the upper-left cell to the lower-left cell of the model grid.


The value of 9 is duplicated to all cells on the West side of the model.

7. Turn on *layer copy* by clicking the *layer copy* button .


Layer copy is on if the *layer copy* button is sunk. The cell values of the current layer will be copied to another layer, if you move to the other model layer while *layer copy* is on.

8. Move to the second layer and the third layer by pressing *PgDn* twice.

The cell values of the first layer are copied to the second and third layers.


9. Choose *Leave Editor* from the *File* menu or click the *leave editor* button .

► **To specify the horizontal hydraulic conductivity**

1. Choose *Horizontal Hydraulic Conductivity* from the *Parameters* menu.
2. Choose *Reset Matrix...* from the *Value* menu (or press *Ctrl+R*), type 0.0001 in the dialog box, then click *OK*.
3. Move to the second layer by pressing *PgDn*.
4. Choose *Reset Matrix...* from the *Value* menu (or press *Ctrl+R*), type 0.0005 in the dialog box, then click *OK*.
5. Repeat steps 3 and 4 to set the value of the third layer to 0.0005.
6. Choose *Leave Editor* from the *File* menu or click the *leave editor* button .

► **To specify the vertical hydraulic conductivity**


1. Choose *Vertical Hydraulic Conductivity* from the *Parameters* menu.
2. Choose *Reset Matrix...* from the *Value* menu (or press *Ctrl+R*), type 0.00001 in the dialog box, then click *OK*.
3. Move to the second layer by pressing *PgDn*.
4. Choose *Reset Matrix...* from the *Value* menu (or press *Ctrl+R*), type 0.00005 in the dialog box, then click *OK*.

5. Repeat steps 3 and 4 to set the value of the third layer to 0.00005.
6. Choose *Leave Editor* from the *File* menu or click the *leave editor* button .

► **To specify the effective porosity**


1. Choose *Effective Porosity* from the *Parameters* menu.

Because the standard value is the same as the prescribed value of 0.25, you may leave the editor and save the changes.

2. Choose *Leave Editor* from the *File* menu or click the *leave editor* button .

The effective porosity is not needed for the flow computation. However, it is necessary for the computation of travel times and transport.

► **To specify the recharge rate**

1. Choose *MODFLOW > Recharge* from the *Models* menu.
2. Choose *Reset Matrix...* from the *Value* menu (or press *Ctrl+R*), enter 8E-9 for *Recharge Flux [L/T]* in the dialog box, then click *OK*.
3. Choose *Leave Editor* from the *File* menu or click the *leave editor* button .

The last step before performing the flow simulation is to specify the location of the pumping well and its pumping rate. In MODFLOW, an injection or a pumping well is represented by a node (or a cell). The user specifies an injection or a pumping rate for each node. It is implicitly assumed that the well penetrates the full thickness of the cell. MODFLOW can simulate the effects of pumping from a well that penetrates more than one aquifer or layer, provided that the user supplies the pumping rate for each layer. The total pumping rate for the multi-layer well is equal to the sum of the pumping rates from the individual layers. The pumping rate for each layer ( $Q_k$ ) can be approximately calculated by dividing the total pumping rate ( $Q_{total}$ ) in proportion to the layer

transmissivity (McDonald and Harbaugh 1988):


$$Q_k = Q_{total} \cdot \frac{T_k}{\Sigma T} \quad (1)$$

where  $T_k$  is the transmissivity of layer  $k$  and  $\Sigma T$  is the sum of the transmissivities of all layers penetrated by the multi-layer well. Unfortunately, as the first layer is unconfined, we do not exactly know the saturated thickness and the transmissivity of this layer at the position of the well. Equation 1 cannot be used unless we assume a saturated thickness for calculating the transmissivity. Another possibility to simulate a multi-layer well is to set a very large vertical hydraulic conductivity (or vertical leakance), e.g. 1 m/s, to all cells of the well. The total pumping rate is assigned to the lowest cell of the well. For the display purpose, a very small pumping rate (say,  $1 \times 10^{-10}$  m<sup>3</sup>/s) can be assigned to other cells of the well. In this way, the exact extraction rate from each penetrated layer will be calculated by MODFLOW implicitly and the value can be obtained by using the *Water Budget Calculator* (see below).

As we do not know the required pumping rate for capturing the contaminated area shown in Fig. 1, we will try a total pumping rate of 0.0012 m<sup>3</sup>/s.

► **To specify the pumping well and the pumping rate**

1. Choose *MODFLOW > Well* from the *Models* menu.
2. Move the grid cursor to the cell [25, 15, 1]
3. Press the right mouse button and type -1E-10, then click *OK*.  
*Note.* A negative value is used to indicate a *pumping* well.
4. Move to the second layer by pressing *PgDn*.
5. Press the right mouse button and type -1E-10 then click *OK*.
6. Move to the third layer by pressing *PgDn*.
7. Press the right mouse button and type -0.0012 then click *OK*.

8. Choose *Leave Editor* from the *File* menu or click the *leave editor* button .
9. Now go back to the vertical hydraulic conductivity menu and modify the value at the location of the well to 1 in all layers

### 2.3 Step 3: Perform the Flow Simulation

Before starting the computation, a solver has to be chosen. Here the default solver PCG2 with its default settings is used automatically.

► **To perform the flow simulation**

1. Choose *MODFLOW > Run...* from the *Models* menu.  
The Run Modflow dialog box appears (Fig. 7).
2. Click *OK* to start the flow computation. Prior to running MODFLOW, PMWIN will use the user-specified data to generate input files for MODFLOW (and optionally MODPATH) as listed in the table of the Run Modflow dialog box. An input file will be generated only if the generate flag is set to . You can click on the button to toggle the generate flag between  and . Normally, you do not need to change the flags, as PMWIN will take care of the settings.

### 2.4 Step 4: Check Simulation Results

During a flow simulation, MODFLOW writes a detailed run record to the listing file *path\OUTPUT.DAT*, where *path* is the folder in which your model data are saved. If a flow simulation is successfully completed, MODFLOW saves the simulation results in various unformatted (binary) files as listed in Table 1. Prior to running MODFLOW, the user may control the output of these unformatted (binary) files by choosing *Modflow > Output Control* from the *Models* menu. The output file *path\INTERBED.DAT* will only be

generated if the Interbed Storage Package is activated.

To check the quality of the simulation results, MODFLOW calculates a volumetric water budget for the entire model at the end of each time step, and saves it in the file *output.dat* (see Table 2). A water budget provides an indication of the overall acceptability of the numerical solution. In numerical solution techniques, the system of equations solved by a model actually consists of a flow continuity statement for each model cell. Continuity should also exist for the total flows into and out of the entire model or a sub-region. This means that the difference between total inflow and total outflow should be equal to 0 (steady-state flow simulation) or to the total change in storage (transient flow simulation). If the accuracy is insufficient, a new run should be made using a smaller

convergence criterion in the iterative solver. It is recommended to check the record file or at least take a glance at it. The record file contains other further essential information. In case of difficulties, this supplementary information can be very helpful.

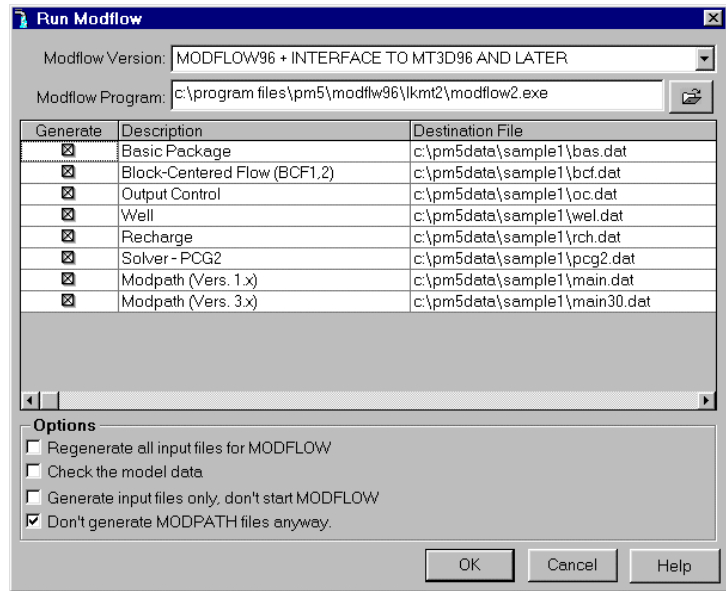


FIG. 7: THE RUN MODFLOW DIALOG BOX

TABLE 1: OUTPUT FILES FROM MODFLOW

File	Contents
<i>path\OUTPUT.DAT</i>	Detailed run record and simulation report.
<i>path\HEADS.DAT</i>	Hydraulic heads.
<i>path\DDOWN.DAT</i>	Drawdowns, the difference between the starting heads and the calculated hydraulic heads.
<i>path\BUDGET.DAT</i>	Cell-by-Cell flow terms.
<i>path\INTERBED.DAT</i>	Subsidence of the entire aquifer and compaction and preconsolidation heads in individual layers.
<i>path\MT3D.FLO</i>	Interface file to MT3D/MT3DMS. This file is created by the LKMT package provided by MT3D/MT3DMS (Zheng 1990, 1998).

- path is the folder in which the model data are saved.

TABLE 2: VOLUMETRIC BUDGET FOR THE ENTIRE MODEL WRITTEN BY MODFLOW

CUMULATIVE VOLUMES L**3	RATES FOR THIS TIME STEP L**3/T
<p>IN:            ----            CONSTANT HEAD = 209690.3590            WELLS = 0.0000            RECHARGE = 254472.9380</p> <p>TOTAL IN = 464163.3130</p> <p>OUT:            ----            CONSTANT HEAD = 350533.6880            WELLS = 113604.0310            RECHARGE = 0.0000</p> <p>TOTAL OUT = 464137.7190</p> <p>IN - OUT = 25.5938</p> <p>PERCENT DISCREPANCY = 0.01</p>	<p>IN:            ----            CONSTANT HEAD = 2.2150E-03            WELLS = 0.0000            RECHARGE = 2.6880E-03</p> <p>TOTAL IN = 4.9030E-03</p> <p>OUT:            ----            CONSTANT HEAD = 3.7027E-03            WELLS = 1.2000E-03            RECHARGE = 0.0000</p> <p>TOTAL OUT = 4.9027E-03</p> <p>IN - OUT = 2.7008E-07</p> <p>PERCENT DISCREPANCY = 0.01</p>


## 2.5 Step 5: Calculate Sub-Regional Water Budget

There are situations in which it is useful to calculate water budgets for various sub-regions of the model. To facilitate such calculations, flow terms for individual cells are saved in the file *path*\BUDGET.DAT. These individual cell flows are referred to as cell-by-cell flow terms, and are of four types: (1) cell-by-cell stress flows, or flows into or from an individual cell due to one of the external stresses (excitations) represented in the model, e.g. pumping well or recharge; (2) cell-by-cell storage terms, which give the rate of accumulation or depletion of storage in an individual cell; (3) cell-by-cell constant-head flow terms, which give the net flow to or from individual fixed-head cells; and (4) internal cell-by-cell flows, which are the flows across individual cell faces—that is, between adjacent model cells. The **Water Budget Calculator** uses the cell-by-cell flow terms to compute water budgets for the entire model, user-specified sub-regions, and flows between adjacent sub-regions.

### ► To calculate sub-regional water budgets

1. Choose *Water Budget* from the *Tools* menu.

A *Water Budget* dialog box appears (Fig. 8). You do not need to change the settings in the *Time* group.

2. Click *Zones*.  
A zone is a sub-region of a model for which a water budget will be calculated. A zone is indicated by a zone number ranging from 0 to 50. A zone number must be assigned to each model cell. The zone number 0 indicates that a cell is not associated with any zone. Follow steps 3 to 5 to assign zone numbers 1 to the first and 2 to the second layer.
3. Choose *Reset Matrix...* from the *Value* menu, type 1 in the dialog box, then click *OK*.
4. Press PgDn to move to the second layer.
5. Choose *Reset Matrix...* from the *Value* menu, type 2 in the dialog box, then click *OK*.
6. Choose *Leave Editor* from the *File* menu or click the *leave editor* button .
7. Click *OK* in the *Water Budget* dialog box.

PMWIN calculates and saves the flows in the file *path*\WATERBDG.DAT as shown in Table 3. The unit of the flows is [L<sup>3</sup>T<sup>-1</sup>]. Flows are calculated for each zone in each layer and each time step. Flows are considered *IN* if they are entering a zone. Flows between sub regions are given in a



*Flow Matrix.* HORIZ. EXCHANGE gives the flow rate horizontally across the boundary of a zone. EXCHANGE (UPPER) gives the flow rate coming from (IN) or going to (OUT) to the upper adjacent layer. EXCHANGE (LOWER) gives the flow rate coming from (IN) or going to (OUT) to the lower adjacent layer. For example, considering EXCHANGE (LOWER) of ZONE=1 and LAYER=1, the flow rate from the first layer to the second layer is 2.587256E-03 m<sup>3</sup>/s. The percent discrepancy in Table 3 is calculated by

$$\frac{100 \cdot (IN - OUT)}{(IN + OUT)/2} \quad (2)$$

In this example, the percent discrepancy of in- and outflows for the model and each zone in each layer is acceptably small. This means the model equations have been correctly solved.

To calculate the exact flow rates to the well, we repeat the previous procedure for calculating sub-regional water budgets.

This time we only assign the cell [25, 15, 1] to zone 1, the cell [25, 15, 2] to zone 2 and the cell [25, 15, 3] to zone 3. All other cells are assigned to zone 0. The water budget is shown in Table 4. The pumping well is abstracting 7.7992809E-05 m<sup>3</sup>/s from the first layer, 5.603538E-04 m<sup>3</sup>/s from the second layer, and 5.5766129E-04 m<sup>3</sup>/s from the third layer. Almost all water withdrawn comes from the second stratigraphic unit, as can be expected from the configuration of the aquifer.

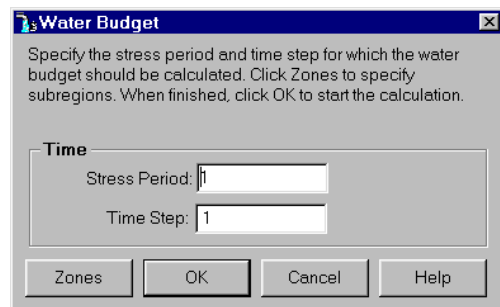


FIG. 8: THE WATER BUDGET DIALOG BOX

TABLE 3: OUTPUT FROM THE WATER BUDGET CALCULATOR

---

FLOWES ARE CONSIDERED "IN" IF THEY ARE ENTERING A SUBREGION  
THE UNIT OF THE FLOWS IS [L<sup>3</sup>/T]

---

TIME STEP	1 OF	STRESS PERIOD	1		
<b>ZONE= 1 LAYER= 1</b>					
FLOW TERM		IN	OUT	IN-OUT	
STORAGE	0.0000000E+00	0.0000000E+00	0.0000000E+00	0.0000000E+00	
CONSTANT HEAD	1.8407618E-04	2.4361895E-04	-5.9542770E-05		
HORIZ. EXCHANGE	0.0000000E+00	0.0000000E+00	0.0000000E+00		
EXCHANGE (UPPER)	0.0000000E+00	0.0000000E+00	0.0000000E+00		
<b>EXCHANGE (LOWER)</b>	<b>0.0000000E+00</b>	<b>2.5872560E-03</b>	<b>-2.5872560E-03</b>		
WELLS	0.0000000E+00	1.0000000E-10	-1.0000000E-10		
DRAINS	0.0000000E+00	0.0000000E+00	0.0000000E+00		
RECHARGE	2.6880163E-03	0.0000000E+00	2.6880163E-03		
.	.	.	.	.	.
SUM OF THE LAYER	2.8720924E-03	2.8308749E-03	4.1217543E-05		
-----					
.	.	.	.	.	.
<b>ZONE= 2 LAYER= 2</b>					
FLOW TERM		IN	OUT	IN-OUT	
STORAGE	0.0000000E+00	0.0000000E+00	0.0000000E+00	0.0000000E+00	
CONSTANT HEAD	1.0027100E-03	1.7383324E-03	-7.3562248E-04		
HORIZ. EXCHANGE	0.0000000E+00	0.0000000E+00	0.0000000E+00		
EXCHANGE (UPPER)	2.5872560E-03	0.0000000E+00	2.5872560E-03		
EXCHANGE (LOWER)	0.0000000E+00	1.8930938E-03	-1.8930938E-03		
WELLS	0.0000000E+00	1.0000000E-10	-1.0000000E-10		
DRAINS	0.0000000E+00	0.0000000E+00	0.0000000E+00		
RECHARGE	0.0000000E+00	0.0000000E+00	0.0000000E+00		
.	.	.	.	.	.
SUM OF THE LAYER	3.5899659E-03	3.6314263E-03	-4.1460386E-05		

---

TABLE 3: OUTPUT FROM THE WATER BUDGET CALCULATOR (CONTINUED)

WATER BUDGET OF SELECTED ZONES:

	IN	OUT	IN-OUT
ZONE( 1):	2.8720924E-03	2.8308751E-03	4.1217310E-05
ZONE( 2):	3.5899659E-03	3.6314263E-03	-4.1460386E-05

WATER BUDGET OF THE WHOLE MODEL DOMAIN:

FLOW TERM	IN	OUT	IN-OUT
STORAGE	0.0000000E+00	0.0000000E+00	0.0000000E+00
CONSTANT HEAD	2.2149608E-03	3.7026911E-03	-1.4877303E-03
WELLS	0.0000000E+00	1.2000003E-03	-1.2000003E-03
DRAINS	0.0000000E+00	0.0000000E+00	0.0000000E+00
RECHARGE	2.6880163E-03	0.0000000E+00	2.6880163E-03
.	.	.	.
.	.	.	.
SUM	4.9029770E-03	4.9026916E-03	2.8545037E-07
DISCREPANCY [%]	0.01		

The value of the element (i,j) of the following flow matrix gives the flow rate from the i-th zone into the j-th zone. Where i is the column index and j is the row index.

FLOW MATRIX:

	1	2
1	0.0000	0.0000
2	2.5873E-03	0.0000

TABLE 4: OUTPUT FROM THE WATER BUDGET CALCULATOR FOR THE PUMPING WELL

FLows ARE CONSIDERED "IN" IF THEY ARE ENTERING A SUBREGION  
THE UNIT OF THE FLOWS IS [L^3/T]

TIME STEP	1 OF STRESS PERIOD	1		
<b>ZONE= 1 LAYER= 1</b>				
FLOW TERM	IN	OUT	IN-OUT	
STORAGE	0.0000000E+00	0.0000000E+00	0.0000000E+00	
CONSTANT HEAD	0.0000000E+00	0.0000000E+00	0.0000000E+00	
<b>HORIZ. EXCHANGE</b>	<b>7.7992809E-05</b>	<b>0.0000000E+00</b>	<b>7.7992809E-05</b>	
EXCHANGE (UPPER)	0.0000000E+00	0.0000000E+00	0.0000000E+00	
EXCHANGE (LOWER)	0.0000000E+00	7.9696278E-05	-7.9696278E-05	
WELLS	0.0000000E+00	1.0000000E-10	-1.0000000E-10	
DRAINS	0.0000000E+00	0.0000000E+00	0.0000000E+00	
RECHARGE	3.1999998E-06	0.0000000E+00	3.1999998E-06	
.	.	.	.	
.	.	.	.	
SUM OF THE LAYER	8.1192811E-05	7.9696380E-05	1.4964317E-06	
.	.	.	.	
.	.	.	.	
<b>ZONE= 2 LAYER= 2</b>				
FLOW TERM	IN	OUT	IN-OUT	
STORAGE	0.0000000E+00	0.0000000E+00	0.0000000E+00	
CONSTANT HEAD	0.0000000E+00	0.0000000E+00	0.0000000E+00	
<b>HORIZ. EXCHANGE</b>	<b>5.6035380E-04</b>	<b>0.0000000E+00</b>	<b>5.6035380E-04</b>	
EXCHANGE (UPPER)	7.9696278E-05	0.0000000E+00	7.9696278E-05	
EXCHANGE (LOWER)	0.0000000E+00	6.4027577E-04	-6.4027577E-04	
WELLS	0.0000000E+00	1.0000000E-10	-1.0000000E-10	
.	.	.	.	
.	.	.	.	
SUM OF THE LAYER	6.4005010E-04	6.4027589E-04	-2.2578752E-07	
<b>ZONE= 3 LAYER= 3</b>				
FLOW TERM	IN	OUT	IN-OUT	
STORAGE	0.0000000E+00	0.0000000E+00	0.0000000E+00	
CONSTANT HEAD	0.0000000E+00	0.0000000E+00	0.0000000E+00	
<b>HORIZ. EXCHANGE</b>	<b>5.5766129E-04</b>	<b>0.0000000E+00</b>	<b>5.5766129E-04</b>	
EXCHANGE (UPPER)	6.4027577E-04	0.0000000E+00	6.4027577E-04	
EXCHANGE (LOWER)	0.0000000E+00	0.0000000E+00	0.0000000E+00	
WELLS	0.0000000E+00	1.2000001E-03	-1.2000001E-03	
.	.	.	.	
.	.	.	.	
SUM OF THE LAYER	1.1979371E-03	1.2000001E-03	-2.0629959E-06	

## 2.6 Step 6: Produce Output

In addition to the water budget, PMWIN provides various possibilities for checking simulation results and creating graphical outputs. The particle-tracking model *PMPATH* can display pathlines and velocity vectors. Using the *Results Extractor*, simulation results of any layer and time step can be read from the unformatted (binary) result files and saved in *ASCII Matrix* files. An ASCII Matrix file contains a value for each model cell in a layer. PMWIN can load ASCII matrix files into a model grid. In the following, we will carry out the steps:

1. Use the *Results Extractor* to read and save the calculated hydraulic heads.
2. Generate a contour map based on the calculated hydraulic heads for the first layer.
3. Use *PMPATH* to compute pathlines as well as the capture zone of the pumping well.

### ► To read and save the calculated hydraulic heads

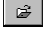
1. Choose *Results Extractor...* from the *Tools* menu  
The Results Extractor dialog box appears (Fig. 9). The options in the Results Extractor dialog box are grouped under four tabs - *MODFLOW*, *MOC3D*, *MT3D* and *MT3DMS*. In the *MODFLOW* tab, you may choose a result type from the Result Type drop-down box. You may specify the layer, stress period and time step from which the result should be read. The spreadsheet displays a series of columns and rows. The intersection of a row and column is a cell. Each cell of the spreadsheet corresponds to a model cell in a layer. Refer to Chapter 5 for more detailed information about the Results Extractor. For the current sample problem, follow steps 2 to 6 to save the hydraulic heads of each layer in three ASCII Matrix files.
2. Choose *Hydraulic Head* from the *Result Type* drop-down box.

3. Type 1 in the *Layer* edit field.  
For the current problem (steady-state flow simulation with only one stress period and one time step), the stress period and time step number should be 1.
4. Click *Read*.  
Hydraulic heads in the first layer at time step 1 and stress period 1 will be read and inserted into the spreadsheet. You can scroll the spreadsheet by clicking on the scrolling bars beside it.
5. Click *Save*.  
A *Save Matrix As* dialog box appears. By setting the *Save as type* option, the result can be optionally saved as an ASCII matrix or a SURFER data file. Specify the file name H1.DAT and select a folder in which H1.DAT should be saved. Click *OK* when ready.
6. Repeat steps 3, 4 and 5 to save the hydraulic heads of the second and third layer in the files H2.DAT and H3.DAT, respectively.
7. Click *Close* to close the dialog box.

### ► To generate contour maps of the calculated heads


1. Choose *Presentation* from the *Tools* menu.  
Data specified in *Presentation* will **not** be used by any parts of PMWIN. We can use *Presentation* to save temporary data or to display simulation results graphically.
2. Choose *Matrix...* from the *Value* menu (or Press Ctrl+B).  
The *Browse Matrix* dialog box appears (Fig. 10). Each cell of the spreadsheet corresponds to a model cell in the current layer. You can load an ASCII Matrix file into the spreadsheet or save the spreadsheet in an ASCII Matrix file by clicking *Load* or *Save*. Alternatively, you may select *Results Extractor* from the *Value* menu, read the head results and use an additional *Apply* button in the *Results Extractor* dialog box to put the data into the *Presentation* matrix.



3. Click the *Load...* button.  
The *Load Matrix* dialog box appears (Fig. 11).
4. Click  and select the file H1.DAT, which was saved earlier by the *Results Extractor*. Click OK when ready. H1.DAT is loaded into the spreadsheet.
5. In the Browse Matrix dialog box, click OK.  
The Browse Matrix dialog box is closed.
6. Choose *Environment* from the *Options* menu (or Press Ctrl+E).  
The *Environment Options* dialog box appears (Fig. 12). The options in the *Environment Options* dialog box are grouped under three tabs. *Appearance* and *Coordinate System* allow the user to modify the appearance and position of the model grid. Use the *Contours* tab to generate contour maps.
7. Click the *Contours* tab, check *Visible*, then click the *Restore Defaults* button.  
Clicking on the *Restore Defaults* button, PMWIN sets the number of contour lines to 11 and uses the maximum and minimum values in the current layer as the minimum and maximum contour levels (Fig. 13). If *Fill Contours* is checked, the contours will be filled with the colours given in the *Fill column* of the table. Use *Label*

*Format* button to specify an appropriate format.

**Note.** PMWIN will clear the *Visible* check box when you leave the *Data Editor*.

8. In the Environment Options dialog box, click OK.  
PMWIN will redraw the model and display the contours (Fig. 14).
9. To save or print the graphics, choose *Save Plot As...* or *Print Plot...* from the *File* menu.
10. Press *PgDn* to move to the second layer. Repeat steps 2 to 9 to load the file H2.DAT, display and save the plot.
11. Choose *Leave Editor* from the *File* menu or click the *leave editor* button  and click *Yes* to save changes to Presentation.

Using the procedure described above, you can generate contour maps based on your input data, any kind of simulation results or any data saved as an ASCII Matrix file. For example, you can create a contour map of the starting heads or you can use the *Result Extractor* to read the concentration distribution and display the contours. You can also generate contour maps of the fields created by the modelling tools *Field Interpolator* or *Field Generator*. See Chapter 5 for details of these modelling tools.

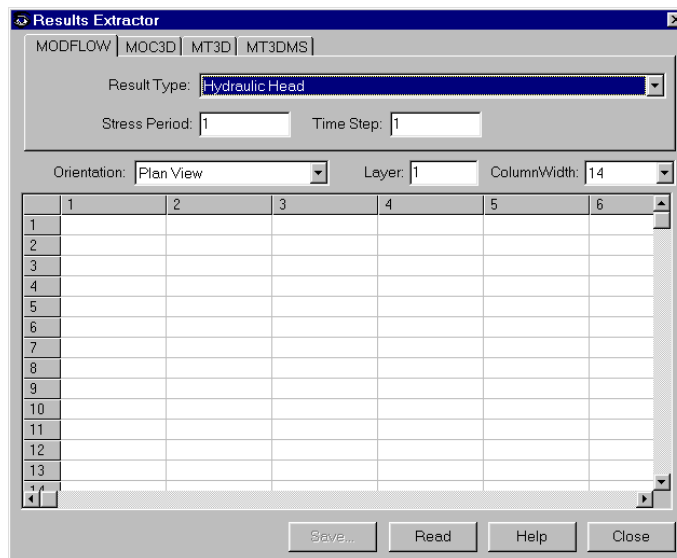


FIG. 9: THE RESULTS EXTRACTOR DIALOG BOX

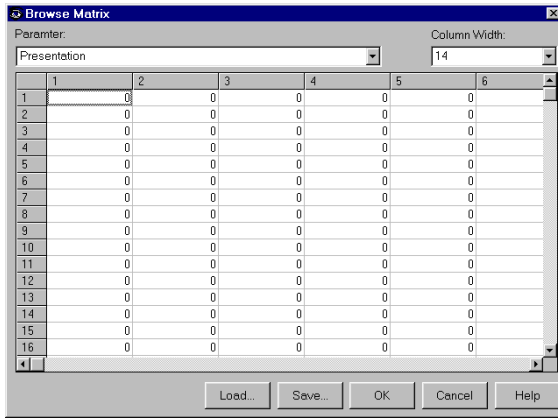


FIG. 10: THE *BROWSE MATRIX* DIALOG BOX

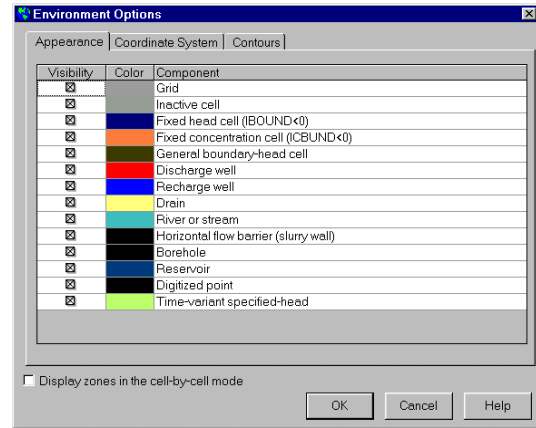


FIG. 12: THE *ENVIRONMENT OPTIONS* DIALOG BOX

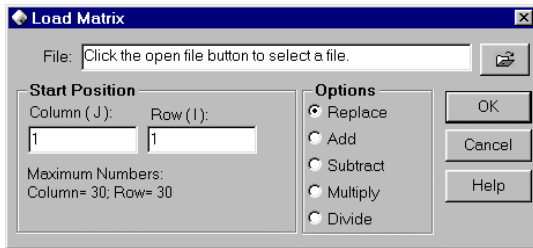


FIG. 11: THE *LOAD MATRIX* DIALOG BOX

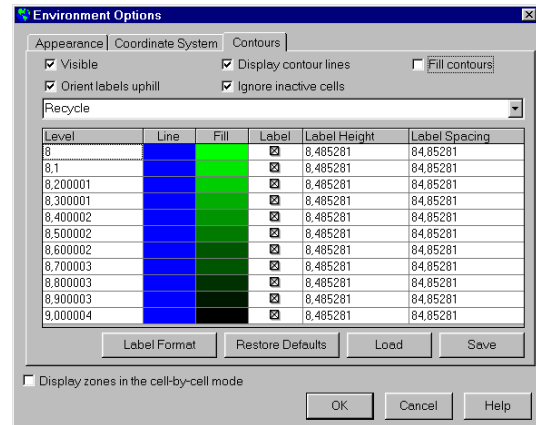


FIG. 13: THE *CONTOURS* TAB OF THE *ENVIRONMENT OPTIONS* DIALOG BOX

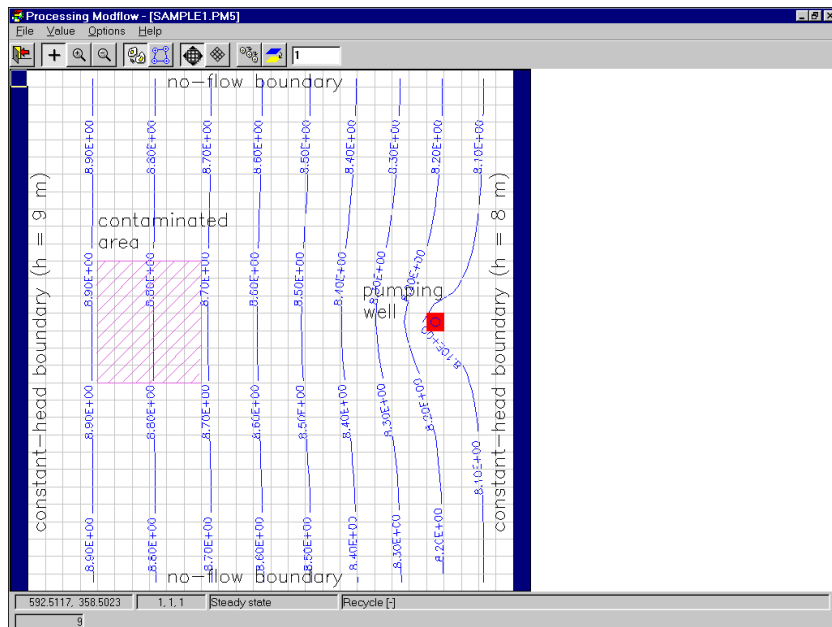


FIG. 14: A CONTOUR MAP OF THE HYDRAULIC HEADS IN THE FIRST LAYER




► **To draw a pathline**



1. Choose *PMPATH* (*Pathlines and Contours*) from the *Models* menu, if you are not already in *PMPATH*.

PMWIN calls the advective transport model *PMPATH* and the current model will be loaded into *PMPATH* automatically. *PMPATH* uses a *grid*


*cursor* to define the column and row for which the cross-sectional plots should be displayed. You can move the grid cursor by holding down the Ctrl-key and clicking the left mouse button on the desired position.

**Note.** If you subsequently modify and calculate a model within PMWIN, you must load the modified model into PMPATH again to ensure that the modifications are recognized by PMPATH. To load a model, click and select a model file with the extension .PM5 from the *Open Model* dialog box.

2. Click the *Set Particle* button .
3. *Right-click* on a point within the model area to set a particle.
4. Click  to start the backward particle tracking.
5. Click  to start the forward particle tracking.


Each time you press one of the buttons  or , particle(s) may move backward or forward for a defined time length.

► **To delineate the capture zone of the pumping well**


1. Choose *PMPATH (Pathlines and Contours)* from the *Models* menu of PMWIN.
2. Click the *Set Particle* button .
3. Move the mouse pointer to the model area. The mouse pointer turns into crosshairs.
4. Place the crosshairs at the upper-left corner of the pumping well, as shown in Fig. 15.
5. Hold down the left mouse button and drag the crosshairs until the window covers the pumping well.
6. Release the left mouse button.

An *Add New Particles* dialog box appears. Assign the numbers of particles to the edit fields in the dialog box as shown in Fig. 16. Click the *Properties* tab and click the coloured button to select an appropriate colour for the new particles. When finished, click *OK*.

7. To set particles around the pumping well in the second and third layers, press PgDn to move down a layer and repeat steps c, d and e. Use other colours for the new particles in the second and third layers.

8. Click  to start the backward particle tracking. PMPATH calculates and shows the projections of the pathlines as well as the capture zone of the pumping well (Fig. 17).

To see the projection of the pathlines on the cross-section windows in greater details, open an *Environment Options* dialog box by choosing *Environment...* from the *Options* menu and set a larger exaggeration value for the vertical scale in the *Cross Sections* tab. Fig. 18 shows the same pathlines by setting the vertical exaggeration value to 10. Note that some pathlines end up at the groundwater surface, where recharge occurs. This is one of the major differences between a three-dimensional and a two-dimensional model. In two-dimensional simulation models, such as ASM for Windows (Chiang et al., 1998), FINEM (Kinzelbach et al., 1990) or MOC (Konikow and Bredehoeft, 1978), a vertical velocity term does not exist (or is always equal to zero). This leads to the result that pathlines can never be tracked back to the ground surface where the groundwater recharge from the precipitation occurs. Note that pathlines can be drawn in three dimensions in PMPATH even if you build a 2D model.

PMPATH can create time-related capture zones of pumping wells. The 100-days-capture zone shown in Fig. 19 is created using the settings in the *Particle Tracking (Time) Properties* dialog box (Fig. 20) and clicking . To open this dialog box, choose *Particle Tracking (Time)...* from the *Options* menu. Note that because of lower hydraulic conductivity (and thus lower flow velocity) the capture zone in the first layer is smaller than those in the other layers.

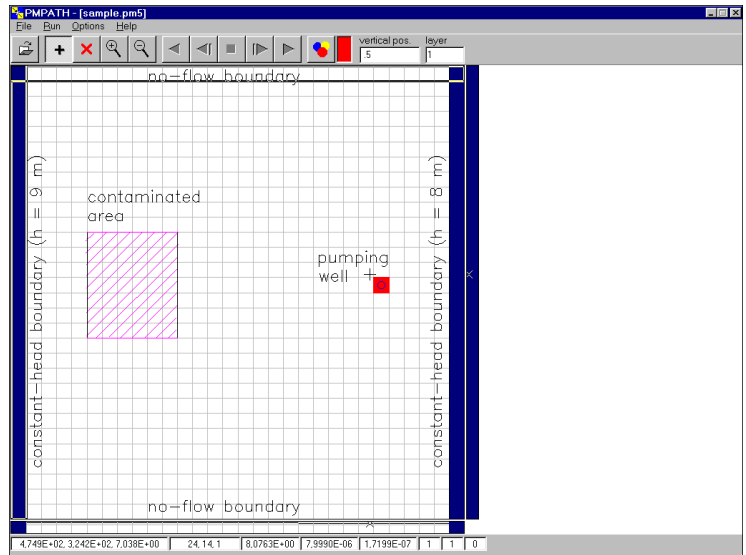


FIG. 15: THE SAMPLE MODEL LOADED IN PMPATH

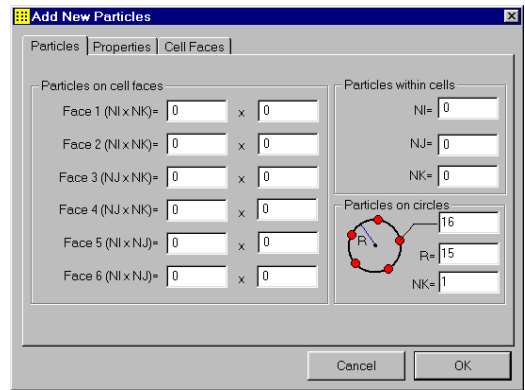


FIG. 16: THE ADD NEW PARTICLES DIALOG BOX

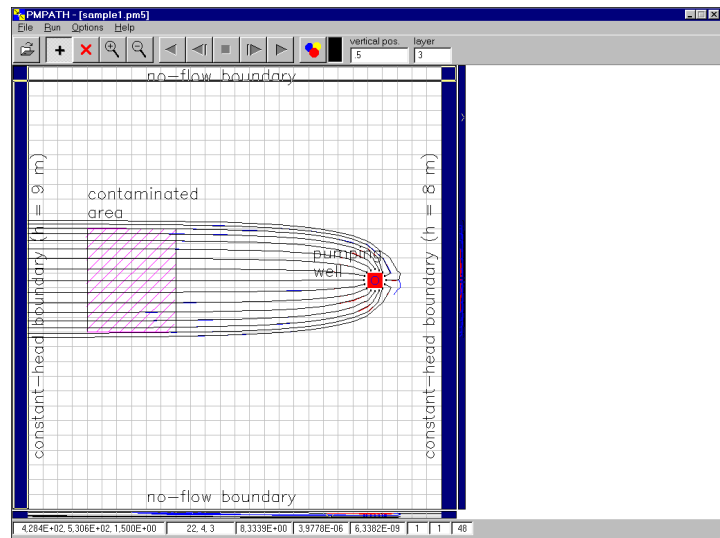


FIG. 17: THE CAPTURE ZONE OF THE PUMPING WELL (WITH VERTICAL EXAGGERATION = 1)

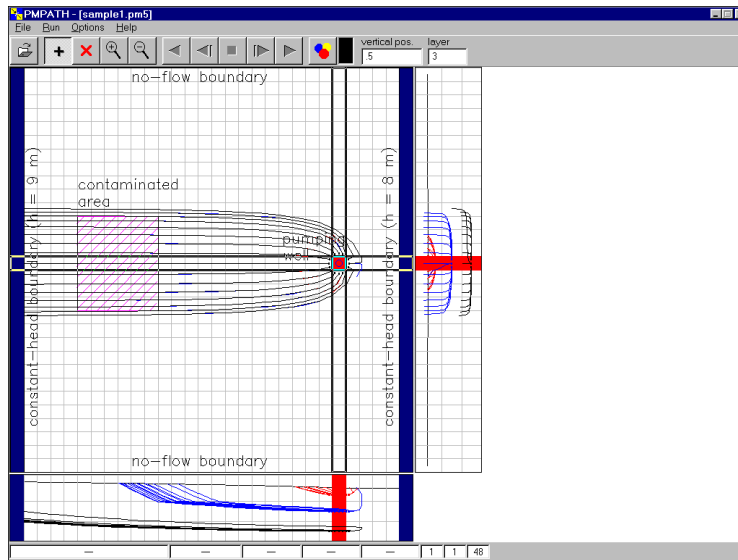


FIG. 18: THE CAPTURE ZONE OF THE PUMPING WELL (WITH VERTICAL EXAGGERATION = 10)

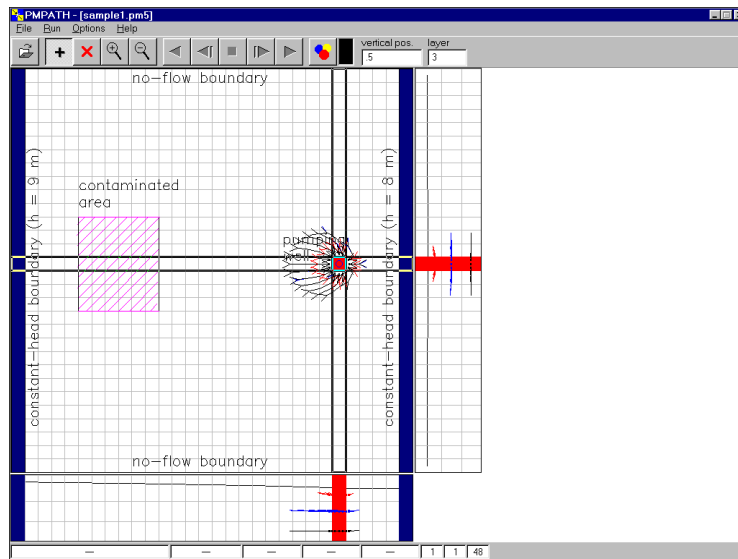


FIG. 19: THE 100-DAYS CAPTURE ZONE CALCULATED BY PMPATH

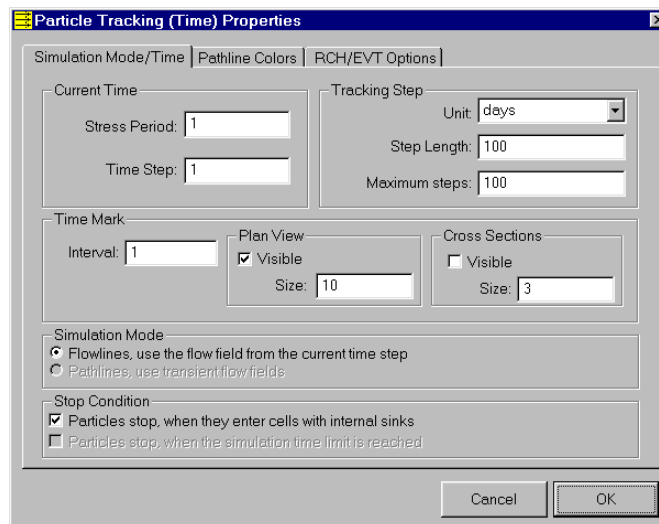


FIG. 20: THE PARTICLE TRACKING (TIME) PROPERTIES DIALOG BOX

### 3 Simulation of Solute Transport

The transport of solutes in porous media can basically be described through three processes: *advection*, *hydrodynamic dispersion* and *physical, chemical or biochemical reactions*.

The MT3D and MOC3D models use the *method-of-characteristics* (MOC) to simulate the advective transport, in which dissolved chemicals are represented by a number of particles and the particles are moving with the flowing groundwater. Besides the MOC method, the MT3D and MT3DMS models provide other methods for solving the advective term.

The hydrodynamic dispersion can be expressed in terms of the *dispersivity* [L] and the *coefficient of molecular diffusion* [ $L^2T^{-1}$ ] for the solute in the porous medium. The types of reactions incorporated into MOC3D are restricted to those that can be represented by a first-order rate reaction, such as radioactive decay, or by a retardation factor, such as instantaneous, reversible, sorption-desorption reactions governed by a linear isotherm and constant distribution coefficient ( $K_d$ ). In addition to the linear isotherm, MT3D supports non-linear isotherms, i.e., Freundlich and Langmuir isotherms.

Prior to running MT3D or MOC3D, you need to define the observation boreholes, for which the breakthrough curves will be calculated.

#### ► To define observation boreholes


1. Choose *Boreholes and Observations* from the *Parameters* menu.  
A *Boreholes and Observations* dialog box appears. Enter the coordinates of the observation boreholes into the dialog box as shown in Fig. 21.
2. Click *OK* to close the dialog box.

### 3.1 Perform Transport Simulation with MT3D


MT3D requires a boundary condition code for each model cell, which indicates whether (1) solute concentration varies with time (active concentration cell), (2) the concentration is kept fixed at a constant value (constant-concentration cell), or (3) the cell is an inactive concentration cell. Use 1 for an active concentration cell, -1 for a constant-concentration cell, and 0 for an inactive concentration cell. Active, variable-head cells can be treated as inactive concentration cells to minimise the area needed for transport simulation, as long as the solute concentration is insignificant near those cells.

Similar to the flow model, you must specify the initial concentration for each model cell. The initial concentration value at a constant-concentration cell will be kept constant during a transport simulation. The other concentration values are used as starting values in a transport simulation.

#### ► To assign the boundary condition to MT3D

1. Choose *Boundary Conditions > ICBUND (MT3D/MT3DMS)* from the *Grid* menu.  
For the current example, we accept the default value 1 for all cells.
2. Choose *Leave Editor* from the *File* menu or click the *leave editor* button .

#### ► To set the initial concentration

1. Choose *MT3D > Initial Concentration* from the *Models* menu.  
For the current example, we accept the default value 0 for all cells.
3. Choose *Leave Editor* from the *File* menu or click the *leave editor* button .

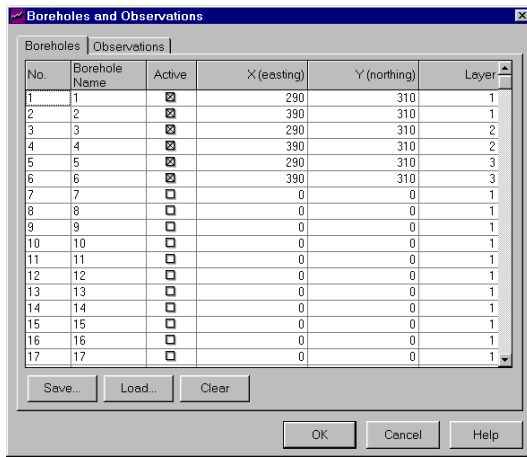


FIG. 21: THE BOREHOLES AND OBSERVATIONS DIALOG BOX

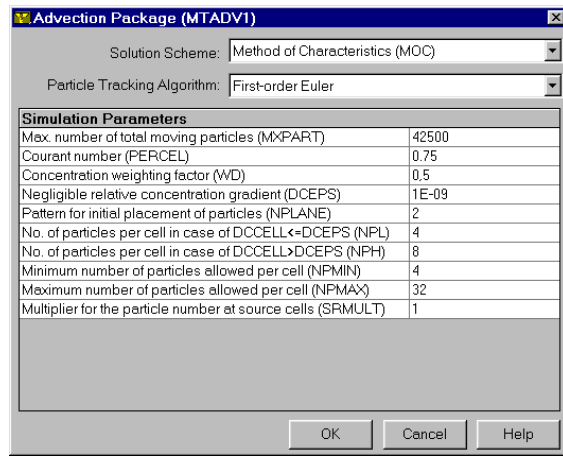



FIG. 22: THE ADVECTION PACKAGE (MTADV1) DIALOG BOX



► **To assign the input rate of contaminants**

1. Choose *MT3D > Sink/Source Concentration > Recharge* from the *Models* menu.
2. Assign 12500 [ $\mu\text{g}/\text{m}^3$ ] to the cells within the contaminated area.  
This value is the concentration associated with the recharge flux. Since the recharge rate is  $8 \times 10^{-9}$  [ $\text{m}^3/\text{m}^2/\text{s}$ ] and the dissolution rate is  $1 \times 10^{-4}$  [ $\mu\text{g}/\text{s}/\text{m}^2$ ], the concentration associated with the recharge flux is  $1 \times 10^{-4} / 8 \times 10^{-9} = 12500$  [ $\mu\text{g}/\text{m}^3$ ].
3. Choose *Leave Editor* from the *File* menu or click the *leave editor* button .

► **To assign the transport parameters to the Advection Package**

1. Choose *MT3D > Advection...* from the *Models* menu.  
An *Advection Package (MTADV1)* dialog box appears. Enter the values shown in Fig. 22 into the dialog box, select *Method of Characteristics (MOC)* for the solution scheme and *First-order Euler* for the particle-tracking algorithm.
2. Click *OK* to close the dialog box.

► **To assign the dispersion parameters**

1. Choose *MT3D > Dispersion...* from the *Models* menu.  
A *Dispersion Package (MT3D)* dialog box appears. Enter the ratios of the transverse dispersivity to longitudinal dispersivity as shown in Fig. 23.
2. Click *OK*.  
PMWIN displays the model grid. At this point you need to specify the longitudinal dispersivity to each cell of the grid.
3. Choose *Reset Matrix...* from the *Value* menu (or press *Ctrl+R*), type 10 in the dialog box, then click *OK*.
4. Turn on *layer copy* by clicking the *layer copy* button .
5. Move to the second layer and the third layer by pressing *PgDn* twice.  
The cell values of the first layer are copied to the second and third layers.
6. Choose *Leave Editor* from the *File* menu or click the *leave editor* button .

► **To assign the chemical reaction parameters**

1. Choose *MT3D > Chemical Reaction > Layer by Layer* from the *Models* menu.  
A *Chemical Reaction Package (MTRCT1)* dialog box appears. Clear the check box *Simulate the radioactive decay or biodegradation* and select *Linear equilibrium isotherm* for the type of sorption. For the linear isotherm, the retardation factor *R* for each cell is

calculated at the beginning of the simulation by equation 3.

$$R = 1 + \frac{\rho_b}{n} \cdot K_d \quad (3)$$

Where  $n$  [-] is the effective porosity with respect to the flow through the porous medium,  $\rho_b$  [ML<sup>-3</sup>] is the bulk density of the porous medium and  $K_d$  [L<sup>3</sup>M<sup>-1</sup>] is the distribution coefficient of the solute in the porous medium. As the effective porosity is equal to 0.25, setting  $\rho_b = 2000$  and  $K_d = 0.000125$  yields  $R = 2$ .

2. Click *OK* to close the *Chemical Reaction Package (MTRCT1)* dialog box (Fig. 24).

The last step before running the transport model is to specify the output times, at which the calculated concentration should be saved.

► **To specify the output times**

1. Choose *MT3D > Output Control...* from the *Models* menu.  
An *Output Control (MT3D, MT3DMS)* dialog box appears. The options in this dialog box are grouped under three tabs: *Output Terms*, *Output Times* and *Misc*.
2. Click the *Output Times* tab, then click the header *Output Time* of the (empty) table.  
An *Output Times* dialog box appears. Enter 3000000 to *Interval* in this dialog box, then click *OK* to accept the other default values.
3. Click *OK* to close the *Output Control (MT3D, MT3DMS)* dialog box (Fig. 25).

► **To perform the transport simulation**

1. Choose *MT3D > Run...* from the *Models* menu.  
The *Run MT3D/MT3D96* dialog box appears (Fig. 26).

2. Click *OK* to start the transport computation.

Prior to running MT3D, PMWIN will use user-specified data to generate input files for MT3D as listed in the table of the *Run MT3D/MT3D96* dialog box. An input file will be generated, only if the *generate* flag is set to . You can click on the button to toggle the *generate* flag between  and . Normally, you do not need to change the flags, as PMWIN will take care of the settings.

► **Check simulation results and produce output**

During a transport simulation, MT3D writes a detailed run record to the file *path\OUTPUT.MT3*, where *path* is the folder in which your model data are saved. MT3D saves the simulation results in various files, which can be controlled by choosing *MT3D > Output Control...* from the *Models* menu.

To check the quality of the simulation results, a mass budget is calculated at the end of each transport step and accumulated to provide summarised information on the total mass into or out of the groundwater flow system. The discrepancy between the in- and outflows of mass serves as an indicator of the accuracy of the simulation results. It is highly recommended to check the record file or at least take a glance at it.

Using *Presentation* you can generate contour maps of the calculated concentration. Fig. 27 shows the calculated concentration in the third layer at the end of the simulation (simulation time=9.467E+07 seconds).

To generate the breakthrough curves, choose *Graphs > Concentration Time > MT3D* from the *Tools* menu. Click on the *Plot* flags of the *Boreholes* table until they are set to  (Fig.28).



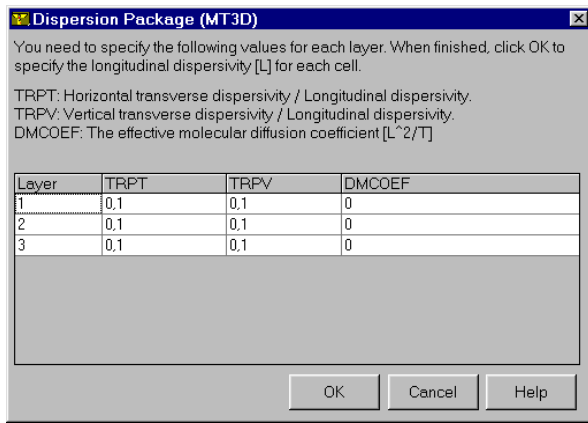


FIG. 23: THE DISPERSION PACKAGE (MT3D) DIALOG BOX

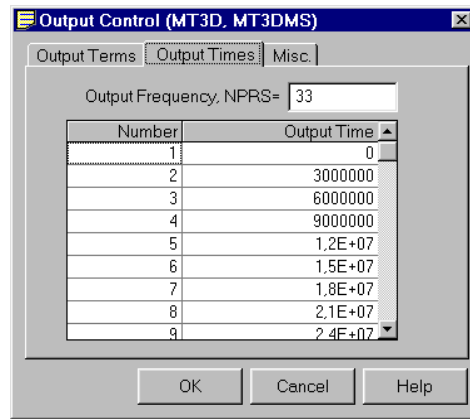


FIG. 25: THE OUTPUT CONTROL (MT3D, MT3DMS) DIALOG BOX

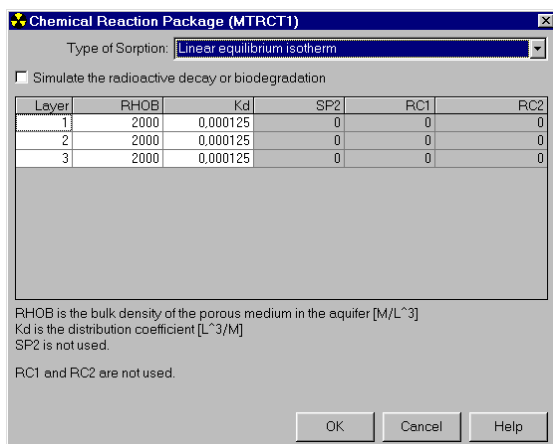


FIG. 24: THE CHEMICAL REACTION PACKAGE (MTRCT1) DIALOG BOX

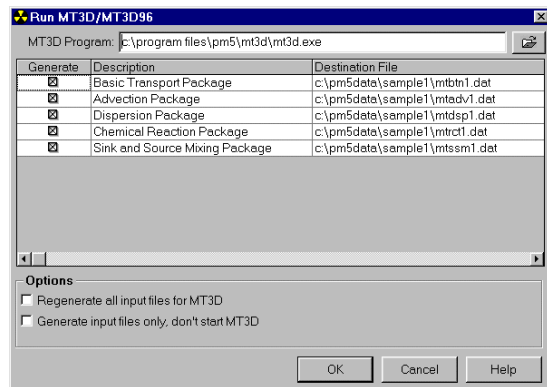


FIG. 26: THE RUN MT3D/MT3D96 DIALOG BOX

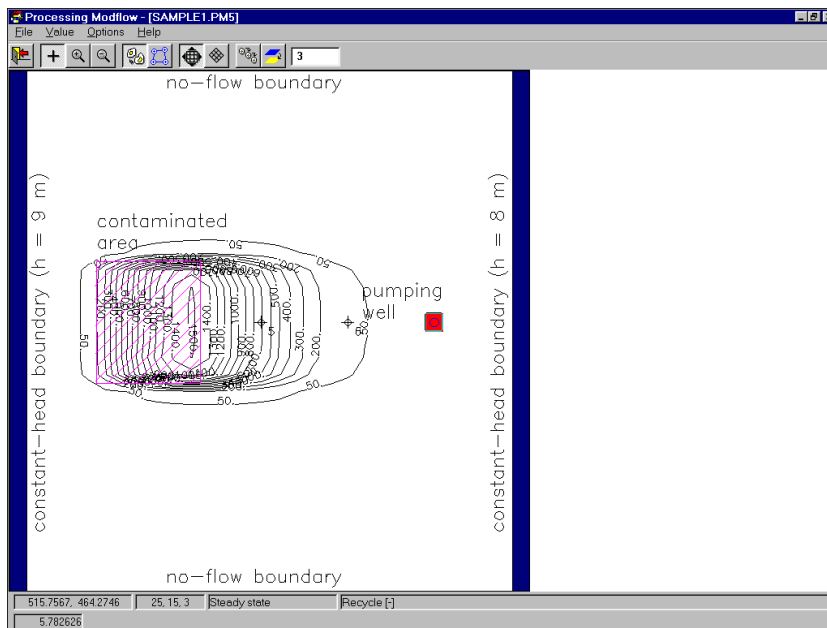


FIG. 27: SIMULATED CONCENTRATION AT 3 YEARS IN THE THIRD LAYER

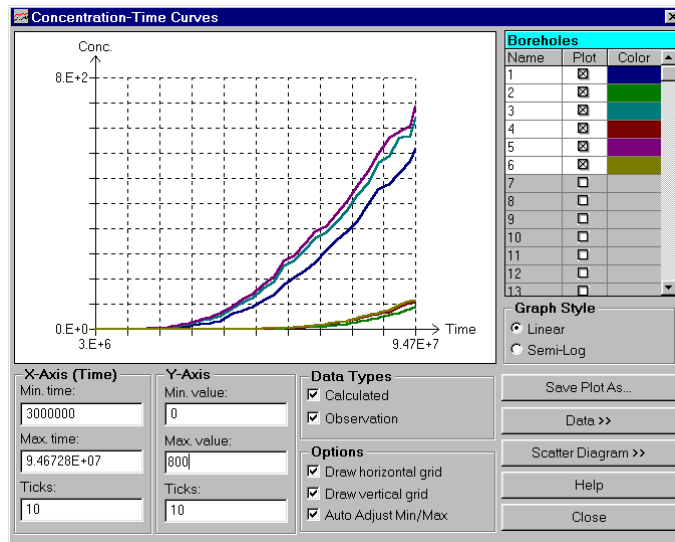


FIG. 28: CONCENTRATION-TIME CURVES AT THE OBSERVATION BOREHOLES 1-6


### 3.2 Perform Transport Simulation with MOC3D

In MOC3D, transport may be simulated within a sub-grid, which is a *window* within the primary model grid used to simulate flow. Within the sub-grid, the row and column spacing must be uniform, but the thickness can vary from cell to cell and from layer to layer. However, the range in thickness values (or product of thickness and effective porosity) should be as small as possible.

The initial concentration must be specified throughout the sub-grid within which solute transport occurs. MOC3D assumes that the concentration outside of the sub-grid is the same within each layer; so only one value is specified for each layer within and adjacent to the sub-grid. The use of constant-concentration boundary condition has not been implemented in MOC3D.

► **To set the initial concentration**

1. Choose *MOC3D* > *Initial Concentration* from the *Models* menu. For the current example, we accept the default value 0 for all cells. Note that PMWIN automatically uses the same initial concentration values for both MOC3D and MT3D.

2. Choose *Leave Editor* from the *File* menu or click the *leave editor* button .

► **To define the transport sub-grid and the concentration outside of the sub-grid**

1. Choose *MOC3D* > *Subgrid...* from the *Models* menu.

The *Subgrid for Transport (MOC3D)* dialog box appears (Fig. 29). The options in the dialog box are grouped under two tabs: *Subgrid* and *C' Outside of Subgrid*. The default size of the sub-grid is the same as the model grid used to simulate flow. The default initial concentration outside of the sub-grid is zero. We will accept the defaults.

2. Click *OK* to accept the default values and close the dialog box.

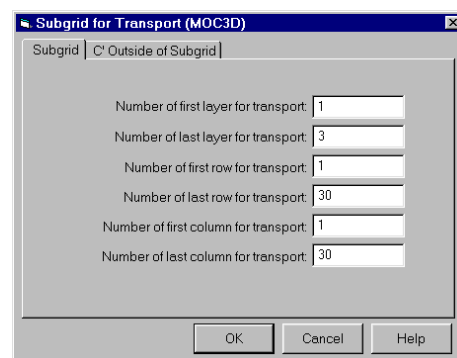



FIG. 29: THE SUBGRID FOR TRANSPORT (MOC3D) DIALOG BOX

► **To assign the input rate of contaminants**

1. Choose *MOC3D* > *Sink/Source Concentration* > *Recharge* from the *Models* menu.
2. Assign 12500 [ $\mu\text{g}/\text{m}^3$ ] to the cells within the contaminated area.  
This value is the concentration associated with the recharge flux. Since the recharge rate is  $8 \times 10^{-9}$  [ $\text{m}^3/\text{m}^2/\text{s}$ ] and the dissolution rate is  $1 \times 10^{-4}$  [ $\mu\text{g}/\text{s}/\text{m}^2$ ], the concentration associated with the recharge flux is  $1 \times 10^{-4} / 8 \times 10^{-9} = 12500$  [ $\mu\text{g}/\text{m}^3$ ].
3. Choose *Leave Editor* from the *File* menu or click the *leave editor* button .


► **To assign the parameters for the advective transport**

1. Choose *MOC3D* > *Advection...* from the *Models* menu.  
A *Parameters for Advection Transport (MOC3D)* dialog box appears. Enter the values as shown in Fig. 30 into the dialog box, and select *Bilinear (X, Y directions)* for the interpolation scheme for particle velocity. As noted by Konikow et al. (1996), if transmissivity within a layer is homogeneous or smoothly varying, bilinear interpolation of velocity yields more realistic pathlines for a given discretization than does linear interpolation.
2. Click *OK* to close the dialog box.

► **To assign the parameters for dispersion and chemical reaction**

1. Choose *MOC3D* > *Dispersion & Chemical Reaction...* from the *Models* menu.  
A *Dispersion / Chemical Reaction (MOC3D)* dialog box appears. Check *Simulate Dispersion* and enter the values as shown in Fig. 31. Note that the parameters for dispersion and chemical reaction are the same for each layer.
2. Click *OK* to close the dialog box.

► **To set Strong/Weak Flag**

1. Choose *MOC3D* > *Strong/Weak Flag* from the *Models* menu.
2. Move the grid cursor to the cell [25, 15, 1].
3. Press the right mouse button and type 1, then click *OK*. Note that a strong sink or source is indicated by the value of 1 in the matrix. When a fluid *source* is strong, new particles are added to replace old particles as they are advected out of that cell. Where a fluid *sink* is strong, particles are removed after they enter that cell.
4. Repeat steps 2 and 3 to assign the value 1 to the cells [25, 15, 2] and [25, 15, 3].
5. Choose *Leave Editor* from the *File* menu or click the *leave editor* button .

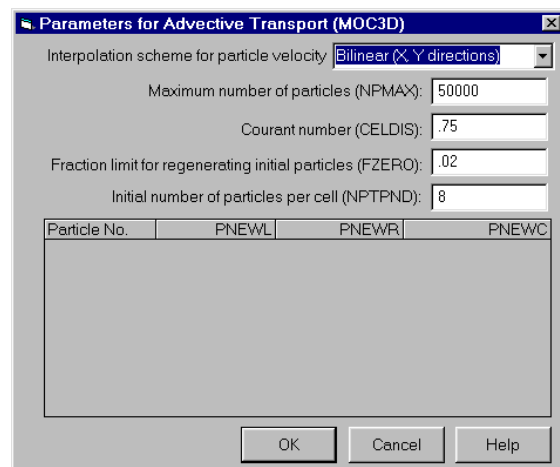


FIG. 30: THE PARAMETERS FOR ADVECTIVE TRANSPORT (MOC3D) DIALOG BOX

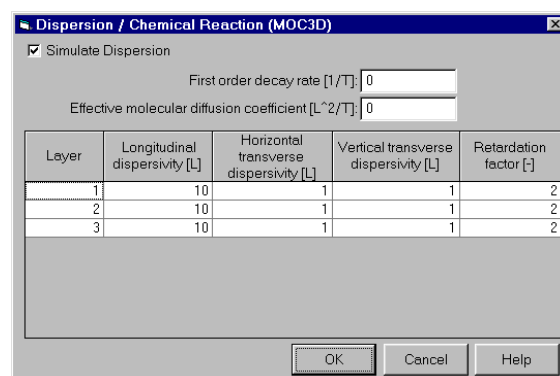


FIG. 31: THE DISPERSION / CHEMICAL REACTION (MOC3D) DIALOG BOX

► **To specify the output terms and times**

1. Choose *MOC3D* > *Output Control...* from the *Models* menu.

An *Output Control (MOC3D)* dialog box appears. The options in the dialog box are grouped under five tabs: *Concentration*, *Velocity*, *Particle Locations*, *Disp. Coeff.* and *Misc.*

- In the *Concentration* tab, select the option “These data will be printed or saved every Nth particle moves” and enter  $N = 20$ .
- Click *OK* to accept all other default values and close the *Output Control (MOC3D)* dialog box (Fig. 32).

► **To perform the transport simulation**

- Choose *MOC3D > Run...* from the *Models* menu.

The *Run MOC3D* dialog box appears (Fig. 33).

- Click *OK* to start the transport computation.

Prior to running MOC3D, PMWIN will use user-specified data to generate input files for MOC3D as listed in the table of the *Run MOC3D* dialog box. An input file will be generated, only if the *generate* flag is set to . You can click on the button to toggle the *generate* flag between  and . Normally, you do not need to change the flags, as PMWIN will take care of the settings.

► **Check simulation results and produce output**

During a transport simulation, MOC3D writes a detailed run record to the file *path\MOC3D.LST*, where *path* is the folder in which your model data are saved.

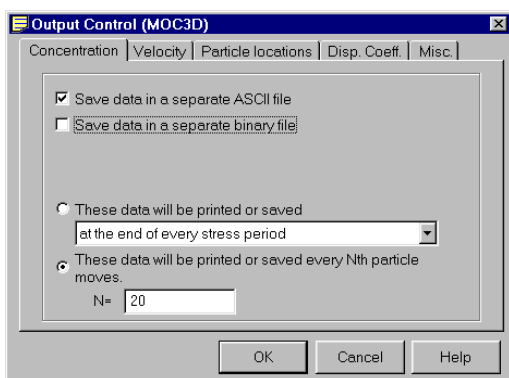


FIG. 32: THE *OUTPUT CONTROL (MOC3D)* DIALOG BOX

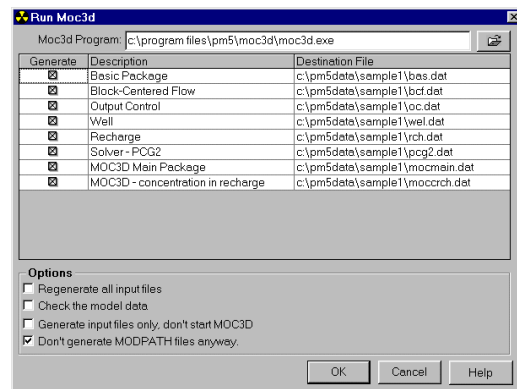


FIG. 33: THE *RUN MOC3D* DIALOG BOX

MOC3D saves the simulation results in various files, which can be controlled by choosing *MOC3D > Output Control...* from the *Models* menu.

To check the quality of the simulation results, mass balance calculations are performed and saved in the run record file. The mass in storage at any time is calculated from the concentrations at the nodes of the transport sub-grid to provide summarised information on the total mass into or out of the groundwater flow system. The mass balance error will typically exhibit an oscillatory behavior over time, because of the nature of the method of characteristics and the finite-difference approximation. The oscillations reflect the fact that **the mass balance calculation is itself just an approximation.**

Using *Presentation* you can generate concentration contour maps of the calculated concentration. Fig. 34 shows the calculated concentration at three years in the third layer (simulation time=9.467E+07 seconds).

To generate the breakthrough curves, choose *Graphs > Concentration Time > MOC3D* from the *Tools* menu. Click on the *Plot* flags of the *Boreholes* table until they are set as in Fig. 35. The fluctuations visible in Fig. 35 are typical for particle based methods. Results from FD-methods are smooth but at the price of more artificial mixing at the same spatial discretization.

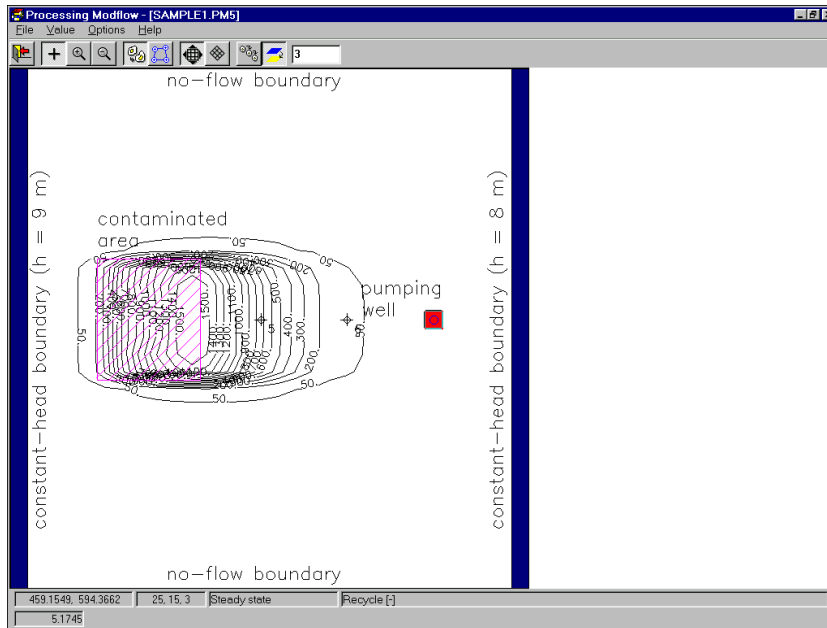


FIG. 34: SIMULATED CONCENTRATION AT 3 YEARS IN THE THIRD LAYER

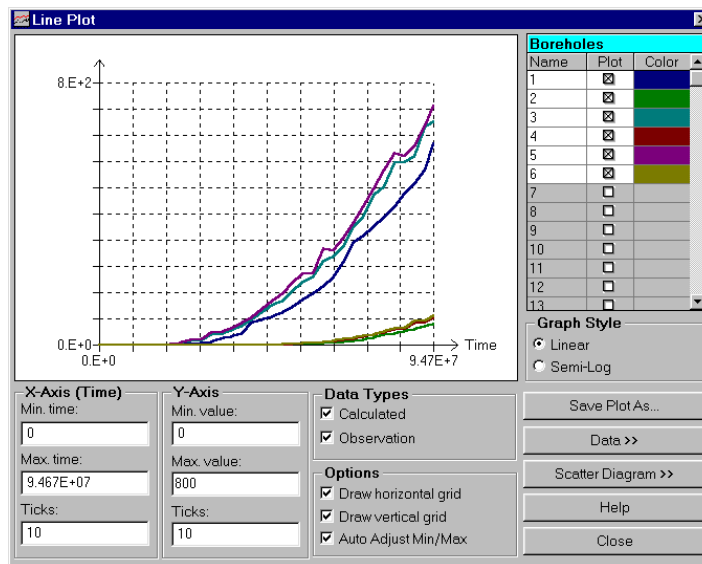


FIG. 35: CONCENTRATION-TIME CURVES AT THE OBSERVATION BOREHOLES


## 4 Parameter Estimation

The process of estimating unknown parameters is one of the most difficult and critical steps in the model application. The parameter estimation (often called calibration) of a flow model is accomplished by finding a set of parameters, hydrologic stresses or boundary conditions so that the simulated heads or ‘drawdowns’ match the measurement values to a reasonable degree. Hill (1998) gives methods and guidelines for model calibration using inverse modeling.

To demonstrate the use of the inverse models PEST and UCODE within PMWIN, we assume that the hydraulic conductivity in the third layer is homogeneous but its value is unknown. We want to find out this value through a model calibration by using the measured hydraulic heads at the observation boreholes listed in Table 5. Three steps are required for the parameter estimation.

1. Assign the zonal structure of each parameter.  
Parameter estimation requires a subdivision of the model domain into a small number of reasonable zones of equal parameter values. The zonal structure is given by assigning to each zone a parameter number in the *Data Editor*.
2. Specify the coordinates of the observation boreholes and the measured hydraulic heads.
3. Specify the starting values, upper and lower bounds for each parameter.

### ► To assign the zonal structure to the horizontal hydraulic conductivity

1. Choose *Horizontal Hydraulic Conductivity* from the *Parameters* menu.
2. Move to the third layer by pressing *PgDn* twice.
3. Choose *Reset Matrix...* from the *Value* menu (or press Ctrl+R).  
A *Reset Matrix* dialog box appears.
4. Enter 1 to the *Parameter Number* edit box, then click *OK*.  
The horizontal hydraulic conductivity of the third layer is set to the parameter #1.
5. Choose *Leave Editor* from the *File* menu or click the *leave editor* button .

**Note.** For layers of type *0:confined* and *2:confined/unconfined* (*transmissivity = const.*), MODFLOW reads transmissivity (instead of hydraulic conductivity) from the model data file. Consequently we are actually estimating the transmissivity values and must use suitable values for the initial guess and lower and upper bounds. Change the layer type to *3:confined/unconfined* (*transmissivity varies*) if you want to estimate the horizontal hydraulic conductivity.

### ► To specify the coordinates of the observation boreholes and measured values

1. Choose *Boreholes and Observations* from the *Parameters* menu and enter the coordinates of the observation

TABLE 5: HYDRAULIC HEADS FOR ESTIMATING PARAMETERS

Borehole	X-Coordinate	Y-Coordinate	Layer	Hydraulic Head
1	130	200	3	8.85
2	200	400	3	8.74
3	480	250	3	8.18
4	460	450	3	8.26

- boreholes into the boreholes table.
- Click the *Observations* tab and enter the values into the observations table as shown in Fig. 36. Note that the observation time, to which the measurement pertains, is measured from the beginning of the model simulation. For a steady state simulation with one stress period (you can run a steady state simulation over several stress periods), the length of the period (9.46728E+07 seconds) is given as the observation time.
  - Click *OK* to close the dialog box.

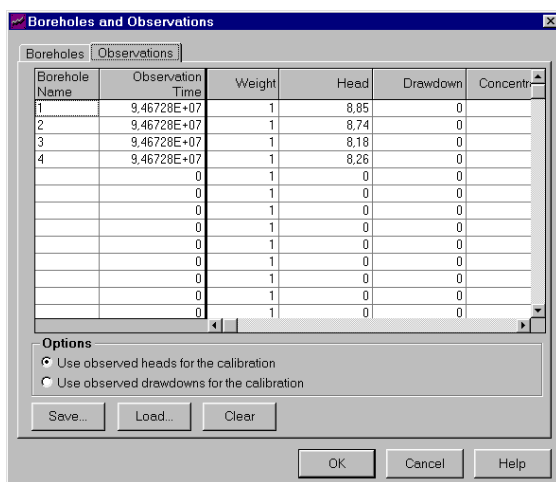


FIG. 36: THE BOREHOLES AND OBSERVATIONS DIALOG BOX

#### 4.1 Parameter Estimation with PEST

##### ► To specify the starting values for each parameter

- Choose *PEST > Parameter List...* from the *Models* menu.

A *List of Calibration Parameters (PEST)* dialog box appears. The options of the dialog box are grouped under five tabs: *Parameters*, *Group Definitions*, *Prior Information*, *Control Data* and *Options*.

- In the *Parameters* tab, activate the first parameter (by setting the *Active* flag to ) from the *Parameters* table and enter values shown in Fig. 37 into the table. *PARVAL1* is the initial guess of the parameter. *PARLBUD* is the lower

bound and *PARUBUD* is the upper bound of the parameter.

##### ► To run PEST

- Choose *PEST (Inverse Modeling) > Run...* from the *Models* menu.

The *Run PEST* dialog box appears (Fig. 38).

- Click *OK* to start PEST.

Prior to running PEST, PMWIN will use user-specified data to generate input files for PEST and MODFLOW as listed in the table of the *Run PEST* dialog box. An input file will be generated only if the *generate* flag is set to . You can click on the button to toggle the *generate* flag between  and . Normally you do not need to change the flags, as PMWIN will take care of the settings.

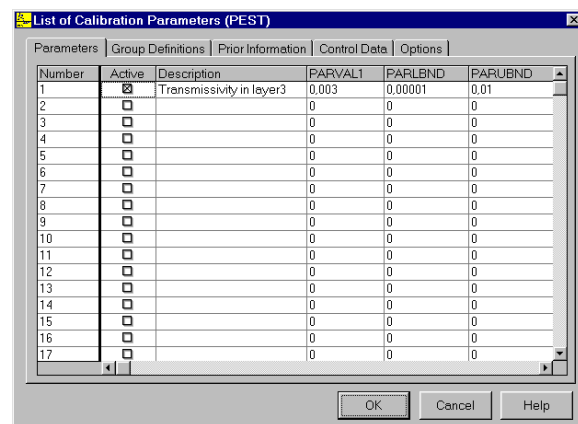


FIG. 37: THE LIST OF CALIBRATION PARAMETERS (PEST) DIALOG BOX

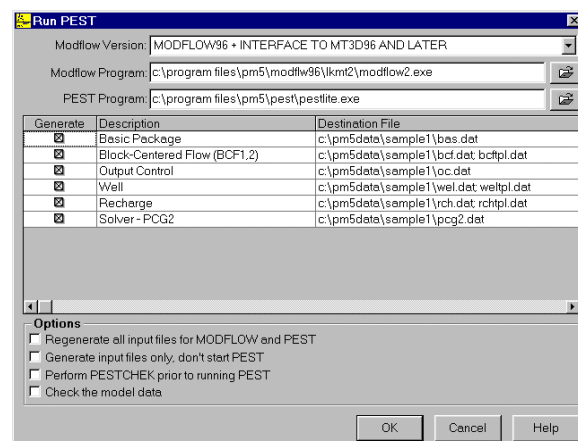


FIG. 38: THE RUN PEST DIALOG BOX



### ► Check the Parameter Estimation Results

Several result files are created through the parameter estimation process. PEST writes the optimised parameter values to the input files of MODFLOW (BCF.DAT, WEL.DAT, etc.) and creates a detailed run record file *path\PESTCTL.REC*, where *path* is the folder in which your model data are saved. The simulation results of MODFLOW are updated by using the optimised parameter values, which are saved in a separate file PESTCTL.PAR.

Note that PMWIN does not retrieve the optimised parameter values into the data matrices. Your original (PMWIN-) model data will not be modified in any way. This provides more security for the model data, because a parameter estimation process does not necessarily lead to a success. If you want to operate on the estimated parameters, you must manually assign them to model cells. Alternatively, you can create a new model with the estimated parameters by using the *Convert Models* dialog.

You can create a scatter diagram to present the result. The observed head values are plotted on one axis against the corresponding calculated values on the other. If there is exact agreement between measurement and simulation, all points lie on a 45° line. The narrower the area of scatter around this line, the better is the match.

### ► To create a scatter diagram for head values

1. Choose *Graph > Head-Time* from the *Tools* menu.  
A *Head-Time Curves* dialog box appears.
2. Click the button *Scatter Diagram* »  
PMWIN shows the scatter diagram (Fig. 39). See Chapter 5 for details about the use of this dialog box.

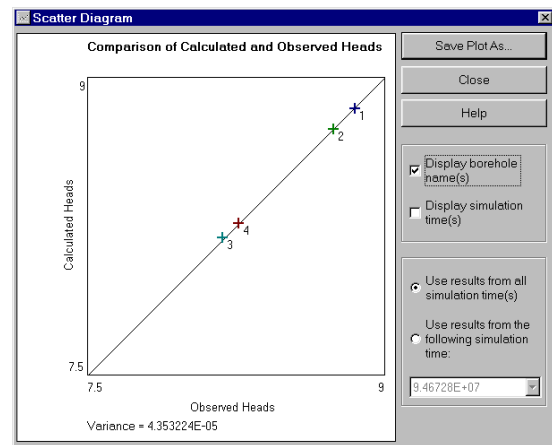


FIG. 39: THE SCATTER DIAGRAM DIALOG BOX

## 4.2 Parameter Estimation with UCODE

### ► To specify the starting values for each parameter

1. Choose *UCODE > Parameter List...* from the *Models* menu.  
A *List of Calibration Parameters (UCODE)* dialog box appears. The options of the dialog box are grouped under five tabs: *Parameters*, *Prior Information*, *Control Data* and *Options*.
2. In the *Parameters* tab, activate the first parameter (by setting the Active flag to ) from the *Parameters* table and enter values shown in Fig. 40 into the table. *Start-value* is the initial guess of the parameter. *Minimum* is the reasonable minimum value and *Maximum* is the reasonable maximum value for the parameter. These two values are used solely to determine how the final optimised value of the parameter compares to a reasonable range of values.
3. Check the *Log-transform* flag to log-transform the parameter. This will ensure that only positive values will be used for the parameter during the calibration.

### ► To run UCODE

1. Choose *UCODE (Inverse Modeling) > Run...* from the *Models* menu.  
The *Run UCODE* dialog box appears (Fig. 41).



2. Click *OK* to start UCODE.

Prior to running UCODE, PMWIN will use user-specified data to generate input files for UCODE and MODFLOW as listed in the table of the *Run UCODE* dialog box. An input file will be generated only if the *generate* flag is set to . You can click on the button to toggle the *generate* flag between  and . Normally you do not need to change the flags, as PMWIN will take care of the settings.

► **Check the Parameter Estimation Results**

Several result files are created through the parameter estimation process. Similar to PEST, UCODE writes the optimised parameter values to the input files of MODFLOW (BCF.DAT, WEL.DAT, etc.) and creates a detailed run record file *path\ucode.\_ot*, where *path* is the folder in which your model data are saved. The simulation results of MODFLOW are updated by using the optimised parameter values, which are saved in a separate file *ucode.\_st*. Similar to PEST, you can create a scatter diagram to present the calibration result (see above).

Note that PMWIN does not retrieve the optimised parameter values into the data matrices. Your original (PMWIN-) model data will not be modified in any way. This provides more security for the model data, because a parameter estimation process does not necessarily lead to a success. If you want to operate on the estimated

parameters, you must manually assign them to model cells. Alternatively, you can create a new model with the estimated parameters by using the *Convert Models* dialog box.

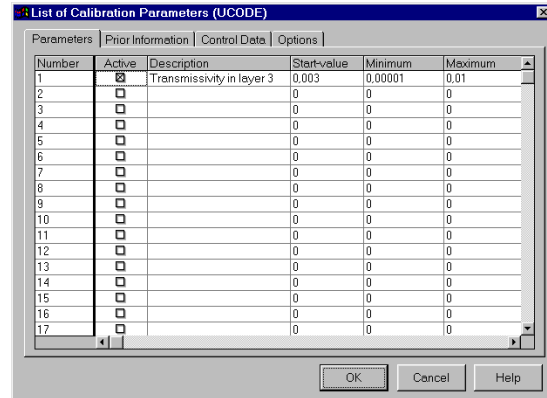


FIG. 40: THE LIST OF CALIBRATION PARAMETERS (UCODE) DIALOG BOX

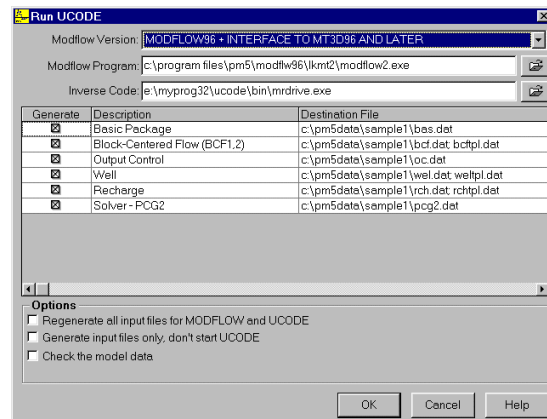


FIG. 41: THE RUN UCODE DIALOG BOX


## 5 Animation

You have already learned how to use the *Presentation* tool to create and print contour maps from calculated head and concentration values. The saved or printed images are static and ideal for paper-reports. In many cases, however, these static images cannot ideally illustrate motion of concentration plumes or temporal variation of hydraulic heads or drawdowns. PMWIN provides an animation technique to display a sequence of the saved images in rapid succession. Although the animation process requires relatively large amount of computer resources to read, process and display the data, the effect of a motion picture is often very helpful.

The *Presentation* tool is used to create animation sequences. The following steps show how to use the *Environment Options* and *Animation* dialog boxes to create an animation sequence for displaying the motion of the concentration plume in the third layer.

### ► To create an animation sequence

1. Choose *Presentation* from the *Tools* menu.
2. Move to the third layer by pressing *PgDn* twice.
3. Choose *Environment...* from the *Options* menu
4. Click the *Contours* tab, clear *Display contour lines*, and check *Visible* and *Fill Colors*.
5. Click the table header *Level*.  
A *Contour Levels* dialog box appears. Set the value for *Minimum* to 100, *Maximum* to 1600 and *Interval* to 100. These values are used, because we already know the range of the concentration values from Fig. 27. When finished, click *OK* to close the dialog box.
6. Click the table header *Fill*.  
A *Color Spectrum* dialog box appears. Set an appropriate colour range by clicking the *Minimum color* and *Maximum color* buttons. When finished, click *OK* to close the dialog box.

7. Click *OK* to close the *Environment Options* dialog box.
8. Choose *Animation...* from the *File* menu.  
The *Animation* dialog box appears (Fig. 42).
9. Click the *open file* button .  
A *Save File* dialog box appears. Select or specify a file name in the dialog box, then click *Open*.
10. Check *Create New Frames*, set *Result Type* to *Concentration (MT3D)* and set *Display Time (s)* to 0.1. *Display Time* is the display duration for each frame.
11. In the *Animation* dialog box, click *OK* to start the animation.

PMWIN will create a frame (image) for each time point at which the simulation results (here: concentration) are saved. Each frame is saved using the filenames *fn.xxx*, where *fn* is the *Frame File* specified in step 9 and *xxx* is the serial number of the frame files. Note that if you have complex DXF-base maps, the process will be slowed down considerably. When all frames are created, PMWIN will repeat the animation indefinitely until the *Esc* key is pressed.

Once a sequence is created, you can play back the animation at a later time by repeating steps 8 to 11 with *Create New Frames* cleared in step 10. You can also use the *Animator* to play back the sequence.

**Note.** The number and the size of the image files can be very large. Make sure that there is enough free space on your hard disk. To reduce the file size, you can change the size of the PMWIN window before creating the frames. You may turn off the display of the model grid in the *Environment Options* dialog box so that the grid is not cluttering the animation.

[www.unep.org](http://www.unep.org)

United Nations Environment Programme  
P.O. Box 30552-00100, Nairobi, Kenya  
Tel: (254 2) 624105  
Fax: (254 2) 624269  
E-mail: [dewainfo@unep.org](mailto:dewainfo@unep.org)  
Web: [www.unep.org](http://www.unep.org)  
[www.unep.net](http://www.unep.net)



For further information

Division of Early Warning and Assessment  
United Nations Environment Programme  
P.O. Box 30552-00100, Nairobi, Kenya  
Tel: (254-2) 624028 Fax: (254-2) 623943 Email: [dewainfo@unep.org](mailto:dewainfo@unep.org)  
Web: [www.unep.org](http://www.unep.org), [www.unep.net](http://www.unep.net)